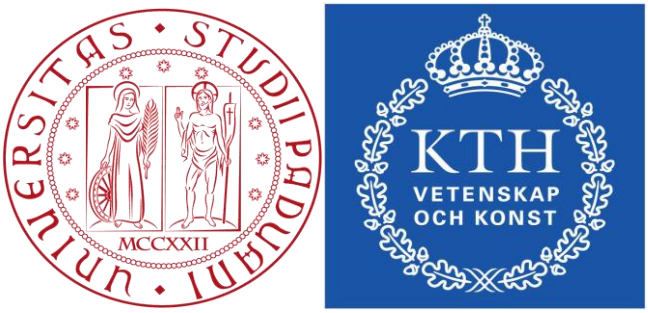

UNIVERSITA' DEGLI STUDI DI PADOVA

KUNGLIGA TEKNISKA HÖGSKOLAN

DIPARTIMENTO DI INGEGNERIA INDUSTRIALE

CORSO DI LAUREA MAGISTRALE IN INGEGNERIA DEI MATERIALI

TESI DI LAUREA

METALLOGRAPHIC INVESTIGATION OF OXIDES IN FRICTION STIR WELDED Cu-OFP

Relatore interno: IRENE CALLIARI

Relatore esterno: ROLF SANDSTRÖM

Laureando: ALBERTO SCHIAVON

Matr.n. 1020411-IR

Anno accademico 2012/2013

Abstract. The purpose of the work is to study the presence of oxides in Cu-OFP. Oxides are typically located in the grain boundaries. Combined with hydrogen they can form water steam pores which can embrittle the material; the object of this work is the analysis of oxides in friction stir welded Cu-OFP joints designated internally FSW90/139 and FSW08/155. Cu-OFP is intended for final disposal of nuclear waste; this method is based on Cu-OFP canisters used as corrosion barriers with an inner cast iron insert.

This work has been focused on the characterization of 2 FSW joints. Each joint has been divided into 5 specimens, these specimens were metallographically prepared using and comparing different methods: mechanical grinding, diamond polishing and chemical etching; mechanical grinding, oxides polishing and chemical etching; mechanical grinding, electro-polishing and etching. Specimens were investigated macro and microscopically using optical microscope, scanning electron microscopy and EDS. The main differences among specimens were disclosed, in particular the oxides area fraction, the inclusion's size, their composition and their orientation and number. Average grain size has also been investigated. Differences between retreating side and advancing side and among the 2 welds have been detected about the area fraction, oxygen content, number of inclusions and average size of inclusions. In both sides of the weld FSW08 oxides area fraction increases getting closer to the edge of the weld, as well as the number of inclusions; considering the average size of inclusions, it grows, as well as the average oxygen content getting further from the edge of the weld. Weld designated FSW08 presents the higher oxides area fraction. Weld designated FSW90 presents the lower oxides area fraction, as for FSW08, oxides area fraction, number of inclusions and average oxygen content grow getting further from the edge of the weld, no remarkable differences have been found concerning the size of inclusions ; as FSW08, FSW90 presents differences between advancing and retreating side even if less obvious. In both welds, besides oxygen and copper, some inclusions with small traces of silicon, calcium, aluminum, sulfur and iron are detected, contrary to FSW08, FSW90 presents almost no voids.

KTH - Materialvetenskap / Università di Padova – Dipartimento di ingegneria industriale

Summary

1 POWER GENERATION IN SWEDEN

Mainly from [4]

More than a third of Sweden's energy supply depends on imports. Domestic energy production is largely limited to electricity generation using nuclear energy and renewable sources (almost exclusively hydro). Energy imports are mainly oil from Denmark, Norway and Russia, with some small quantities of hard coal imports. Industry exhibits a relatively high share of final energy consumption compared to other EU Member States. Given the relatively low presence of fossil fuels in the energy mix, Sweden has low CO_2 emissions and CO_2 intensity factor. Low carbon energy is a high priority in government policy.

As presented in *figure 1*, swedish energy supply depends mainly on nuclear energy, oil and renewable sources, Sweden is a significant producer of nuclear energy holding the third place among EU.

Final Energy Consumption in Sweden has remained fairly constant since 1990. Industry and transport are the major energy-consuming sectors, with a 39% and a 24% share respectively in final energy consumption in 2004. The share is much higher than the EU-27 average, particularly for demand in the industrial sector. Oil and electricity dominate in terms of the type of energy consumed (67% of total).

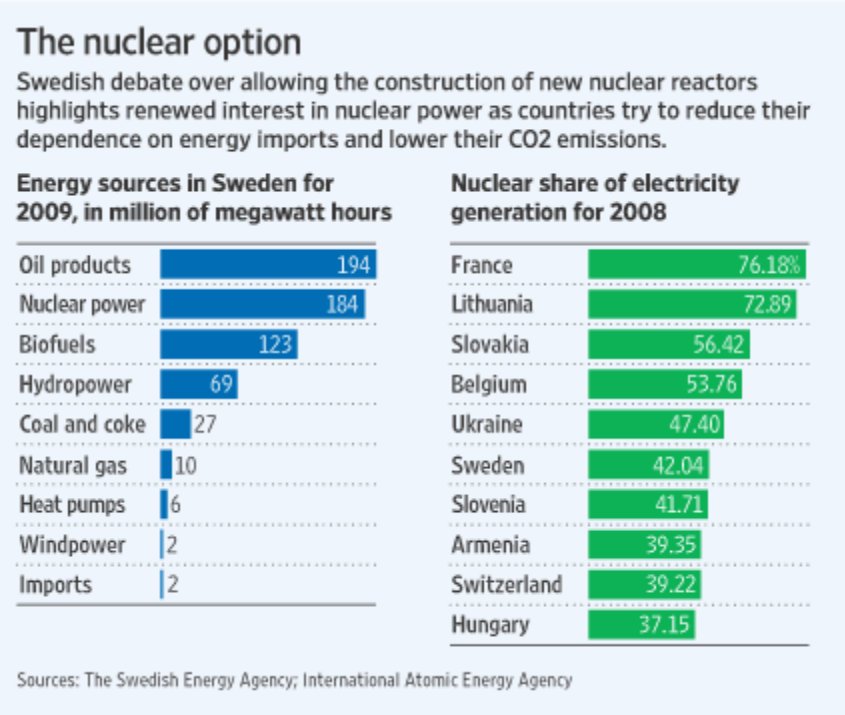

Fig. 1 Energy sources and nuclear share of electricity in Sweden [4].

1.1 Nuclear power plants in Sweden

Mainly from [4]

In order to investigate Swedish nuclear waste program it's useful to give a background of the Swedish energy production program; electricity production in Sweden is dominated by hydroelectricity and nuclear power. Sweden began research into nuclear energy in 1947; in 1954 Sweden built its first small research heavy water reactor; this first reactor was followed by 2 heavy water reactors, Agesta and Marviken .The first light water reactor was developed at Oskarshamn in 1972. Today 10 reactors are in operation: three boiling water reactors at Forsmark, three boiling water reactors at Oskarshamn, one boiling water and three pressurized water reactors at Ringhals. After the partial meltdown of Three miles island in US in 1979, there was a referendum about the future of nuclear power in Sweden, the result of the referendum was that no further nuclear power plants should be built, and that a nuclear phase-out should be completed in 2010. The topic of nuclear security was raised again in 1986, after Cernobyl disaster. In June 2005 radioactive water was detected leaking from the nuclear waste store in Forskmark. On the 17 June of 2010 the Riksdag adopted a decision allowing

the replacement of the existing reactors with new nuclear reactors, starting from 1 January 2011.

The principal strategy for high-level radioactive waste disposal in Sweden is to enclose the spent fuel in tightly sealed copper canisters that are embedded in clay about 500 m down in the Swedish bedrock.

1.2 Final repository for spent nuclear fuel in the world

Mainly from [10]

About thirty countries use nuclear power to produce electricity and totally about 430 nuclear reactors are in operation worldwide, then the problem of spent nuclear fuel is widely common for the most industrialized country in the world.

Table 1: Spent fuel inventory and policy among different countries [10]

Country	Spent Fuel Inventory (tons)	Spent Fuel Policy
Canada	38.400	Direct disposal
Finland	1.600	Direct disposal
France	13.500	Reprocessing
Germany	5.850	Direct disposal
Japan	19.000	Reprocessing
Russia	13.000	Some reprocessing
South korea	10.900	Storage, disposal undecided
Sweden	5.400	Direct disposal
United Kingdom	5.850	Reprocessing but future unclear
United States	61.000	Direct disposal

In a few countries, spent fuel is sent to a reprocessing plant. Where the fuel is dissolved and the plutonium and uranium recovered for potential use in reactor fuel; usually plutonium is involved in the development of nuclear weapons. Reprocessing can be re-used as fuel, this is economic only when uranium prices are high.

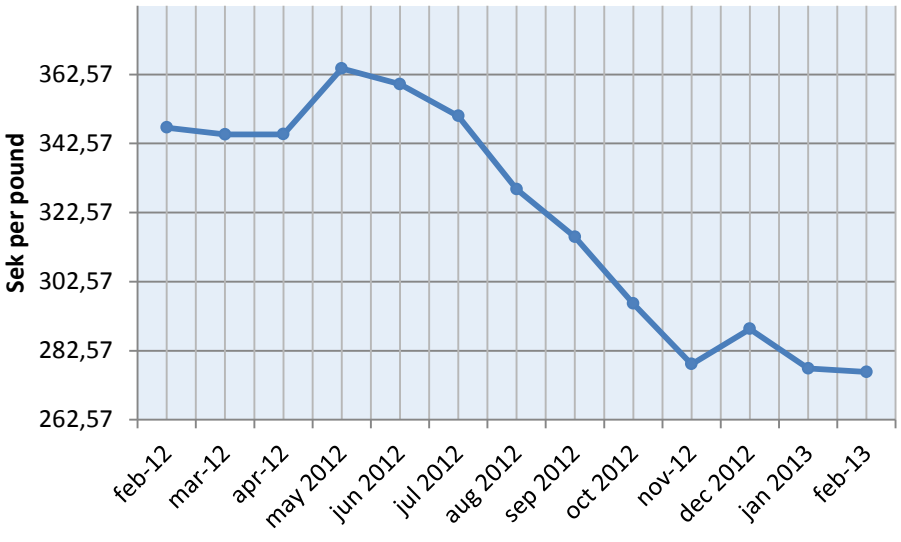

Fig. 2: Uranium price (sek per pound), data from [5].

Nuclear reprocessing reduces also the volume of high-level waste even if it doesn't avoid the need for a geological waste repository; this kind of processes have always been politically controversial because of the potential contribute to nuclear proliferation. Nuclear reprocessing is widely performed in Europe, Russia and Japan; anyway nuclear reprocessing does not eliminate the requirement for a repository, an example of industrial reprocessing is the nuclear center of Tricastin in southern France. In France is pursued an intense policy of reprocessing so that in Japan; Germany, Switzerland, the Netherlands, Belgium and Italy have shipped their wastes for reprocessing here in the past or are currently doing so; even US, after Obama shut down the project of Yucca Mountains repository for political reasons, are starting to develop French's knowledge in this field. In contrast with this policy, Sweden and Finland are the countries that are most advanced in repository siting without reprocessing; finding sites for repositories has proven politically very difficult. This has almost always resulted in strong local opposition, leading to the abandonment of the sites, a clear example is Obama administration's decision to abandon the Yucca Mountain repository project ; in the United Kingdom, in 1981, in face of the intense local opposition, the government abandoned efforts to investigate the geology at possible sites that it had identified for high-level repository and decided not to resume the effort for 50 years; another European example is Germany, in 1977, the state government of Lower-Saxony chose Gorleben as a place to dispose of spent fuel and high-level reprocessing waste; after this decision the site became the focus of intense

demonstrations, so in 2000 the government halted work there, social scientists call this NIMBY (not in my back yard). For this initial failures, several countries developed a more consultative process in which local communities determine whether or not they wish to be included in site assessments; in this field in 1970, the British sociologist Richard Titmuss published a comparative study of blood donation systems in UK and the US, in this study he finds out that monetary compensation "crowded out" the finer motivations and resulted in fewer blood donors, this theory was then tested in the field of nuclear waste facilities by two Swiss economists who demonstrate that sense of altruism supplies social motivation rather than monetary compensation; the key, as O'Hare supposes, is to find indirect ways of compensating the local community that builds on a sense of pride in the facility.

1.3 Final repository for spent nuclear fuel in Sweden

Mainly from [4]

Sweden and Finland are the countries that are most advanced in repository siting without reprocessing; According to the KBS-3 concept, the spent fuel will be inserted in an inner pressure resistant component made by nodular cast iron. The insert will be put into copper canisters with a lid and possibly a bottom sealed by Friction Stir Welding (FSW). The candidate canister has a diameter of 1050 mm, a length of 4850 mm, and a wall thickness of 50 mm, The copper canisters will be transported to a deep repository around 500 m in the granite bedrock and will be embedded in bentonite, which will swell and encase the canisters after groundwater fills the space between the rock and the clay, the canister is designed to be a corrosion barrier which should stay intact for at least 100,000 years.

The canister isolates, the buffer seals and the rock protects; the materials used for this kind of repository are present naturally in the earth's crust in order to imitate nature as closely as possible. The copper isolates the spent fuel from the surrounding environment, the canister is then surrounded by a layer of bentonite clay that protects the canister against small movements in the rock, prevents direct contact with the groundwater and acts as a filter trapping radionuclides; then the repository is filled with rock in order to protect the canister and the buffer from mechanical damage.

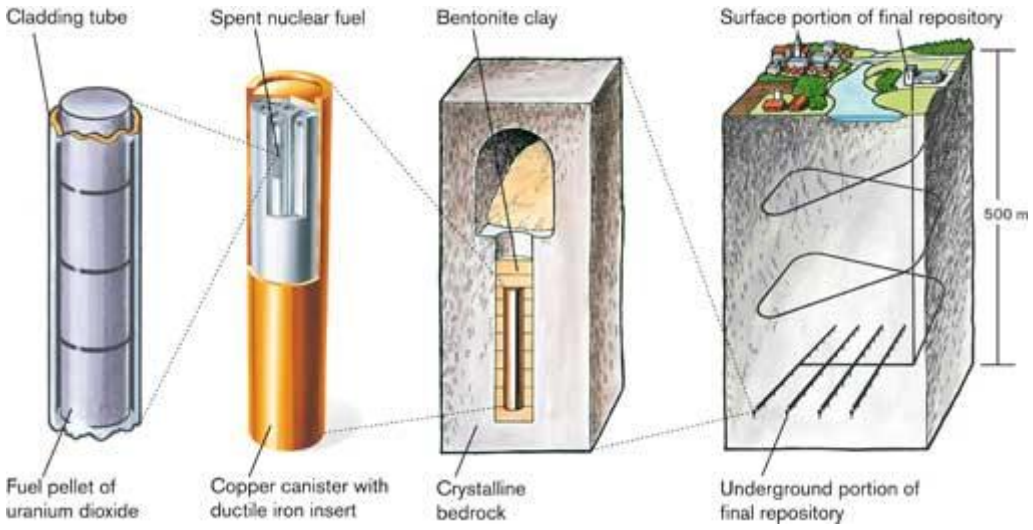

Fig. 3: Final disposal scheme [4].

SKB manages and disposes of three types of nuclear waste: operational waste, decommissioning waste and spend nuclear fuel.

- *Operational waste*: This kind of waste constitutes 85 per cent of all nuclear waste, most is low and intermediate-level waste, which requires isolation for at least 500 years. Low level waste doesn't need any radiation shielding, so it can be transported and stored in ordinary steel-plate containers. Intermediate level waste needs a radiation shielding and must be poured into concrete or steel containers at the nuclear power plants.
- *Decommissioning waste:* When a nuclear power plant is dismantled large quantities of scrap metal and concrete are generated which can be considered as low and intermediate level wastes. A small part of the decommissioning waste are reactor rods and other core components which are classified as long-lived and must be isolated for thousands of years.
- *Spent nuclear fuel:* The smallest but most hazardous part of the total quantity of waste is spent nuclear fuel; this waste must be shielded and cooled throughout handling, transportation and storage and isolated for at least 100000 years.

The responsible of the development of KBS-3 is SKB, SKB stands for Svensk Karnbranslehantering AB and it's the Swedish nuclear fuel and waste management company; its aim is to manage and dispose spent nuclear fuel and other radioactive waste, in order to guarantee a good disposal SKB presents an R&D program every three years. The 1976

Parliamentary election in Sweden resulted in a coalition government which imposed extremely stringent requirements for the waste produced by Swedish nuclear power plants, the industry responded with a crash study, the KBS project where KBS stands for Karnabranslesakerher that means Nuclear Fuel Safety, in 1977 the industry presented a complete scheme for absolutely safe storage of nuclear waste in engineered facilities located at about 500 m depth in the bedrock, this project was called KBS-1, this first study was later followed by KBS-2, the first project was redacted in 1977 (KBS-1), and the second in 1978 (KBS-2).

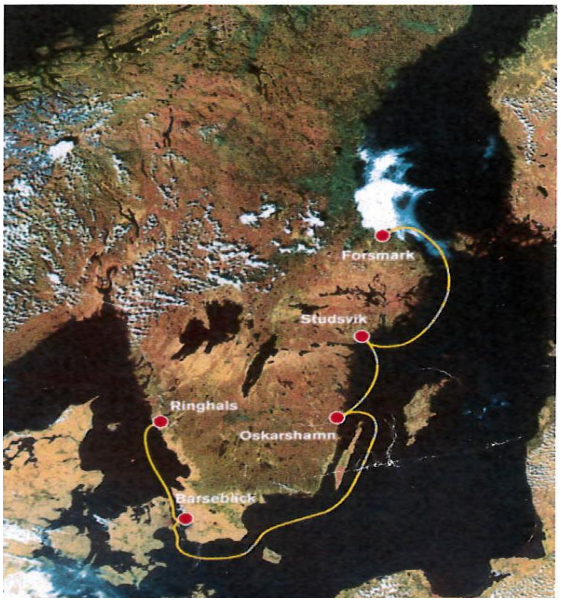

Fig. 4: Nuclear facilities in Sweden [4]

In 1982 SKB built M/S Sigyn, a special vessel for the transportation of wastes from the nuclear power plants to the interim storage facility for spent nuclear fuel and the final repository for radioactive shortlived waste. In 1983 report KBS-3 was published, this report showed that direct disposal is a viable method and that the geological conditions for a safe repository can be found in Swedish crystalline bedrock with barriers of natural materials, for this reason reprocessing was no longer required.

In 1985, after swedish government support, started the operation for an interim storage facility for nuclear fuel (Clab), this facility is located on the Simpevarp Peninsula near the Oskarshamn Nuclear Power Plant. In 1988 started the building of SKB's final repository for short lived waste (SFR), it's located nearby Forsmark and receives low- and intermediate-level waste; in 1995 was inaugurated Aspo Hard Rock Laboratory, a renowned and prestigious laboratory for research on geological storage, the laboratory offers a realistic environment for different experiments and tests under the conditions that will prevail in a deep repository, this laboratory is situated near the Oskarshamn Nulcear Power Plant. In 1998 SKB inaugurated another renowned facility: the canister laboratory, which is the centre for further development of the encapsulation technology and related safety issues, its primary purpose is to develop methods for welding the lid onto the copper canister and inspecting the weld for quality. After some year of investigation, in 2009 Forsmark was chosen as site for the final repository of spent nuclear fuel, a deposition permit is expected then in 2017, then a

trial operation with 200-400 canisters will start followed by an evaluation before the regular operation, it's believed that SKB's mission will be completed in 2060. All Swedish nuclear power plants and present waste management facilities are situated on the coast, this because of the easier transport from a site to another. The storage operation starts with a storage in water pools situated at the power plants for about nine months, after all the waste is transported to an interim storage facility, where it will be stored for about 30 years; the final operation is the encapsulation in cooper canisters and the storage in a deep repository. In order to understand the magnitude of this problem it's useful to compare the amount of nuclear waste upon 40 years operation of the nuclear power plants with the size of the "Globen" stadium in Stockholm.

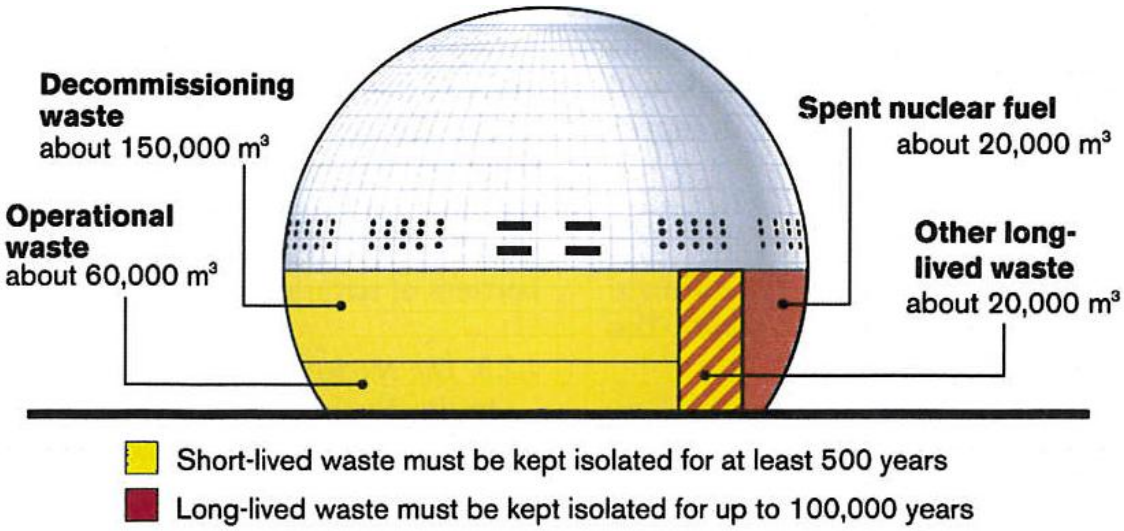

Fig. 5: Total ammount of nuclear wastes [4].

Nuclear power has given Sweden electricity at reasonable prices for years, the main disadvantage is that it creates radioactive residual products that are harmful to humans and the environment, for this reason an intensive research is needed so the nuclear power utilities pay a special fee for future expenses for safe management of spent nuclear fuel and decommissioning and dismantling of nuclear reactors, this fund finances SKB activities.

1.4 Swedish nuclear waste fund

Mainly from [1]

In the early 80's the Swedish parliament devised a financing system to finance the cost of future management and disposal of nuclear fuel, the holder of a nuclear facility that increase the national waste production pay a special fee to the state; this fee is paid at a given rare per KWh of electricity delivered by the nuclear power plants. Before 1996 this fees were deposited in accounts at the Swedish central bank, after 1996, these fees are controlled by the Swedish nuclear waste fund, so nuclear power industry must be responsible for the waste disposal costs. Every year the Fund redacts a report to point out the situation.

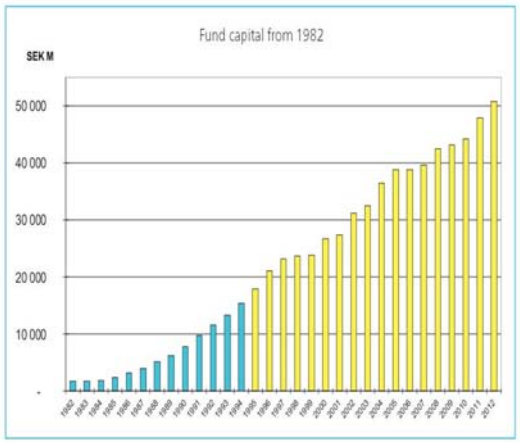

Fig.6: Nuclear waste fund [1].

Being this a crucial problem for the present and the future also Swedish politics has pronounced: first of all the waste from Swedish nuclear power plants must be disposed of within the country's borders, secondly Sweden will not dispose of fuel from other countries in its repositories, the spent fuel will not be reprocessed (as in France), the waste must not be passed on to future generations, but rather be managed and disposed of today. The challenge of SKB is to prove a million years life of an engineering barrier for storage of nuclear waste, as said, the strategy is to enclose the spent fuel in tightly sealed copper canister that are embedded in clay.

1.5 Collaboration among countries

Mainly from [3]

Many countries have their own research and development programs to resolve issues involving the handling and storage of radioactive waste; several international organizations such as IAEA, OECD/NEA and EC are working intensively on radioactive waste issues. There are also international agreements in palace, like IAEA's "Joint Convention on the Safety of Spent Fuel Management and on the Safety of Radioactive Waste Management". In order to collaborate with other countries, SKB International Ab, a subsidiary of SKB, is active in international work related to technology transfer, it offers its international customers the knowledge and experience that SKB has built in these years, its field extend from low and intermediate-level waste to high level waste and spent nuclear fuel. Recently has been studied the impact that would an ice sheet have on the Swedish final repository for spent nuclear fuel, for this SKB is participating in a major international research project in western Greenland that investigates how glacial meltwater flows through and under the ice sheet and forms groundwater that, in turn, would be able to affect the safety of the repository, this project is called Greenland Analogue Project; SKB is also involved in a research on what happens at the ground surface in a permafrost landscape, in order to study how does the water at the surface flow in a landscape where the ground is constantly frozen. The attempt of this kind of studies is to examine what could happen to the nuclear fuel repository during several ice age cycles.

2 FRICTION STIR WELDING

Mainly from [6,7,8,9]

Friction Stir Welding (FSW) was developed by The Welding Institue in 1991 in order to find a welding method also for aluminum and its alloys, copper and its alloys, lead, titanium and its alloys, magnesium alloys, zinc, plastics, and mild steel. In this welding method a non consumable tool with no filler material and with no need of shielding gas is used. This technology has been used for the manufacture of butt welds, overlap welds, T-sections, fillet, and corner welds; the industries using FSW is the shipbuilding and marine industries, aerospace industry, railway industry, construction industry and electrical industry, since it's a solid phase welding process it can be used in many position. FSW is rapid, clean and can guarantee high quality level for long periods of production, indeed the other welding processes depend widely on the operator's skills. The heat is due to friction between the tool and the welded material, which causes the weld material to soften at temperature less than its melting point. The side on which the tool rotation is parallel to the weld direction is called advancing side and the side on which the tool rotation is opposite to the weld direction is called retreating side. The tool shoulder has two roles, first it generates the necessary heat, secondly it controls the flow of the material in order to have a more uniform flow.

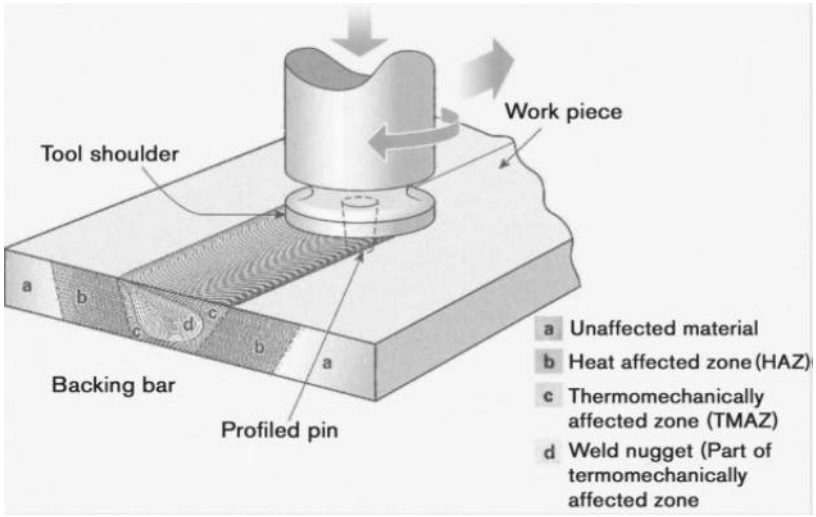

Fig. 7: Friction stir welding scheme [8].

As for any welding process, FSW has a large number of parameters that can be controlled to avoid defects; first of all the thickness of the weld, the tool geometry, the side clamping force, the rotation speed of the tool, the tilt angle, the tool cooling, the tool axial welding force, the physical stops to prevent further movement of the welding head and the altered welding force. If those parameters are not optimal, voids and excess flashes can be formed and they can lead to tool's pin breakage.

Even if FSW looks like a simple welding method, the physics behind is very complex; it involves heat generation and mass and heat transportation. Many efforts have been spent to understand how the matter flows in a FSW process, several methods have been developed by Xu, Reynolds, Fourment, Colegrove, Shercliff and Colligan; the latter describes the material flow caused by the rotating pin. For this purpose Colligan used as tracer material 14 steel balls of 0,38mm in size, these balls tent to travel around the rotating pin, weld was subsequently radiographed to reveal the distribution of the tracer material as it transitioned from its original position, around the welding tool and into the welded joint; results showed that material around the pin is lifted and extruded around the pin in the rotating direction, for this reason materials in the advancing side is carried around to the retreating side.

3 Cu- OFP

Mainly from [11]

Cu-OFP is the material that is employed in canisters for spent nuclear fuel, before going any further, it is useful to consider its compounds from the chemical and the thermodynamic point of view.

Copper forms compounds in the oxidation states +1 and +2 in its normal chemistry, although under special circumstances some compounds of trivalent copper can be prepared. It has been shown that trivalent copper survives no more than a few seconds in an aqueous solution. With oxidation state +1 in presence of oxygen reaction (1) takes place, with oxidation state +2 reaction (2) takes place.

$$4Cu + O_2 \rightarrow 2Cu_2O \qquad (1)$$

$$2Cu + O_2 \rightarrow CuO \qquad (2)$$

Reaction (1) forms Cuprite, reaction (2) Tenorite, these compounds differ in the crystallographic structure, Cuprite has a cubic structure, Tenorite a monoclin crystal structure.
In order to understand which compound is more stable depending on the conditions, phase diagrams have to be investigated:

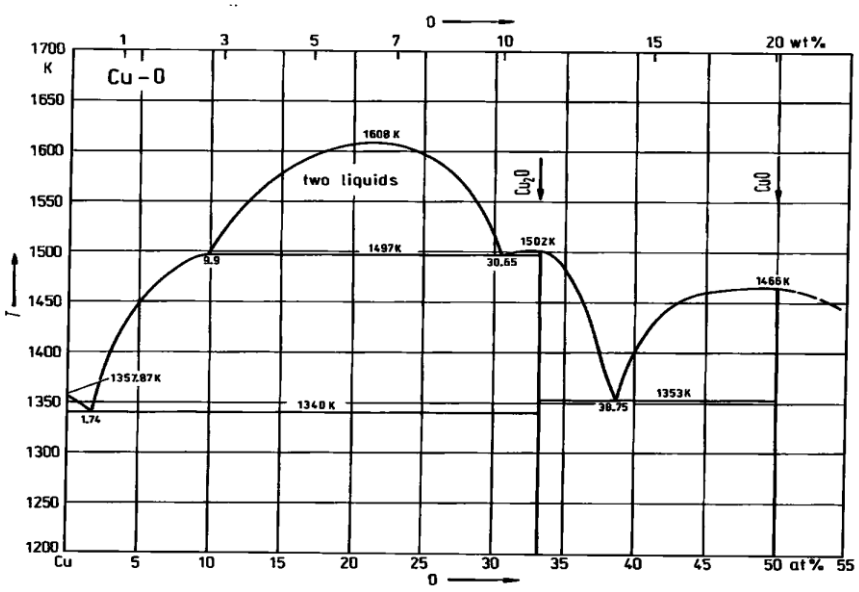

Fig. 8: Oxygen and Copper phase diagram [11]

From diagram in *figure 8* it's clear that Cuprite is stable for lower oxygen content than Tenorite. Taking into account also the pressure and the temperature:

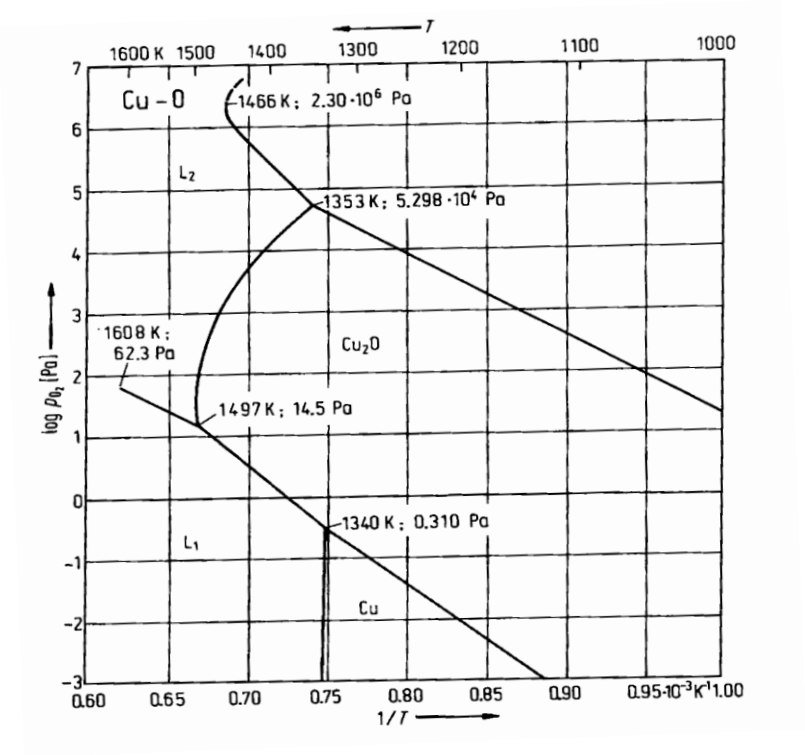

Fig. 9: Relation between pressure and temperature in copper stability [11].

Diagram in *figure 9* shows that Cu_2O is stable for relatively low temperature and low oxygen pressure, being Cu-OFP almost oxygen free, the oxide that could be formed is Cu_2O .Besides rock movement, the biggest threat to the canister in the repository is corrosion, copper will last if proper environmental conditions are established and maintained. We already know that copper can show high corrosion rates in some environments, that it can reveal local corrosion under certain conditions. Considering the final repository for spent nuclear fuel, the deep groundwater can vary considerably in salinity providing a different environment from the corrosion's behavior point of view. Initially oxygen free high conductivity copper (Cu-OFHC) has been considered as a candidate material for the canisters, since its thermodynamic stability in reducing ground water was considerable. Howerer, Cu-OFHC shows inadequate creep ductility, for this reason, two candidates were oxygen free copper with 30-60 ppm phosphorus (Cu-OFP), and pure copper with 0.1 % silver. Since Cu-OFP was expected to give the least negative influence on the corrosion properties, it was selected. In addition the cost of Cu-OFP is essentially lower than that of Cu-0.1%Ag. Cu-OFP is then designed for

canisters acting as a corrosion barrier for disposal of spent nuclear waste. Purposely, Cu-OFP has a very low oxygen content of 5 wt. ppm to prevent hydrogen sickness when the canister is welded. In addition phosphorus is added which combines with some of the oxygen to reduce the free oxygen content even more.

Table 2: Chemical composition of Cu-OFP [14]

Ag	As	Fe	Ni	O	P	S	Sb	Cu+P
13	<1	2	2	1-2	45-60	5	1	≥99,99%

Concerning Cu-OFP, various attempts have been made to develop a model that can predict its behavior, in Cu-OFP different compounds are present in equilibrium the more stable are chalcocite (α and β) (Cu_2S), digenite (Cu_9S_5), $Cu_2P_2O_7$, $Cu_3P_2O_8$, P_4O_{10}, CuO and Cu_2O.

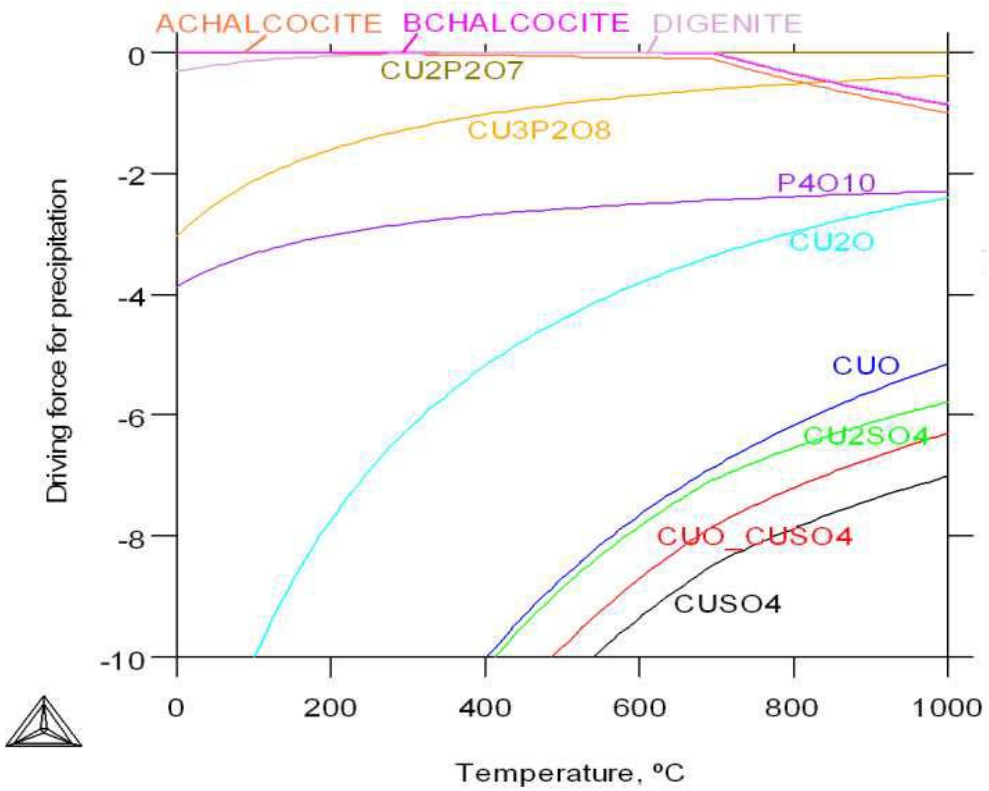

Fig. 10: Driving force for precipitation calculated for copper with 50ppm phosphorous, 6ppm sulfur and 3ppm oxygen [12].

Considering the thermodynamic graph present in *figure 10* it's possible to assert that $Cu_2P_2O_7$ and $Cu_3P_2O_8$ are all more stable that Cu_2O and CuO, this because phosphorous present in copper tends to combine with oxygen limiting the quantity of oxygen free to form Cu_2O and CuO. For this reason phosphorous has a very important role, limiting the quantity of free

oxygen it hinders the formation of oxides, this role is underlined also from the comparison between the graphs in *figure 11* and *12*.

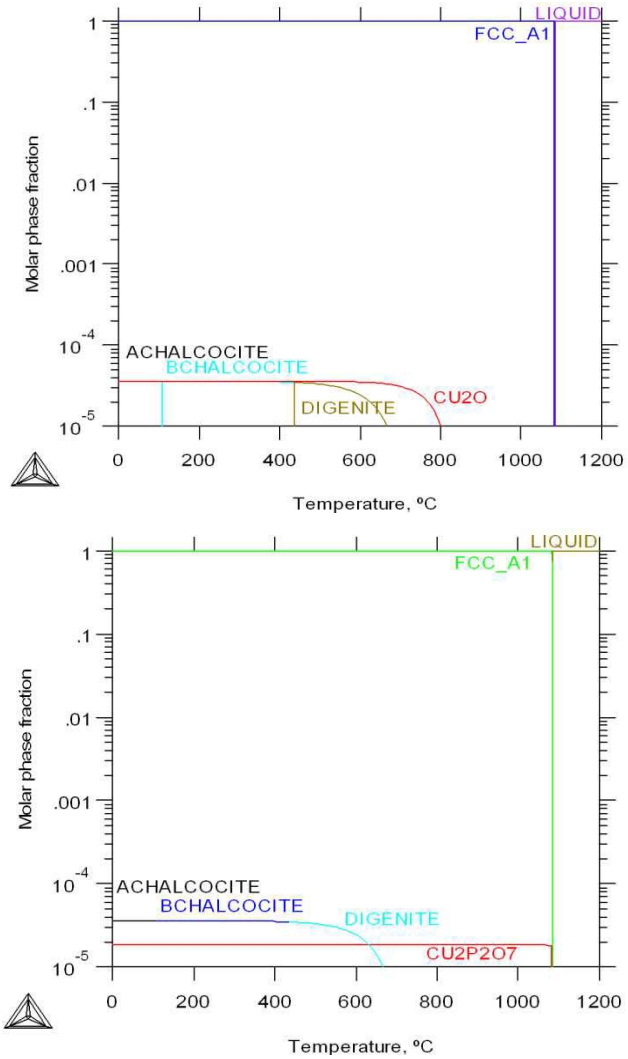

Fig. 11-12: Calculated equilibrium for copper with 50 ppm P, 6 ppm S, 3 ppm O; in fig. 11 without P [12].

Even though in Cu-OFP phosphorous tends to form phosphates reacting with oxygen, the larger part of phosphorous present in the material is in the form of free phosphorous. The concept expressed in the graph in *figure 10* is presented also in *figure 13*. It' is clear, also from this graph, that $Cu_2P_2O_7$ is the most stable compound at high temperature.

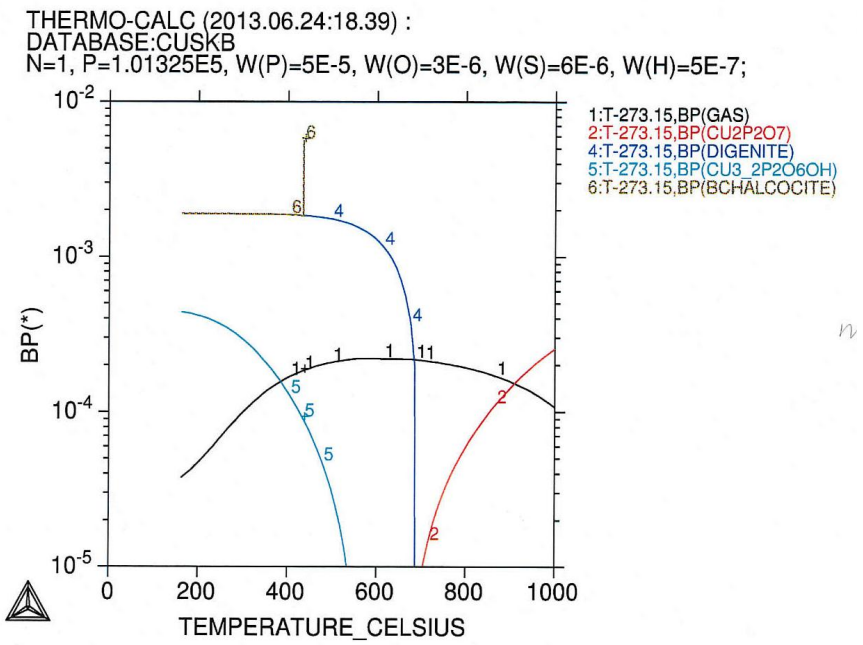

Fig. 13: Thermodinamic stability of Cu-OFP.

3 .1 Hydrogen embrittlement in copper

Mainly from [13,14]

The classical form of hydrogen embrittlement of copper has been attributed to formation of voids generated by reaction between diffusing hydrogen and cuprous oxide inclusions, these water bubbles, particularly those formed at the grain boundaries, lower the ductility of copper considerably, this is known as hydrogen sickness. Hydrogen is expected to be accumulated in a metal that is exposed to an anoxic environment on all sides. The copper canister in a repository will eventually be exposed to a strictly anoxic environment and hydrogen charging due to anoxic corrosion. Copper is not particularly sensitive to hydrogen embrittlement but the problem exists and the mechanical properties are affected negatively before any serious embrittlement occurs, absorption of hydrogen in copper and the influence of hydrogen on the mechanical properties and the role of the microstructure have been studied for over 50 years. Only molecular hydrogen can remain in copper as a stable species at ambient temperatures, this because of the high H_2 dissociation energy (35-40 $kcal\ mol^{-1}$) of molecular hydrogen on copper surface then the solubility of atomic hydrogen in copper is very low at room

temperatures according to the experimental data obtained by McLellan, where T is the temperature in Kelvins.

$$ln\theta = \frac{6{,}62*10^3}{T} \qquad (3)$$

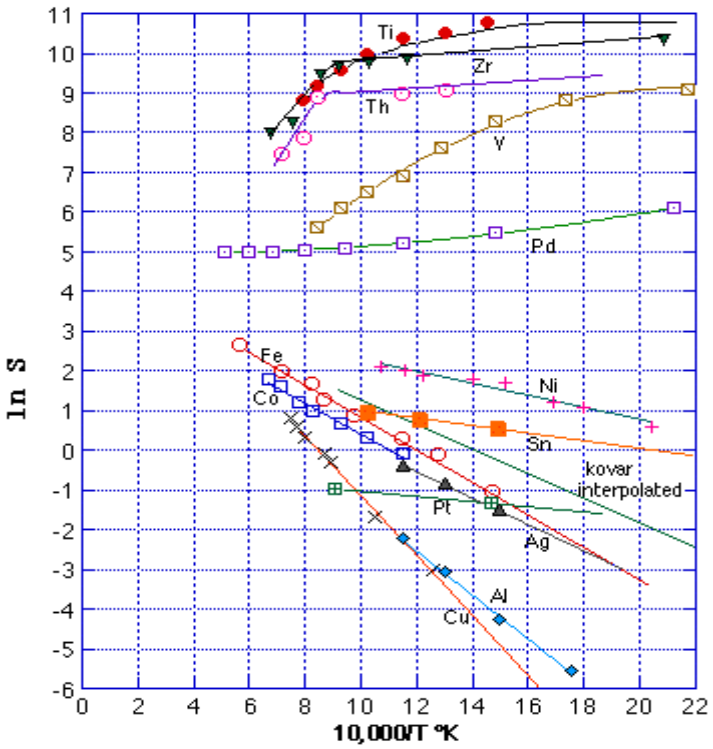

Fig. 14: Hydrogen solubility in various metals [13]

Afterwards the activation energy for dissociation of molecular hydrogen into atomic hydrogen by copper surface is very large (35-40 $kcal^{-1}$), this fact suggests that when molecular hydrogen enters into copper lattice as bubbles, it does not readily diffuse out of copper by the dissociation mechanism

$$H_2 \rightarrow H + H \qquad (4)$$

As it involves a large activation energy. Therefore a combination of both high pressure and high temperature is required to observe the hydrogen effect on proprieties of copper. Transfer of hydrogen to bubbles was analyzed by Wampler, he proposed a relation for the hydrogen flux to a bubble:

$$J_H = D\nabla_{CH} = D\frac{C_H}{r} \qquad (5)$$

Considering r the radius of the bubble.

The amount of hydrogen absorbed will depend on the efficiency of the dissociation process which, in turn, depends on the condition of the metal surface. Thin oxide films on metal surfaces significantly reduce the ability of hydrogen to dissociate, once the ductility is lost, it can be restored after some months at room temperature or after heating. Adsorbed hydrogen interacts with alloying or impurity elements in the microstructure, in copper, oxygen strongly segregate on grain boundaries and form oxides than can interact with hydrogen generating steam, these are elevated temperature processes that generally lead to the formation of grain boundary cavities.

$$Cu_2O + 2H \rightarrow 2Cu + H_2O \quad (6)$$

Oxides reacting with hydrogen to form steam are generally associated with grain boundaries thus continued bubble development tends to force the grain apart, and can cause grain boundary fracture. This form of embrittlement occurs in copper alloys containing oxygen and copper oxides, but since oxygen free copper has become easy to produce, steam embrittlement is not frequent. Frequent embrittlement situation occurs when copper is annealed and quenched in hydrogen environments, in this situation the use of hydrogen atmosphere facilitates the reduction of oxides, but if copper contains a significant amount of oxygen, the hydrogen can react with the oxygen leading to water bubble growth at grain boundaries. The amount of gas bubbles depends on the quenching rate and on the temperature. As pointed out the exposure of copper to high temperatures and high hydrogen pressures can degrade the strength and ultimately cause fracture.

When the copper canister is placed in the repository is subjected to high temperature and pressure.

If the diffusion of hydrogen into the material is controlled just by conventional diffusion of hydrogen atoms, it would satisfy the diffusion equation:

$$\frac{dc_H}{dt} = D\frac{d^2c_H}{dy^2} \quad (7)$$

Where c_H is the hydrogen concentration in solid solution, t is the time and D is the diffusion constant for hydrogen and y is the distance from the surface. At room temperature $D = 2{,}2x10^{-4}\frac{m}{s^2}$..

3.2 Hydrogen interaction with defects in metals

Mainly from [21]

The interaction of hydrogen with lattice imperfections are important and often dominant in determining the mechanism of hydrogen embrittlement, nevertheless, in general, these interactions are far less understood at a fundamental level than the behavior of hydrogen in perfect lattices. As well as reflecting the natural progression of research, this situation results from the variety and complexity of hydrogen-defect interactions and from the experimental and theoretical difficulties that have been encountered in their study.

The simplest defect in metals in the vacancy, hydrogen is strongly bound to this imperfection in copper, whenever the surface chemisorption state of hydrogen is energetically favored over interstitial solution. Also grain boundaries can affect the interaction between copper and hydrogen.

4 EXPERIMENTAL APPARATUS

4.1 Grinding disks

The surface of the specimens is ground with rotating manual grinding disks in order to remove any surface defects and to get the slightest roughness.
This step is very important since in SEM analysis high roughness or a surface not completely finished is not optimal, since the light beam is distorted due to small pads on the surface.
Moreover other parameters must be considered:

- The choice of the abrasive papers: they must present harder grains than the specimen in exam.
- Grinding rate: disks must be replaced when they are consumed.

With grinding processes it is possible to remove all the superficial damage suffered during cutting process; abrasive disks are used with decreasing grain size, in order to obtain a properly ground sample, some steps must be followed:

- Grinding process must be carried out in presence of water in order to minimize the heating of the sample and to wash out metallic dust that can be deposited between the abrasive grains lowering the efficiency of the process.
- Pressure must be enough to permit a fast polishing without any damages to the surface in exam.
- In between the changing from two papers with different grain size, the sample must be carefully washed with water in order to avoid that abrasive grain of the previous paper can damage the next paper.

Grinding papers are often made of silicon carbide, aluminum oxide, emery, ceramic composites and diamond. These materials are always linked to papers or abrasive disks.

Fig. 15: Grinding manual machine.

4.2 Oxides and diamond polishing

Diamond

Usually polishing is performed with abrasive-water suspension on rotating drapes, with diamond paste lubrication is required and the choice, also concerning drapes and grain size of abrasive, has to be carried out taking into account the general features of the material under polishing.

Fig. 16: Polishing manual machine.

Oxides

The interaction between mechanical and chemical material removal is the important issue during oxide polishing. Sole mechanical abrasion always results in some kind of deformation, whereas exclusive chemical material removal produces relief between various phases.
However, by combining the right abrasive with the correct chemical reagent, superb results can be obtained. The chemicals that are often used for copper are ammonia water and hydrogen peroxide. This process is not performed with the conventional rotating drapes, but it is carried out using the automatic polishing machine, with a magnetic disk and a neoprene disk glued on it, with this machine it is possible to control the rotating speed, the lubrication and the polishing time in a larger range than the manual polishing machine; in this case since the samples are not small enough to fill into the automatic arm, finger pressure has to be used.

Etching:

Etching is the process that reveals microstructural details that would otherwise not be evident on the as-polished sample, this process is not always required, in our case etching is fundamental in order to reveal the grain boundaries where there could be oxides inclusions; usually this process is performed immersing the sample in an etchant, this chemical selectively corrodes the surface of the metal sharpening the microstructural features, immersion time or etching time is highly dependent on the system and in most cases requires experience.

4.3 Electrolytic polishing

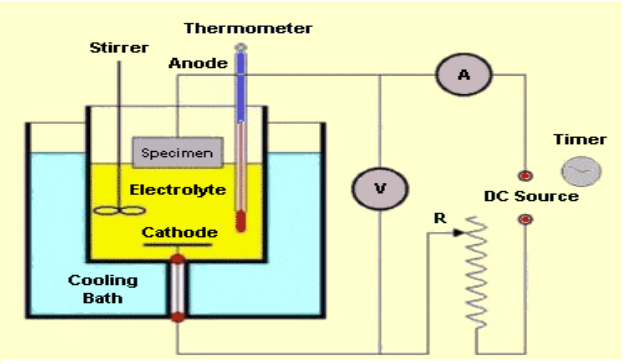

Fig. 17: Electrolytic polishing [20].

A commonly used polishing method is electrolytic polishing. This method is commonly known as anodic dissolution, is the best way to polish very soft materials which are prone to smearing and deformation. Materials that work well for electropolishing include soft austenitic stainless steels, aluminum and aluminum alloys. The primary requirement for electropolishing is that the specimen has to be conductive. Electrolytic polishing essentially dissolves the higher surface energy sites

associated with rough surfaces by smoothing the rough ridges or peaks. This is accomplished by making the specimen surface the anode in an electrolytic cell. The voltage-current density plot represents the mechanism by which electrolytic etching and polishing occurs. In Zone I, the primary mechanism is the direct dissolution of the metal. In this region, etching occurs. Zone II represents the voltage-current density conditions where the metal begins to form a passivation layer. In Zone III, the passivation layer is stable and dissolution of the metal is primarily by diffusion through the passivated layer. In this region, the higher surface area peaks dissolve preferentially to the lower surface area valleys, providing a polishing, or smoothing, effect to the surface. By increasing the voltage into Zone IV, the passivation layer breaks down as the oxygen evolution occurs at the surface. In this zone, the metal will begin to pit.

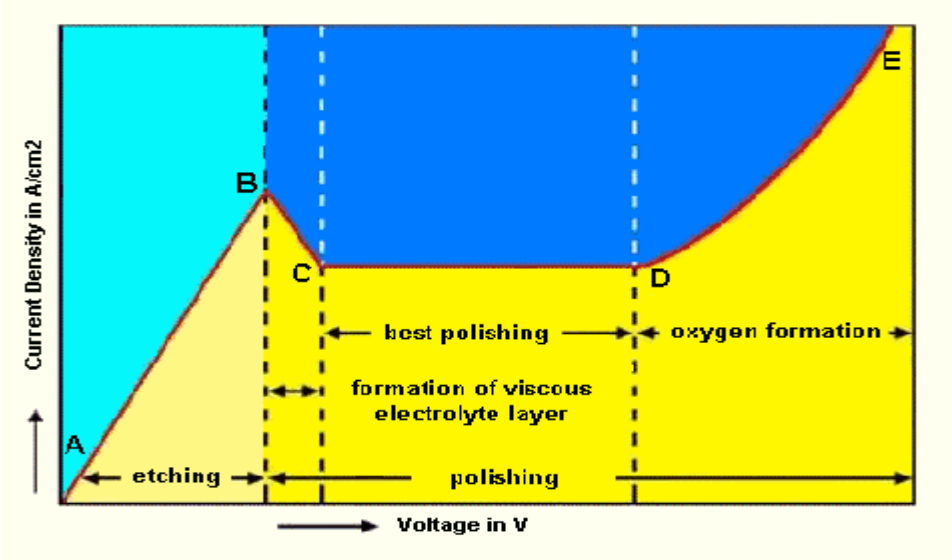

Fig. 18: Relation between current intensuty and voltage in electropolishing [20].

Important variables in the electrolytic polishing are the surface area to be polished, the orientation of sample in bath, the orientation of cathode in bath, choice of cathode in bath, choice of cathode material, the ratio of cathode to anode surface area, the anode to cathode spacing, the depth of sample below solution surface, the composition of sample, including impurities, electrolyte bath age and composition changes, bath temperature, degree of bath agitation, current density and voltage, time, degree of preliminary mechanical treatment. The need to control all these variables can be an obstacle and has reduced the utilization of this kind of polishing. However for laboratories that routinely examine the same materials, once the operating conditions are established, an inexperienced metallographer can be quickly trained and can obtain excellent results.

In developing a suitable procedure for electropolishing a metal or alloy, it is generally helpful to compare the position of the major component of the alloy with elements of the same general group in a periodic table and to study the phase diagram, if avaible, to predict the number of phases and their characteristics. Single-phase alloys generally are easy to electropolish, whereas multiphase alloys are likely to be difficult or impossible to polish with electrolytic techniques. Even minor alloying additions to a metal may significantly affect the response of the metal to polishing in a given electrolyte. The possibility of polishing a metal and the conditions for polishing metal in a given electrolyte can sometimes be ascertained by plotting current density versus electrode potential.

Electrolytes:

Table 3: Formula and use of main electrolytes.

Formula	Use
800 mL ethanol, 140 mL Distilled H2O, 60 mL HClO4	Aluminium and alloys, lead, magnesium, stainless steel
800 mL ethanol, 200 mL HClO4	Stainless steel, aluminium
700 mL ethanol, 120 mL distilled H2O, 100 mL 2-butoxyethanol, 80 mL HClO4	Steel, cast iron, aluminium, titanium, beryllium
175 mL distilled water, 825 mL H3PO4	Pure copper
500 mL diethylene glycol monoethyl ether, 500 mL H3PO4	Steel
500 mL distilled water, 250 mL ethanol, 250 mL H3PO4	Copper and copper-base alloys
625 mL ethanol, 375 mL H3PO4	Magnesium-Zinc
250 mL H2O, 750 mL H2SO4	Stainless steel

Usually, when electropolishing is performed the operator has to set properly the device considering also his skills, for example there could be various problem and the operator has to change the process-parameter until the result is good, for example in *table 4* there are some problems with their solutions.

Table 4: Electropolishing troubles and suggestions.

Trouble	Possible cause	Suggested correction
Pitting	Poloshing too long, voltage too high	Decrease voltage, decrease time, try different electrolyte
Phase in relief	Insufficient polishing film	Increase voltage, use better preparation, decrease time
Unpolished spots (bullseyes)	Gas bubbles	Increase agitation, decrease voltage
Roughness or matte surface	Insufficient or no polishing film	Increase voltage, use more viscous electrolyte
Sludge settling on surface	Insoluble anode product	Try new electrolute, increase temperature, increase voltage
Pitting or etching at edges of specimen	Too viscous or thick film	Decrease voltage, increase agitation, use less viscous electrolyte
Centre of specimen deeply etched	No polishing film at centre of specimen	Increase voltage, decrease agitation, use more viscous electrolyte

4.4 Optical microscope

Optical microscopy is a basic method for structural analysis of materials.

Enlarging a section of the material enable us to study the structure, the latter gives us important information about use of material, mechanical features and corrosion and usury resistance. This device can be used to check how grinding, polishing and etching processes are carried out, furthermore, it gives us information about previous heat treatment of the sample, welds and coatings.

Optical microscope uses optical elements to produce an image of an object. The two most common elements for imaging objects are the converging lens and the concave mirror; lenses are more common in optical microscopes, concave mirrors are used for imaging purposes in reflective telescopes.

Fig. 19: LOM device.

All lenses create a "hot spot" when pointed at the sun. This point is called the *focal point*. The distance from the center of the lens to this focal point is called *focal length*. When reproducing this experiment with different types of converging lenses, one will discover that the focal length mainly depends on the curvature of the lens. In fact, a smaller radius of the curvature results in a shorter focal length. Another fact will be discovered: lenses with a large diameter are more "effective" than those with a smaller one. With this conclusion we have already defined two of the most important benchmark data of a lens: focal length and opening (diameter). The handling of the lens diameter it is generally expressed in relation to the focal length. In the field of microscopy this parameter is called *aperture*. Numerical aperture is defined $NA = n \sin \alpha$, where n is the refractive index of the medium filling the space between the object and the lens, and α is the half-angle of the maximum cone of light that can enter the lens. Pointing the eyes on the focal point is possible then to analyze the sample. Usually optical microscopes have more than one lens, every lens is concerning a particular grade of magnification.

Light from high intensity source is centered and collimated from diaphragms and capacitance and affects on a semi reflecting mirror that diverts the light to the sample's surface through the lens. The light reflected from the surface crosses again the mirror and focus on the lens; is then placed a prism reflector which deflects the light on the ocular lens allowing the enlargement of the sample in exam.

All the structure is supported by a stand which has on his body 2 screws to adjust the magnification.

A defect of optical microscopy is the inability to focus different parts of a sample that lie outside the best focal plane, for this reason, before the analysis, we must polish one side of the sample in order to expose to light a planar part of our sample.

4.5 Scanning electron microscopy

The scanning electron microscope (SEM) uses a focused beam of high energy electrons to generate a variety of signals at the surface of solid specimens. The fundamental principle of SEM sides on the interactions between electron and sample; accelerated electrons carry a significant amount of kinetic energy, this energy is dissipated with the interaction with the solid sample.

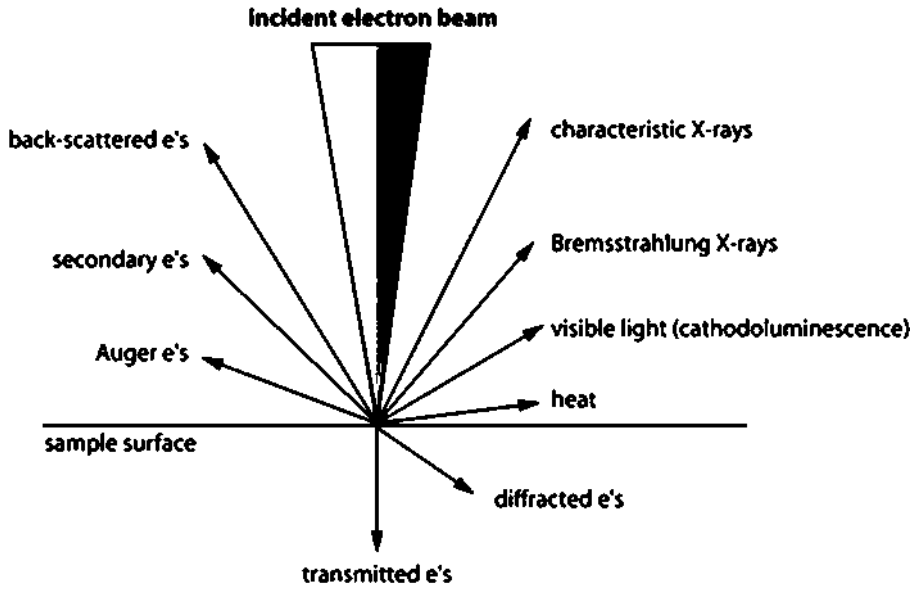

Fig. 20: Interaction between electrons and matter.

When electrons interact with a sample they produce signals, these include secondary electrons, diffracted backscattered electrons, photons, visible light and heat.

- *Back scattered electrons*: Elastic scattering changes the trajectory of the incoming beam electrons when they interact with a target sample without any significant change in their kinetic energy, in this case we can think in terms of a "billiard ball model".

- *Secondary electrons*: Produced by inelastic interactions of high energy electrons with valence electrons of atoms in the specimen which cause the ejection of the electrons from the atoms.

- *Characteristic X-Rays*: Characteristic X-rays are emitted from heavy elements when their electrons make transitions between the lower atomic energy levels.

- *Bremsstrahlung X-Rays*: When electrons are decelerated they give off electromagnetic radiation, and when the energy of the bombarding electrons is high enough, that radiation is in the X-ray region of the electromagnetic spectrum.

- *Auger's electrons*: When a core electron is removed leaving a vacancy, an electron from a higher energy level may fall into the vacancy, resulting in a release of energy; sometimes this energy is released in the form of an emitted photon; energy can also be transmitted to another electron, this electron is called Auger electron.

- *Cathodoluminescence*: Is an optical phenomenon in which electrons impacting a sample cause the emission of photons which may have wavelengths in the visible spectrum.

Secondary electrons and backscattered electrons are commonly used for imaging samples (SE and BSE imaging), indeed secondary electrons are most valuable for showing morphology and topography on samples and backscattered electrons are most valuable for illustrating contrasts in composition in multiphase samples. X-rays are produced by inelastic collisions of the incident electrons with electrons in discrete shells of atoms, when these electrons return in the original state they release X-rays. Scanning electron microscopy is a non-destructive analysis.

Components of SEM device are summarized in figure below

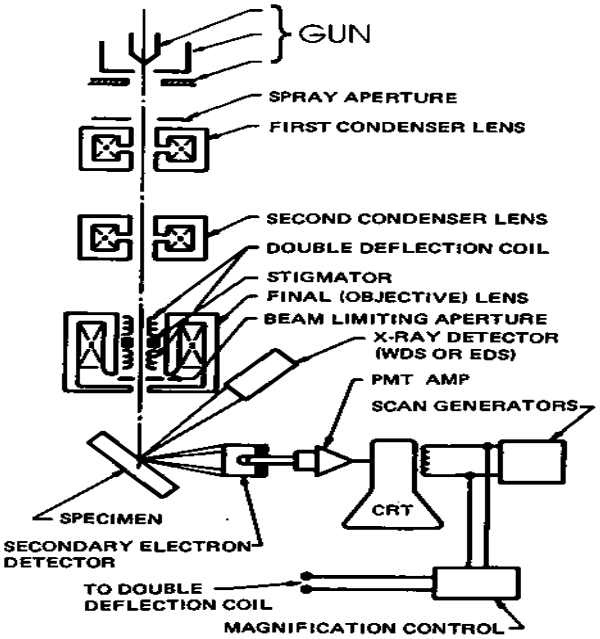

Figure 1.11. Schematic drawing of the electron and x-ray optics of a combined SEM–EPMA.

Fig.21: Schematic drawing of SEM.

Electrons are produced in the "Gun" this electron gun is an electrical component that produces an electron beam that has a precise kinetic energy. And hot cathode emits electrons via thermoionic emission, between the cathode and the anode there is an electric field which focus the beam onto the specimen. Another essential component is the electron lenses and the sample stage. The signals are detected by detectors for all signals that could interest, these signals are sent to output devices. Furthermore there are other important components such as power supply, vacuum system, cooling system, vibration-free floor and a room free of ambient magnetic and electric fields.

As any other analysis device SEM has his own strengths and limitations; most of SEM's are comparatively easy to operate, with user-friendly interfaces, the samples need a minimal preparation (polishing); on the other side samples must be solid and they must fit into the microscope chamber, the maximum size accepted is about 10 cm, vertical dimension 40mm; usually $10^{-5} - 10^{-6}$ vacuum is needed, for this reason samples likely to outgas at low pressure are unsuitable for examination in conventional SEM's.

4.6 EDS

EDS make use of X-Ray spectrum emitted by a solid sample bombarded with a focused beam of electrons to obtain a localized chemical analysis. All elements from atomic number 4 (Be) to 92 (U) can be detected in principle, though not all instruments are equipped for light elements (Z < 10). To explain further, when the sample is bombarded by the electron beam of the SEM, electrons are ejected from the atoms on the specimen's surface. A resulting electron vacancy is filled by an electron from a higher shell, and an X-ray is emitted to balance the energy difference between the two electrons. The EDS X-ray detector measures the number of emitted X-rays versus their energy to produce the EDS spectrum. Qualitative analysis involves the identification of the lines in the spectrum and is fairly straightforward owing to the simplicity of X-ray spectra. Quantitative analysis (determination of the concentrations of the elements present) entails measuring line intensities for each element in the sample and for the same elements in calibration standards of known composition.

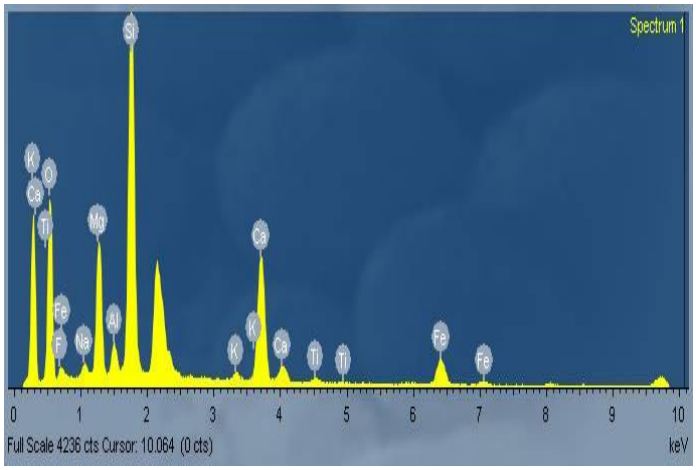

Fig.22: EDS output.

X-ray intensities are measured by counting photons and the precision obtainable is limited by statistical error. For major elements it is usually not difficult to obtain a precision (defined as 2 σ) of better than ± 1% (relative), but the overall analytical accuracy is commonly nearer ± 2%, owing to other factors such as uncertainties in the compositions of the standards and errors in the various corrections which need to be applied to the raw data.

Modern SEM-EDS instruments are operated using sophisticated software. These software programs allow unattended feature analysis and "mapping" of the composition of the elements on the specimen's surface.

5 MATERIALS PRESENTATION

SKB has provided 2 samples internally designated FSW90/139 and FSW08/155; these samples are extracted at position 139° and 155° from a circle friction stir weld between the lid and the tube.

Fig. 23: Segment of lid and but welded together

For simplicity FSW08 will be recognized as Weld 1, FSW90 as Weld 2. Weld 1 was conducted in air, Weld 2 under Argon as shielding gas, both samples are extracted from a steady state welding condition.

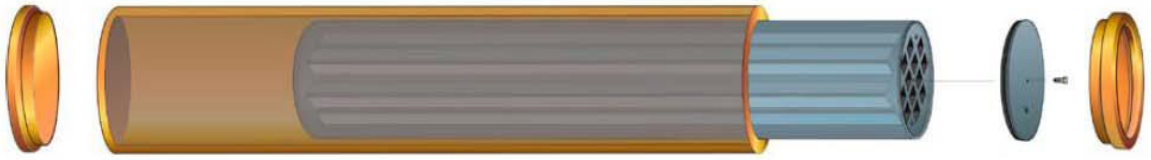

Fig. 24: Scheme of the canister [21].

After an initial visual analysis the welded zone has been disclosed, as pointed out before, in the welded zone the grains are different from the grains in base material, the samples have been ground with grinding paper with increasing P grade number, starting with 80 and ending with 1200, after grinding the samples have been chemically etched in order to underline the welded zone.

Fig. 25: Friction stir welded join cross section after grinding.

The aim of the thesis is to check the oxygen content in the welded zone, so after a first visual analysis, samples have been divided into smaller samples to facilitate further analysis. 5 squares of equal area have been drawn in each sample and then using as cutting tool an hacksaw they were separated from the main samples.

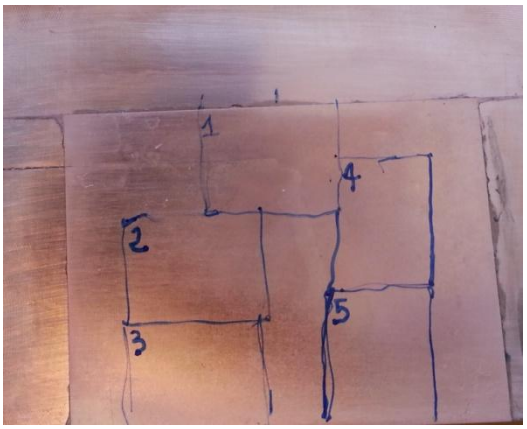

Fig. 26: Division of the joint into 5 specimens.

Each sample was numbered from 1 to 5 in weld 1 and from 6 to 10 in weld 2.

6 EXPERIMENTAL PART

Before SEM and EDS analysis, in order to provide an high quality of results, sample 2, as reference, has been ground and polished with different methods:

- Grinding + 3μm diamond paste polishing + chemical etching.
- Grinding + 1μm diamond paste polishing + chemical etching.
- Grinding + oxides polishing + chemical etching.
- Grinding + electrolytical polishing + electrolytical etching.

Grinding:

Grinding was the starting step for each of the 4 methods, the sample was ground using different rotating abrasive disks with increasing P grade number, starting from 80 continuing with 320 and 600 and ending with 1200, the sample was kept in every step for about 2 minutes, turning it of 90 degrees every 20-30 seconds, each step was performed with fluent water on the disk and before changing abrasive disk the flatness of the sample was carefully checked, between every step the sample was washed with water.

Mechanical Polishing:

After grinding, sample 2 has been polished with diamond paste of 3 micron and 1 micron size respectively, the final surface should be mirror-like with no scratches, since the diamond paste is dry the sample, during polishing, was often lubricated, after this step the sample was carefully washed with water and ethanol and dried, the process took several minutes, since copper is a soft material compared to other metals, in order to avoid unexpected scratches the polishing drapes have to be carefully washed with fluent water to remove metallic residuals.

Chemical and electrolytical etching:

Oxides Cu_2O are generally located at the grain boundaries, so in order to find them easily, an etching treatment has been performed, after this, sample 2 has been analyzed with SEM/EDS/LOM. Etching can be chemical or electrolytical, after mechanical polishing the sample was chemically etched, the composition of the etching solution changes with the

purpose of the analysis, in our case etching has to show grain boundaries and grain areas then the composition was:

Table 5: Composition of the chemical etching solution

Quantity [ml]	Chemical
25	Distilled water
25	Ammonia water
5 - 25	Hydrogen peroxide 3%

When the interest of the process is to show grain boundaries less hydrogen peroxide has to be added.

Electrolytic polishing and etching:

Electrolytic polishing was performed first to sample 2 that had been previously re-ground with grinding paper of decreasing grain size.

This process, according with Rui Wu, was performed using as electrolyte 125ml of 85% H_3PO_4 and 125ml of distilled water, as cathode a specimen of stainless steel was used; copper and stainless steel samples were connected to a voltage generator through 2 terminals and 2 cables.

Mixing together in the solution distilled water and phosphoric acid the following reactions took place:

$$H_3PO_4 + H_2O \rightarrow H_3O^+ + H_2PO_4^- \quad (8)$$

$$H_2PO_4^- + H_2O \rightarrow H_3O^+ + HPO_4^{2-} \quad (9)$$

$$HPO_4^{2-} + H_2O \rightarrow H_3O^+ + PO_4^{3-} \quad (10)$$

Since the reaction is exothermic we put carefully phosphoric acid in water rather than water in acid.

In order to analyze the process and point out the correct parameters, a trial session has been carried out on a spare specimen of copper. After some iteration the following process parameters have been found out.

Table 6: Electrolytical polishing and etching parameters

	Time	Temperature (°C)	Voltage (Volt)	Current (A)
Etching	10-20 s	25	2	0,8
Polishing	2-4 min	25	3-6	2-3

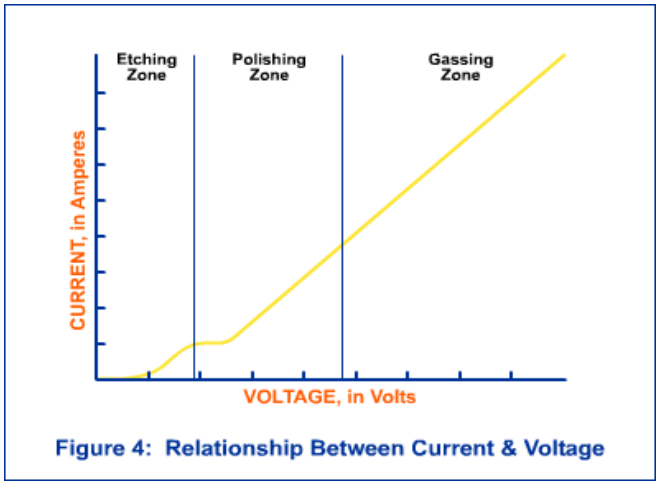

Fig. 27: Relation between current and voltage.

Parameters are strongly dependent on the shape of the sample, indeed, after some trials was discovered that decreasing the size of the sample it's worth to decrease the polishing voltage, in fact the situation tends to be unstable at higher voltage values. Other important parameters are the conditions of the electrolytic bath and the distance between anode and cathode. In order to obtain an even surface attention must be paid on the voltage, indeed if the latter is higher than 6 Volt the sample undergoes pitting corrosion, this case is very disadvantageous firstly because the surface is no longer even, secondly because, in order to restore the surface, another grinding process has to be carried out. The voltage range proposed in *table* is suitable for a variety of shapes and dimensions, for this reason is 3V wide; considering the sample cut from the cross section joint:

Fig. 28: Sample 1 after electrolytical polishing and etching.

The value of voltage which better suited our needs was about 4V, a voltage higher than 4V made the process unstable leading to the formation of bubbles, besides this, the bigger was the sample the higher was the current intensity at the same voltage value. As pointed out before in order to gain good surfaces in which it's possible to distinguish inclusions, it was mandatory to avoid bubbles on the sample surface, and the voltage must be high enough to avoid the passivation of the sample. During the process stirring conditions were mandatory. As seen in *figure 28*, due to the current flow the surface of the sample is not completely even in the surface portion where the terminals were attached, in order to limit this problem (even if partially), was recommended to operate with the terminals below the electrolyte's level, though terminals were subjected to a stronger and faster oxidation.

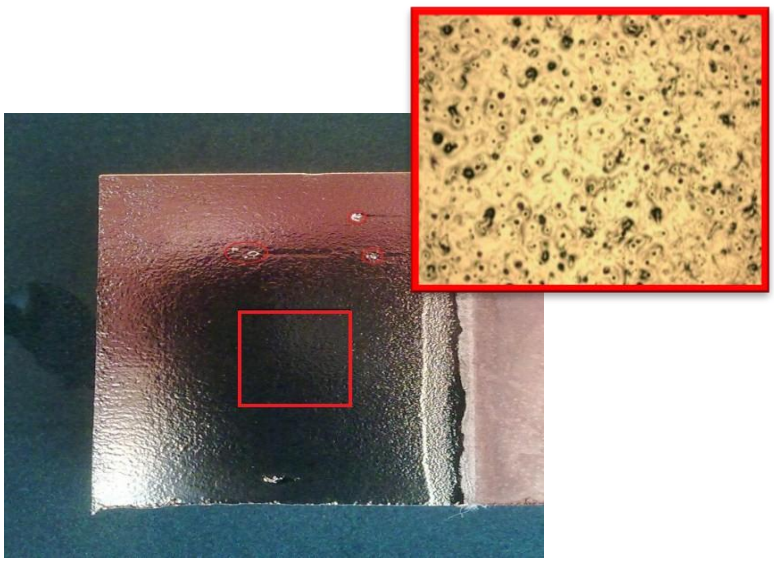

Fig.29: Example of pitting.

Electro-polishing is a polishing method that is strongly dependent on the operator's skills, for this reason in order to get an even surface, localized oxidation must be avoided, in particular the region of the cable's terminals was subjected to an uneven oxidation:

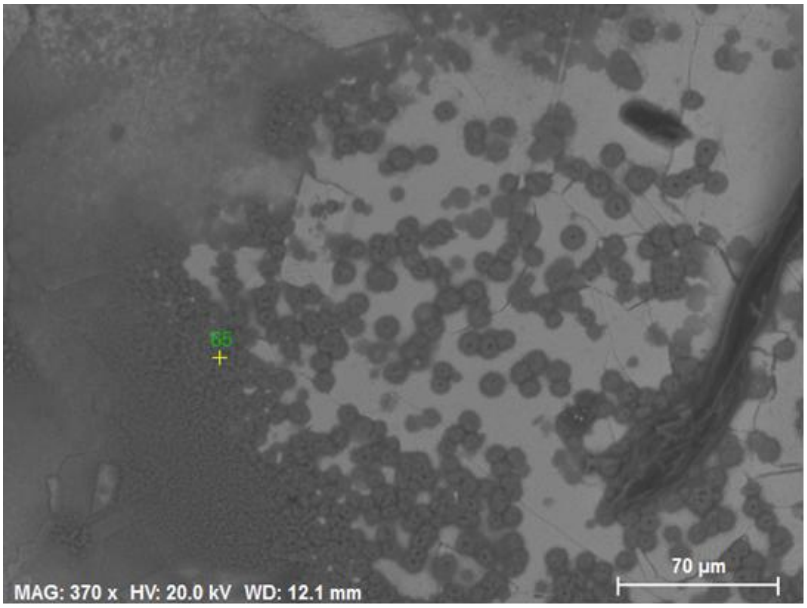

Fig. 30: Oxidation caused by electrolytical polishing.

Spectrum: 65

Element	Series	norm. C [wt.%]	Atom. C [at.%]
Oxygen	K-series	41.54	66.90
Phosphorus	K-series	22.03	18.33
Copper	K-series	36.43	14.77
	Total:	100.00	100.00

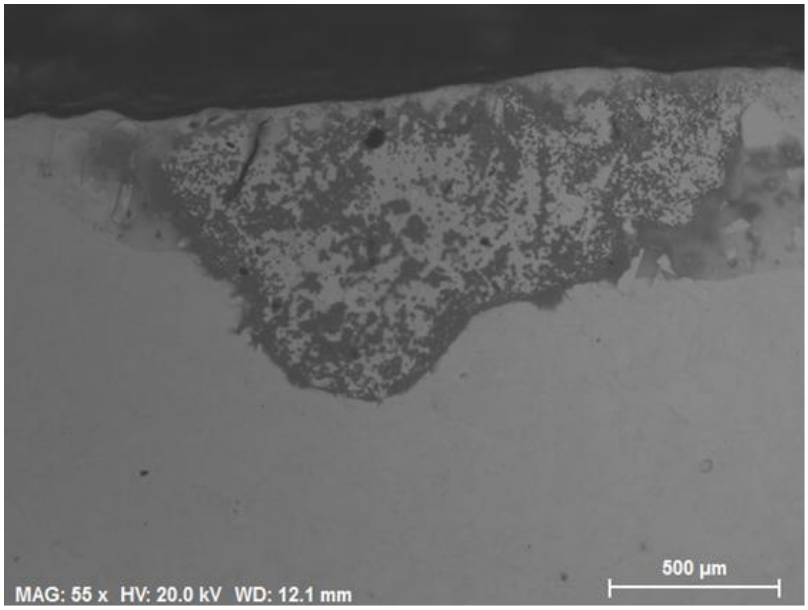

Fig. 31: Oxidation caused by electrolytical polishing.

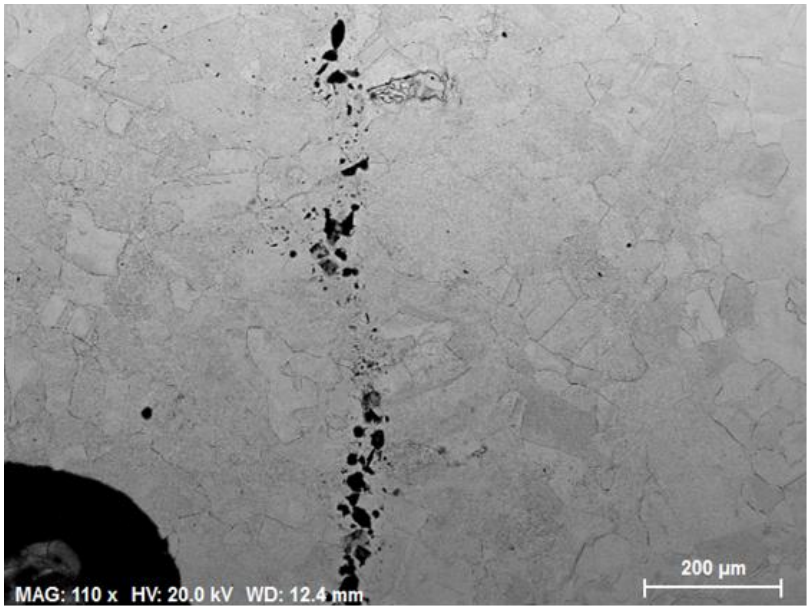

Fig. 32: Oxidation caused by electrolytical polishing.

Fig.34: Electrolytic bath with copper residuals

Another important parameter that can affect the result is the dimension and shape of the stainless steel cathode, in this case we used a stainless steel sample 2x3cm. While the

Fig. 33: Stainless steel cathode covered in copper

copper sample was polishing the cathode was covered in copper residuals, same thing for the cathode terminal. During the process the electrolytic solution tended to stain of blu, this because of the Cu^{2+} ions dissolved from the anode, so it was necessary to restore the electrolyte several time as it tended to fill with copper residuals. Etching is very important since allows to underline the grain boundaries, this process shouldn't exceed 10-15 s to avoid overetching, an overetched surface can make difficult the identification of oxides inclusions since the boundary appears thicker.

Oxides polishing and chemical etching:

This method is generally softer than diamond polishing and it was performed using also chemicals, in this method 96 ml of Silicon Dioxide colloidal particles have been mixed with 2 ml of ammonia water (25%) and 2ml of hydrogen peroxide (3%), since commercial hydrogen peroxide is in the concentration 30%, stoichiometric calculations have been made to gain the exact concentration. With this suspension polishing took around 1-2 minutes. Chemical etching, as pointed out before, was performed with 25 ml of distilled water, 25 ml of ammonia water and 5-25 ml of hydrogen peroxide 3%, the total amount of hydrogen peroxide depends on the purpose of our etching, in our case since the task of our process was to reveal grain boundaries, a solution with less hydrogen peroxide has been prepared. The sample was put in a becker with inside the cited solution, after some seconds the solution tended to color in dark blue, after several minutes the sample was removed from the becker, dried and analyzed in the LOM. It is noted that this method of etching is softer than electrolytic etching and it is easier to control, another difference between the 2 etching method is in the color of the etching solution and of the electrolyte, the first is darker and the second is brighter.

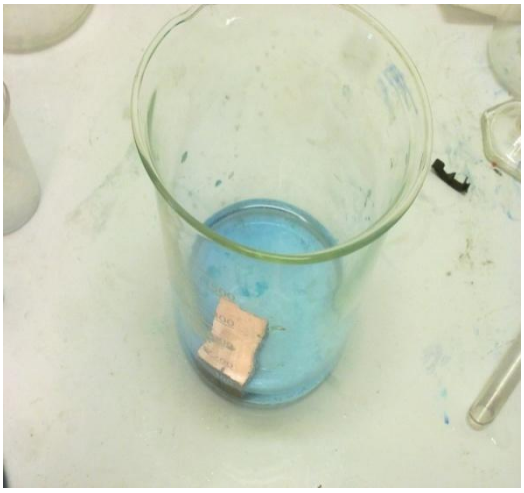

Fig. 35: Chemical etching.

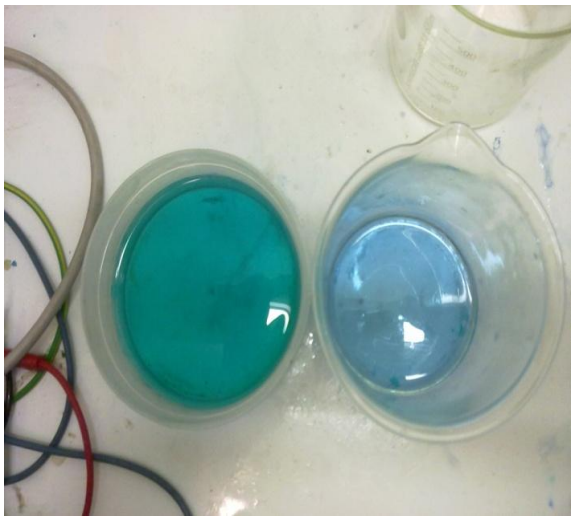

Fig.36: Comparison between electrolytic bath and etching solution

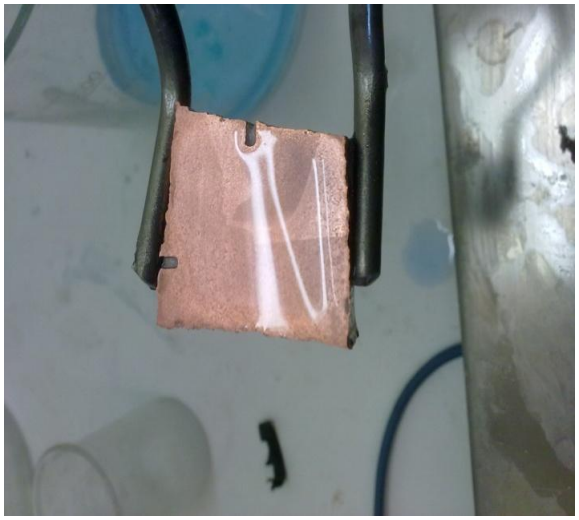

Fig.37: Sample after chemical etching

7 RESULTS AND DISCUSSION

7.1 Average grain size

In order to give a wider point of view of the joint, a general analysis of the weld is given here. Using light optical microscope it is possible to underline the main feature of the sample; for example *figure 38* and *39* focus on the Slit and on the Joint Line Hooking, the latter is a discontinuity that usually follow the slit. In both figures it is clear how the grains in the upper part of the images are bigger since the grain size in the friction stir welded zone and in the lid differs apparently.

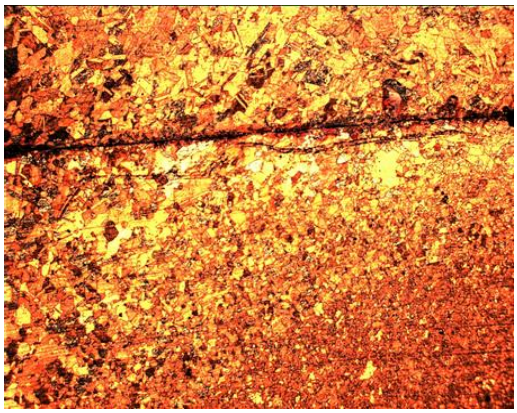

Fig. 38: Slit 25X

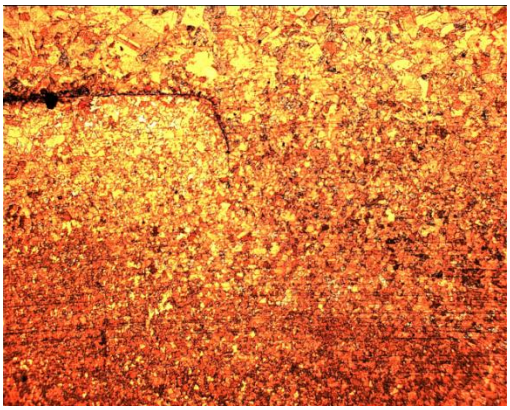

Fig.39: Joint Line Hooking 25X

The joint can be divided into 3 parts: base material, heat affected zone and friction zone. Each part was subjected to different mechanical and thermal stresses, for this reason they present a different microstructure. Just after etching it is possible to see how the average grain size is different, these differences have been pointed out using light optical microscope.

Fig.40: LOM image, base material 100X Weld 1

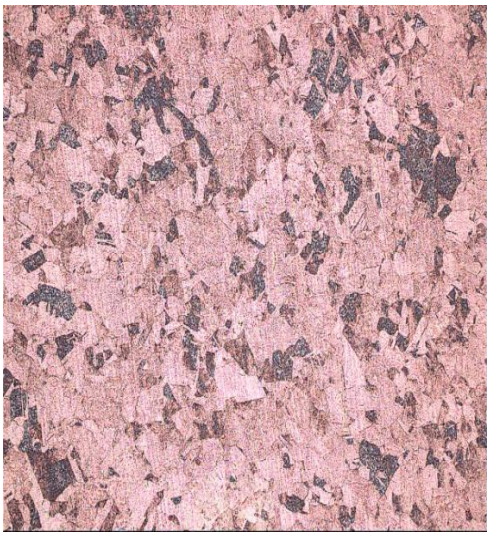

Fig. 41: LOM image, heat affected zone 100X Weld 1

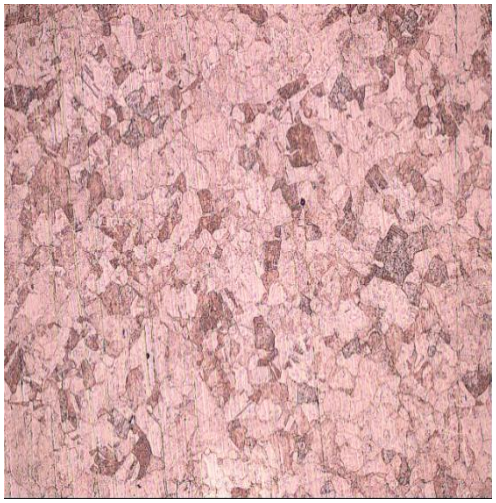

Fig. 42: LOM image, friction zone 100X Weld 1

Fig. 43: LOM image, base material 100X Weld2

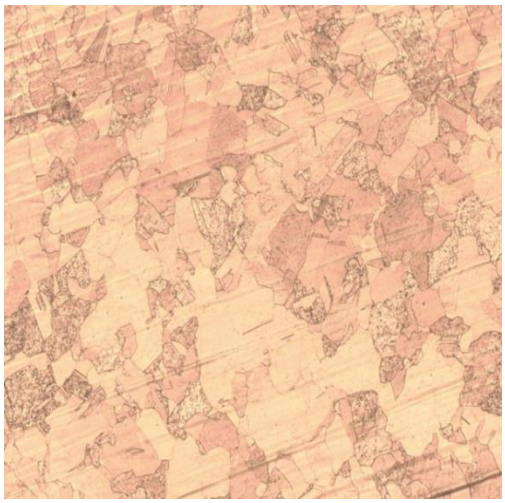

Fig. 44: LOM image, heat affected zone, 100X Weld 2

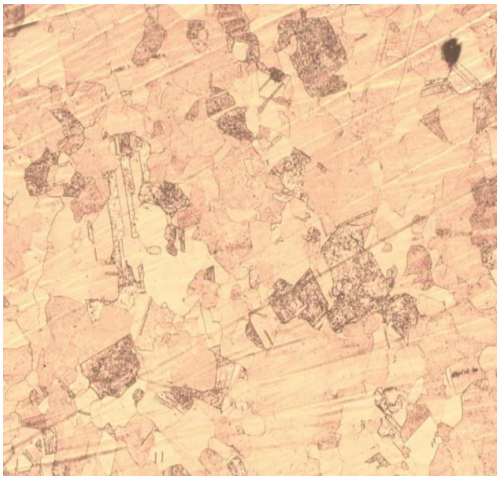

Fig. 45: LOM image, friction zone, 100X Weld 2

Different pictures have been taken at different position in the weld, then the average grain size was calculated using ASTM method; this method is based on the following equation:

$$N = 2^{n-1} \qquad (11)$$

Where N is the number of grains in the circle of square area $1in^2$ when the sample is examined at 100 power micrograph, in this calculation are included also grains intercepted by the circumference, in this case this number figure in the calculation but divided by 2; n is the ASTM number.

In order to obtain, after the count of the grains inside the circle and cut by the circumference, the ASTM number, the previous equation has to change in this way:

$$n = \frac{lnN}{ln2} + 1 \qquad (12)$$

The results obtained are listed in *table 8,* the average size of grains among the 2 samples is almost the same among base material, heat affected zone and friction zone, and as was expected grains are bigger in the base material followed by heat affected zone and friction zone.

The ASTM number is linked to the average grain size:

Table 7: Relation between average grain size and ASTM number

ASTM number	Average grain diameter [mm]
-3	1
-2	0,75
-1	0,5
0	0,35
1	0,25
2	0,18
3	0,125
4	0,091
5	0,062
6	0,044
7	0,032
8	0,022
9	0,016
10	0,011
11	0,008
12	0,00096

Using *equation 12* the average grain size dimension has been calculated for the joints:

Table 8: Average grain size in BM, HAZ, FZ, Weld 1 and 2

	BM	HAZ	FZ
Weld 1	120µm	80µm	55µm
Weld 2	119µm	85µm	62µm

7.2 SEM/EDS results

As mentioned at the beginning of chapter 6, sample 2 has been taken as reference to understand which polishing method is suitable for the whole analysis. In the following sections different polishing methods are presented and compared in the results they provided.

Grinding + Mechanical polishing with 3µm diamond paste

This kind of mechanical polishing has shown an inefficient outcome since the surface of the sample presented several parallel scratches and the analysis with SEM was literally impossible. For this reason, no results are presented for this method.

7.2.1 Grinding + Mechanical polishing with 3µm and 1µm diamond paste + chemical etching

After this method of grinding and polishing, sample 2 presented several oxides, as in is seen in *figure 46,47,48* and *49* they were in the form of single spots usually at grain boundaries, no oxide strings are documented. The average size of these spots is 3,98µm, their average oxygen content and total area fraction is respectively 41,5%at and 4,7E-06, these particles are composed mainly by copper, oxygen, silicon and aluminium; a small number of inclusion present also in small traces sulfur, magnesium, potassium, sodium, nitrogen, iron, calcium, zinc and phosphorous.

Table 9: Average chemical composition of inclusions after mechanical polishing and chemical etching.

Oxygen (%at)	Aluminium (%at)	Silicon (%at)
41,5	8,5	8

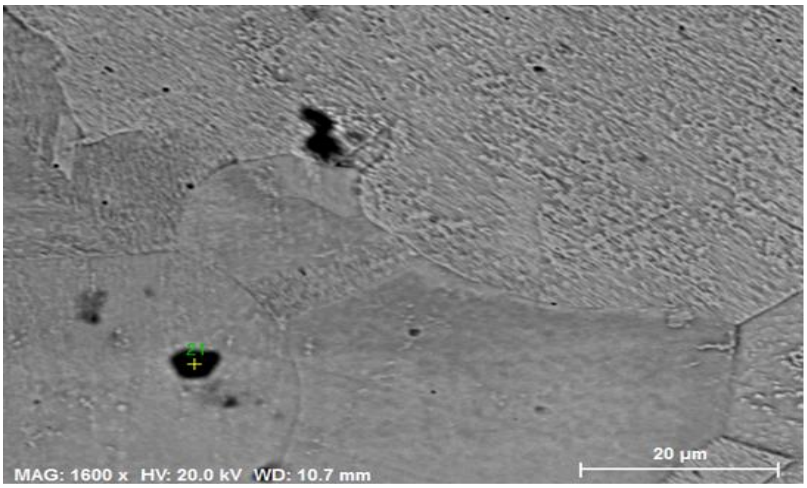

Fig. 46: Inclusions after mechanical polishing and chemical etching.

Spectrum: 21

Element	Series	norm. C [wt.%]	Atom. C [at.%]
Oxygen	K-series	25.40	51.85
Aluminium	K-series	8.21	9.93
Silicon	K-series	6.33	7.36
Copper	K-series	60.06	30.86
	Total:	100.00	100.00

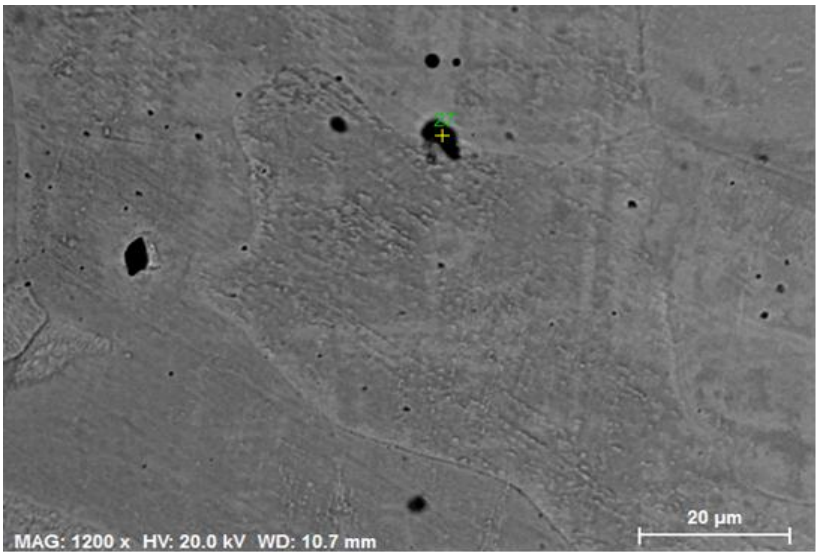

Fig. 47: Inclusions after mechanical polishing and chemical etching.

Spectrum: 27

Element	Series	norm. C [wt.%]	Atom. C [at.%]
Oxygen	K-series	18.16	43.13
Aluminium	K-series	5.63	7.93
Silicon	K-series	4.47	6.04
Copper	K-series	71.75	42.90
	Total:	100.00	100.00

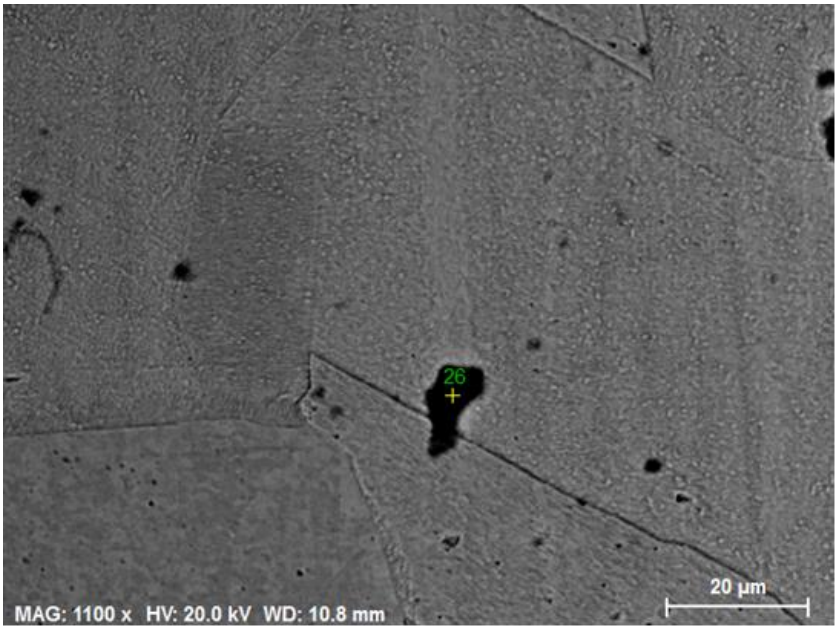

Fig. 48: Inclusions after mechanical polishing and chemical etching.

Spectrum: 26

Element	Series	norm. C [wt.%]	Atom. C [at.%]
Oxygen	K-series	33.55	57.00
Aluminium	K-series	14.18	14.29
Silicon	K-series	11.76	11.38
Copper	K-series	40.51	17.33
Total:		100.00	100.00

As shown in *figure 49*, there are also several particles with high content of carbon, these particles are probably dirt, coming from the polishing process, these particles are often bigger than the oxides inclusions.

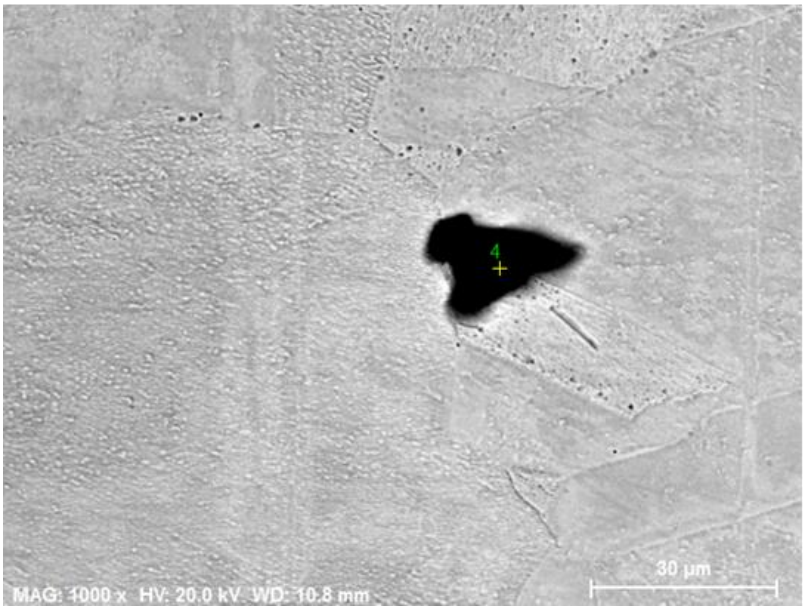

Fig. 49: Dirt inclusion after mechanical polishing and chemical etching.

Spectrum: 4

Element	Series	norm. C [wt.%]	Atom. C [at.%]
Carbon	K-series	51.49	72.23
Nitrogen	K-series	6.88	8.27
Oxygen	K-series	10.19	10.72
Aluminium	K-series	0.08	0.05
Silicon	K-series	0.10	0.06
Sulfur	K-series	0.19	0.10
Chlorine	K-series	0.67	0.32
Potassium	K-series	0.87	0.38
Calcium	K-series	0.28	0.12
Copper	K-series	29.25	7.76
	Total:	100.00	100.00

7.2.2 Grinding + oxides polishing + chemical etching

This method was suggested by Struers, as presented in *figure 50,51,52* and *53*, with this methods some oxide strings are disclosed, their average oxygen content is 37,8%at and their average size is 1,44µm. Considering all oxide strings, their area fraction is 2,66E-07, furthermore inclusions presented an average silicon content of 12,80 %at. Few inclusions presented traces of phosphorous, sulfur, aluminum and calcium.

Fig. 50: Inclusions after oxides polishing and chemical etching.

Spectrum: 149

Element	Series	norm. C [wt.%]	Atom. C [at.%]
Oxygen	K-series	20.27	45.53
Silicon	K-series	13.16	16.83
Copper	K-series	66.57	37.64
	Total:	100.00	100.00

Spectrum: 148

Element	Series	norm. C [wt.%]	Atom. C [at.%]
Oxygen	K-series	30.17	55.61
Silicon	K-series	20.44	21.47
Copper	K-series	49.39	22.92
	Total:	100.00	100.00

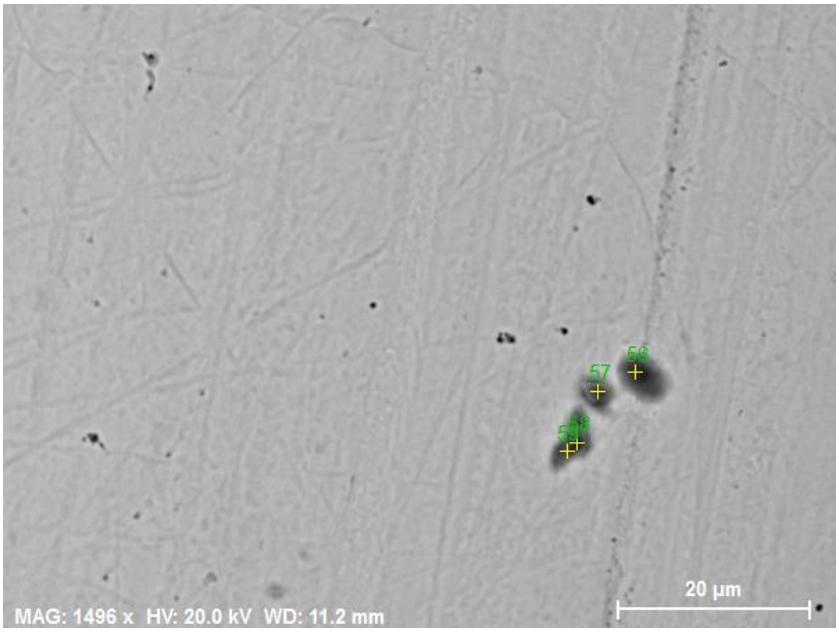

Fig. 51: Inclusions after oxides polishing and chemical etching.

Spectrum: 59

Element	Series	norm. C [wt.%]	Atom. C [at.%]
Oxygen	K-series	22.41	49.83
Calcium	K-series	20.55	18.24
Copper	K-series	57.04	31.93
	Total:	100.00	100.00

Spectrum: 58

Element	Series	norm. C [wt.%]	Atom. C [at.%]
Oxygen	K-series	16.84	41.31
Calcium	K-series	20.23	19.81
Copper	K-series	62.93	38.87
	Total:	100.00	100.00

Spectrum: 57

Element	Series	norm. C [wt.%]	Atom. C [at.%]
Oxygen	K-series	40.69	68.84
Calcium	K-series	23.68	15.99
Copper	K-series	35.63	15.17
	Total:	100.00	100.00

Spectrum: 56

Element	Series	norm. C [wt.%]	Atom. C [at.%]
Oxygen	K-series	22.66	48.45
Silicon	K-series	13.40	16.32
Phosphorus	K-series	1.44	1.59
Copper	K-series	62.50	33.64
Total:		100.00	100.00

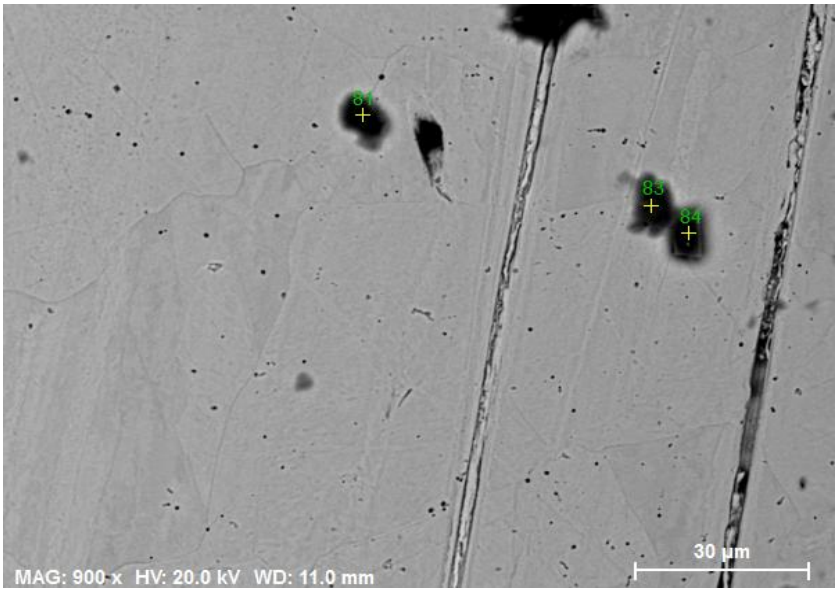

Fig. 52: Inclusions after oxides polishing and chemical etching.

Spectrum: 84

Element	Series	norm. C [wt.%]	Atom. C [at.%]
Oxygen	K-series	43.14	63.68
Silicon	K-series	32.39	27.23
Copper	K-series	24.47	9.09
Total:		100.00	100.00

Spectrum: 83

Element	Series	norm. C [wt.%]	Atom. C [at.%]
Oxygen	K-series	25.83	51.59
Silicon	K-series	17.50	19.92
Copper	K-series	56.67	28.50
Total:		100.00	100.00

Spectrum: 81

Element	Series	norm. C [wt.%]	Atom. C [at.%]
Oxygen	K-series	34.24	59.17
Silicon	K-series	22.26	21.91
Copper	K-series	43.50	18.92
	Total:	100.00	100.00

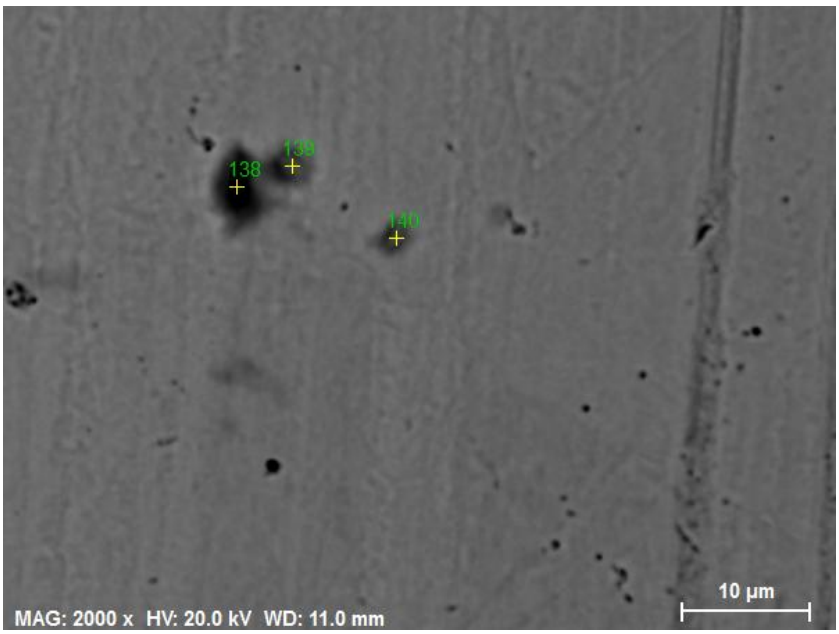

Fig. 53: Inclusions after oxides polishing and chemical etching.

Spectrum: 140

Element	Series	norm. C [wt.%]	Atom. C [at.%]
Oxygen	K-series	18.07	43.48
Silicon	K-series	9.03	12.37
Copper	K-series	72.90	44.15
	Total:	100.00	100.00

Spectrum: 139

Element	Series	norm. C [wt.%]	Atom. C [at.%]
Oxygen	K-series	24.66	52.43
Silicon	K-series	10.72	12.98
Copper	K-series	64.63	34.59
	Total:	100.00	100.00

Spectrum: 138

Element	Series	norm. C [wt.%]	Atom. C [at.%]
Oxygen	K-series	24.89	50.62
Silicon	K-series	16.86	19.54
Copper	K-series	58.25	29.84
	Total:	100.00	100.00

7.2.3 Grinding + electrolytical polishing and etching

The procedure described in chapter 4 has been followed for the analysis of sample 2, the results obtained are presented in *figure 54,55,56* and *57* and they are quite similar to the previous methods, strings are usually located at grain boundary, their average oxygen content is 29,5 %at, their average size is 1,37µm; almost every inclusion in sample 2 is characterized the constant presence of phosphorous coming from the electrolyte , also in this case small traces of sulfur, aluminum and calcium have been detected. Oxides area fraction is 2,7E-07.

Fig. 54: Inclusions after electrolytic polishing and etching

Spectrum: 27

Element	Series	norm. C [wt.%]	Atom. C [at.%]
Oxygen	K-series	1.30	4.97
Copper	K-series	98.70	95.03
Total:		100.00	100.00

Spectrum: 28

Element	Series	norm. C [wt.%]	Atom. C [at.%]
Oxygen	K-series	3.33	12.04
Copper	K-series	96.67	87.96
Total:		100.00	100.00

Spectrum: 29

Element	Series	norm. C [wt.%]	Atom. C [at.%]
Oxygen	K-series	6.37	21.26
Copper	K-series	93.63	78.74
Total:		100.00	100.00

Spectrum: 30

Element	Series	norm. C [wt.%]	Atom. C [at.%]
Oxygen	K-series	8.00	25.67
Copper	K-series	92.00	74.33
Total:		100.00	100.00

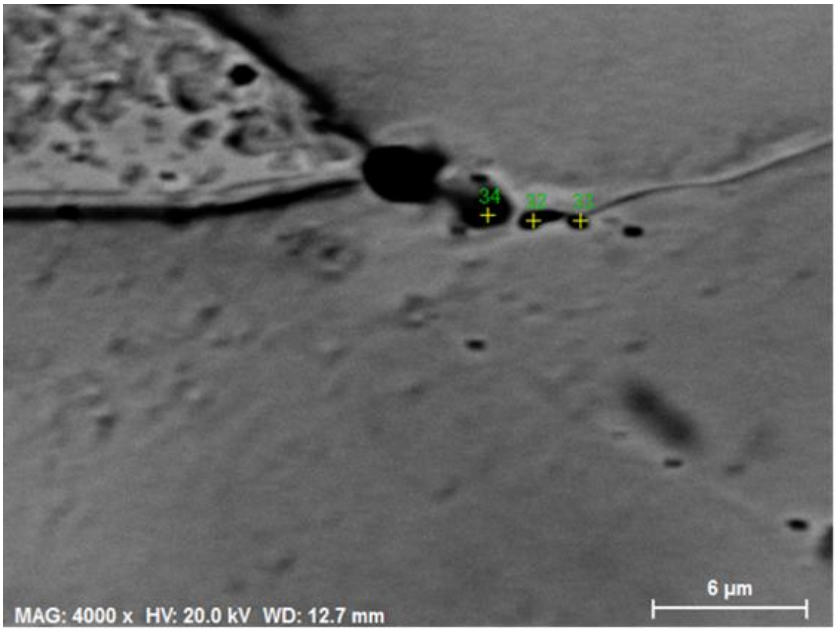

Fig. 55: Inclusions after electrolytic polishing and etching.

Spectrum: 32

Element	Series	norm. C [wt.%]	Atom. C [at.%]
Oxygen	K-series	3.13	11.39
Copper	K-series	96.87	88.61
Total:		100.00	100.00

Spectrum: 33

Element	Series	norm. C [wt.%]	Atom. C [at.%]
Oxygen	K-series	2.06	7.70
Copper	K-series	97.94	92.30
Total:		100.00	100.00

Spectrum: 34

Element	Series	norm. C [wt.%]	Atom. C [at.%]
Oxygen	K-series	10.89	32.67
Copper	K-series	89.11	67.33
Total:		100.00	100.00

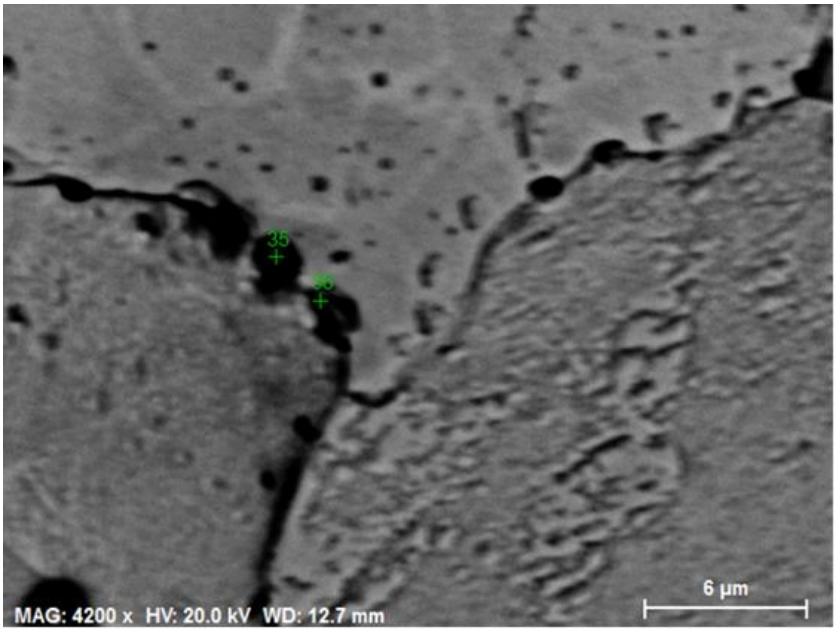

Fig. 56: Inclusions after electrolytic polishing and etching.

Spectrum: 35

Element	Series	norm. C [wt.%]	Atom. C [at.%]
Oxygen	K-series	3.16	11.48
Copper	K-series	96.84	88.52
Total:		100.00	100.00

Spectrum: 36

Element	Series	norm. C [wt.%]	Atom. C [at.%]
Oxygen	K-series	6.27	20.99
Copper	K-series	93.73	79.01
Total:		100.00	100.00

Fig. 57: Inclusions after electrolytical polishing and etching.

Spectrum: 47

Element	Series	norm. C [wt.%]	Atom. C [at.%]
Oxygen	K-series	4.51	15.81
Copper	K-series	95.49	84.19
Total:		100.00	100.00

Spectrum: 48

Element	Series	norm. C [wt.%]	Atom. C [at.%]
Oxygen	K-series	9.56	29.57
Copper	K-series	90.44	70.43
Total:		100.00	100.00

Spectrum: 49

Element	Series	norm. C [wt.%]	Atom. C [at.%]
Oxygen	K-series	8.47	26.87
Copper	K-series	91.53	73.13
Total:		100.00	100.00

7.3 Comparison between polishing methods

At this point, after all these analysis, an efficient polishing method has to be chosen in order to gain good results extending the analysis also to all the samples. First of all, 3µm diamond paste polishing has to be avoided since it doesn't provide an even surface. It's possible to compare the results obtained after electrolytic polishing, oxides polishing and 1 micron diamond polishing among average size, average oxygen content and specific area.

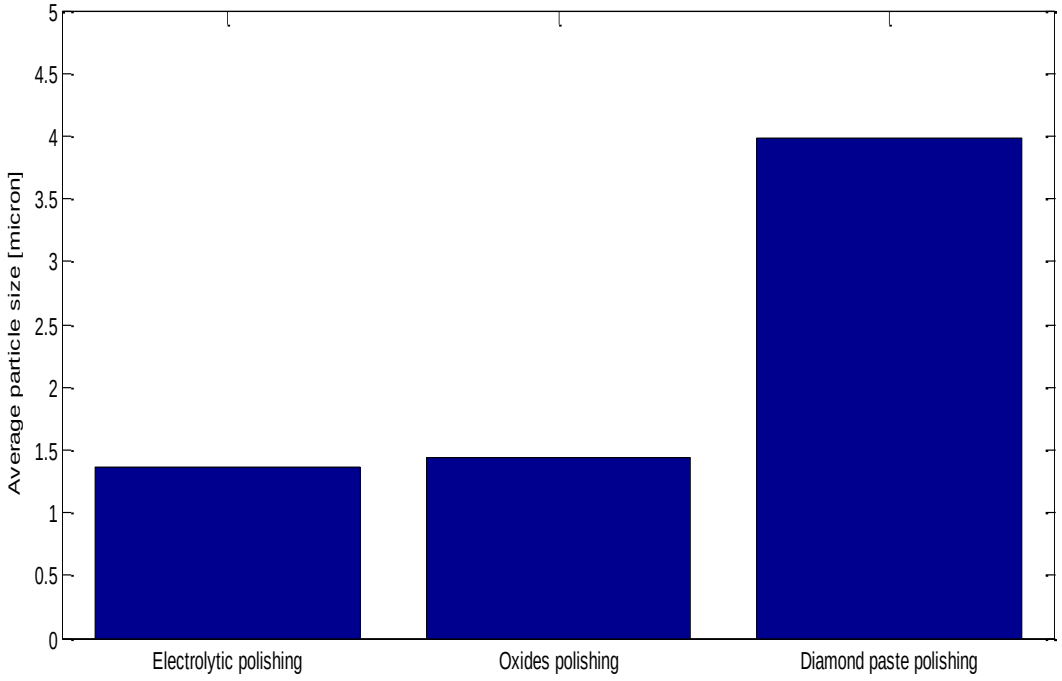

Fig.58: Relation between average particle size among different polishing methods.

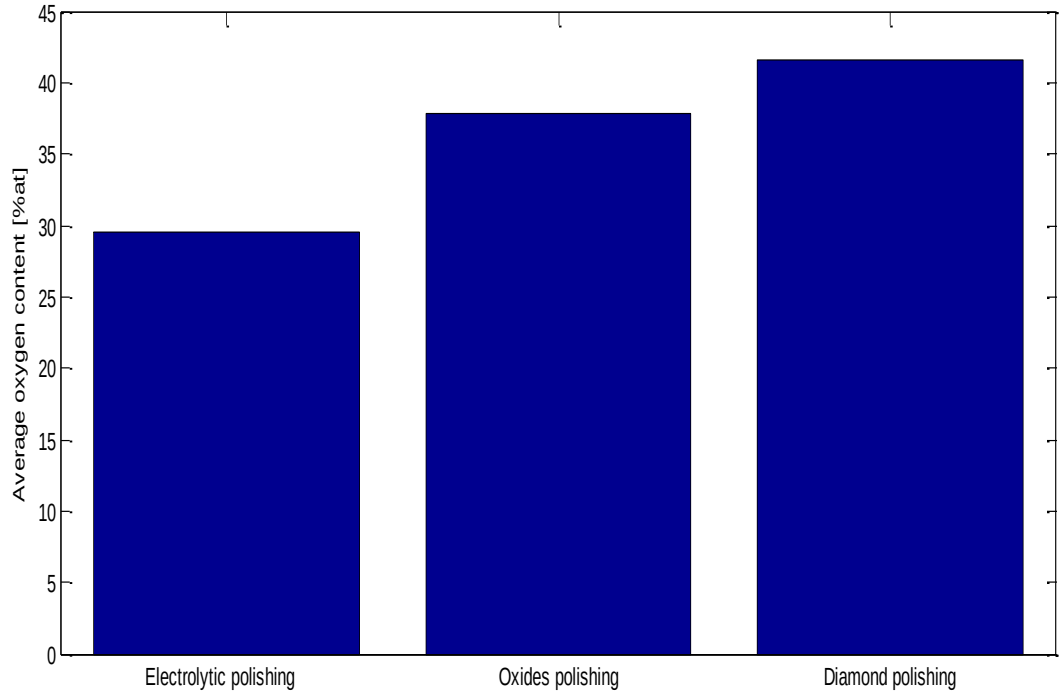

Fig. 59: relation between oxygen content among different polishing methods.

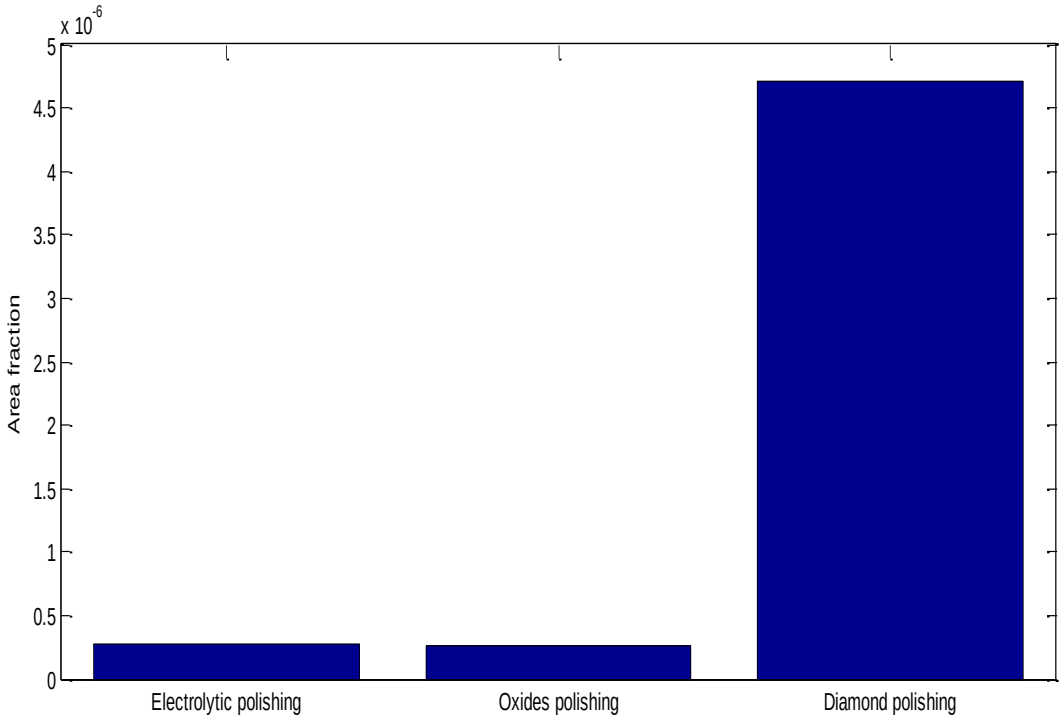

Fig. 60: Relation between area fraction among different polishing methods.

From graphs in *figure 58,59* and *60* it is clear that inclusion showed up after diamond polishing are bigger by 176% if compared to oxides polishing, 190% if compared to

electrolytic polishing, with an higher oxygen content respectively by 9% and 40%, as a consequence they have an higher area fraction by 17% and 16%, the main difference between diamond polishing and the other polishing method is that in the surface analysed after diamond polishing no strings where detected but only isolated inclusions with a bigger size and higher oxygen content; since our analysis is focused on the presence of oxide strings, being them much more interesting, this method has to be set aside. Considering now electrolytic polishing and oxides polishing, they present similar average inclusion size and area fraction, considering the average oxygen content, oxides polishing shows up an higher oxygen content (37,8%at) this difference is probably due to the polishing suspension which is composed by SiO_2; these two polishing methods present then similar results, for this reason the other samples have been analysed after grinding+electrolytical polishing and etching.

7.4 Analysis and discussion

Weld 1:

Weld 1 presents the higher oxides area fraction between the two welds, the welding process was performed in air atmosphere; sample 4 and 5 belong to the retreating side, sample 2 and 3 belong to the advancing side. As expected the oxides content is not the same in the weld. Oxides distribution is not even, more oxide strings are found closer to the edge of the weld and their concentration decreases getting further from the latter, in the retreating side higher oxide strings concentration is found on the right boundary of the weld, this inhomogeneity is not detected in the advancing side. Oxide strings concentration decreases until the slit region in sample 1, where a number of strings is detected following all the slit until the Joint Line Hooking. As a result, oxides area fraction is higher in sample 5 (2,36E-06) and decreases in sample 4 (1,56E-06) by 33%, similarly, in the advancing side, oxides area fraction is higher in sample 3 (3,37E-07) and decreases in sample 2 (2,71E-07) even if this decreasing is lower if compared to the retreating side (18%), oxides area fraction in the advancing side is lower by 84% if compared to the retreating side. Together with oxide strings concentration, also oxides area fraction grows in the slit region, this increase is due to the strong oxidation occurred in the slit line and Joint Line Hooking which increases the oxides area fraction in sample 1 by 457% from 1,42E-07 to 7,92E-07 including the slit oxidation.

String's morphology is not unique, in the retreating side strings can be both composed by more than 3 or 4 strings usually separated by more than 15μm and by 3,4 inclusion very close

to each others; the first category is not usually following any grain boundary whereas the second category is usually situated at grain boundaries, since strings are composed by an high number of inclusion it is discovered that their average orientation to the edge line is around 90° in sample 4 and 45° in sample 5.

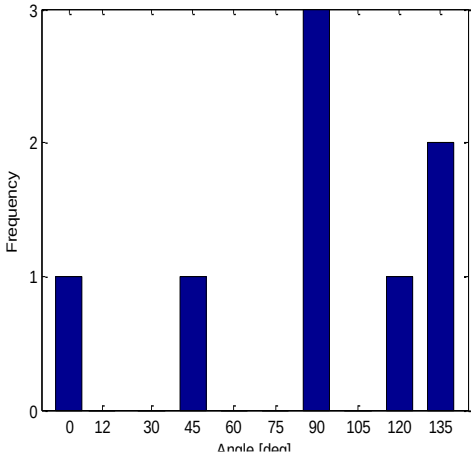

Fig.61: Orientation of strings to the edge line, sample 4

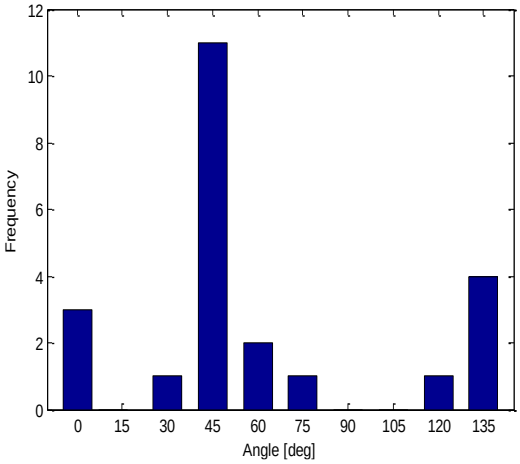

Fig.62: Orientation of strings to the edge line, sample 5

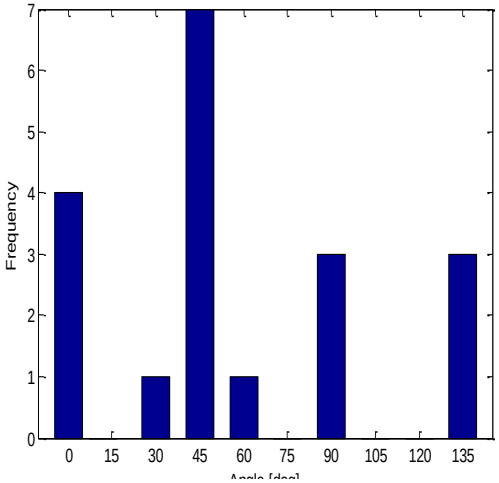

Fig. 63: Orientation of strings to the edge line, sample 3

This occurrence is no longer present in the advancing side when inclusions are usually closer and situated at grain boundaries, and the number of inclusions per string decreases getting further from the edge of the weld, for this reason closer to the edge of the weld strings are composed by an high number of inclusion with an average orientation to the edge line of around 45° (sample 3). In the slit region, oxide inclusions are organized in small strings composed by 2,3 inclusions very close to each other and can be situated both in the middle of the grain or at grain boundaries without any particular orientation, considering the inclusions following the slit and the Joint Line Hooking, they are not organized in strings but they follow the slit line and the Joint Line Hooking.

Fig. 64: Slit oxidation, SEM secondary electrons, weld 1

As well as for morphology, strings differs from each other also for size and oxygen content of the inclusions inside them; in the retreating side the average inclusions size is 2,93µm, in the advancing side is 1,24µm with an increase between advancing and retreating side of 137%, in both sides of the weld, decreases getting closer to the edge of the weld, then inclusions size is bigger in sample 4 (3,27µm) and the average inclusion's size is 2,29µm; considering the oxygen content of inclusions inside strings, it is detected that in the advancing side oxide inclusions present a lower oxygen content than in the retreating side where, likewise size, also the oxygen content is higher by 105%. Considering the advancing side, oxygen content increases, from sample 3 to 2, getting further from the edge of the weld by 120% from 13,36%at in sample 3 to 29,48%at in sample 2, this occurs also in the retreating side from sample 5 to 4, but with an increase of 19% from 36,31%at in sample 5 to 43,44%at in sample 4; exploring average oxygen content and average size of inclusion, it is possible to pull out a linear correlation between average oxygen content and average size.

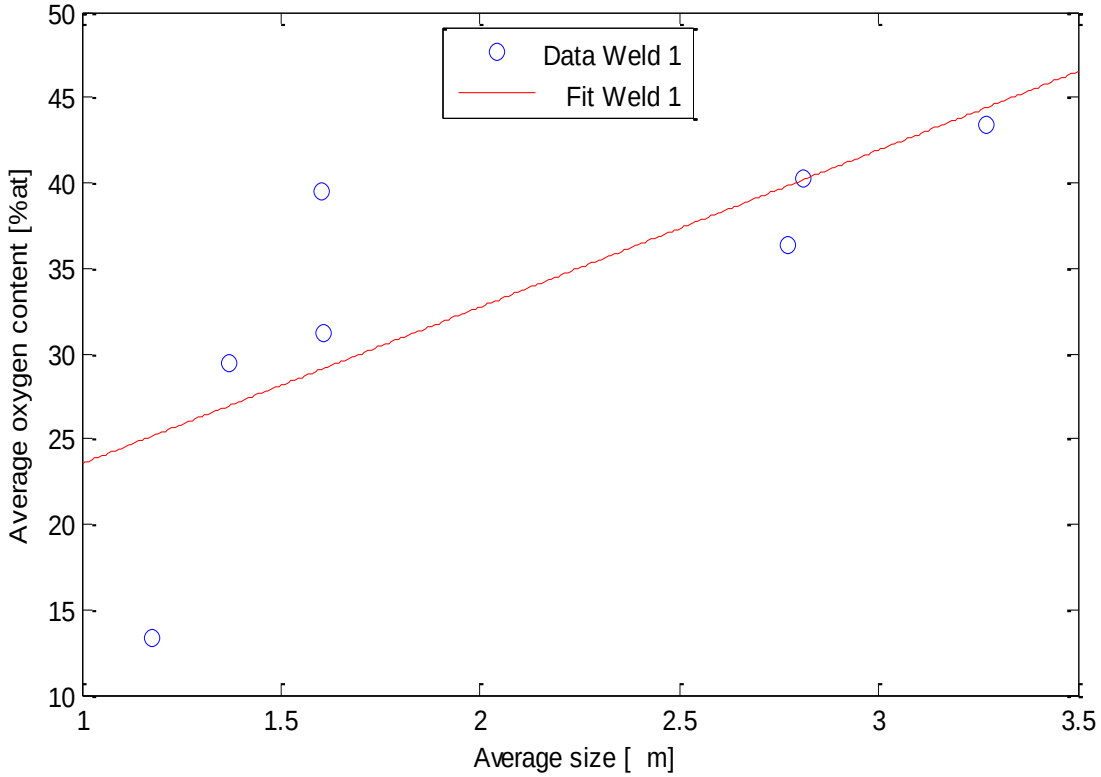

Fig. 65: Relation between average oxygen content and average size of inclusion disclosed in weld 1

Considering the slit region, a further clarification is needed: oxides inclusions detected in this part of the weld can be divided into 2 categories: inclusion uniformly distributed among sample 1 and inclusions that follow the slit and the Joint Line Hooking, the latter are usually bigger in size and with an higher oxygen content respectively by 217% and 145%. Another important parameter that is investigated is the number of inclusions, as expected the number of inclusion is higher in the retreating side than in the advancing side by 32% and it decreases getting further from the edge of the weld, 50% decrease from sample 5 (139) to 4 (69) and 49% from 3 (104) to 2 (53); this decrease is attenuated in the slit region, where, as pointed out before, the slit is subjected to a strong oxidation during welding. Inclusions disclosed in all the weld are mainly composed by copper and oxygen even though also traces of phosphorous, aluminium, silicon, and, in some cases very small traces of sulphur have been

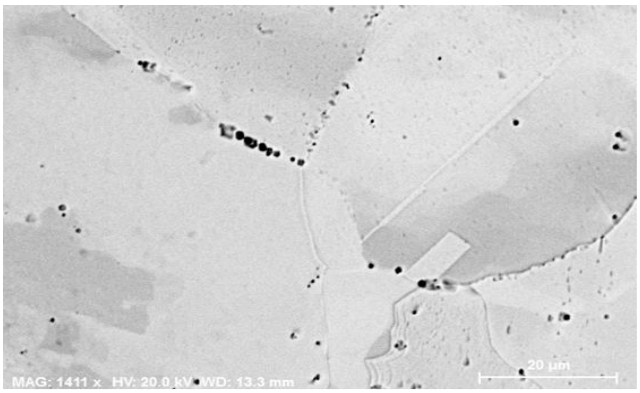

Fig. 66: Voids disclosed at grain boundaries, SEM backscattered electrons, weld 1.

detected; some voids have been detected mainly in the edge region of the advancing side, it is not possible to declare if this voids are intrinsic or are generated by the polishing.
As well as the advancing side, retreating side and slit region, also the nugget has been analyzed; as expected compared to the rest of the weld, it presents a lower number of inclusions (29) and a lower oxides area fraction (1,83E-07), the average size of oxides inclusion and their oxygen content is in line with the average values disclosed for the rest of the weld, also in this case some voids have been detected.

Weld 2:

Weld 2 presents the lower oxides content between the two welds since welding was performed using Argon as shielding gas; samples 7 and 8 belong to the advancing side, samples 9 and 10 belong to the retreating side. Also in this weld, as expected, the oxides content is not changeless in all weld, more oxides strings are found closer to the edge of the weld and their amount decreases getting further from the latter and getting closer to the slit region. Likewise in weld 1, in weld 2 a difference in oxides content is detected between the advancing side and the retreating side, even if this difference is not as heavy as in weld 1. In addition to this the concentration of strings is higher in the left side of the retreating side closer to the edge of the weld, nearby the friction zone; and, among samples, there are some areas in which oxides are more concentrated.
As a consequence, oxides area fraction is higher closer to the edge of the weld and decreases getting further from the latter, in the advancing side from sample 8 (8,05E-07) to 7 (5,19E-07) with 35% decrease and in the retreating side, from sample 10 (1,06E-06) to 9 (5,86E-07) with 44% decrease. Comparing the relation between oxides area fraction and average distance from the edge of the weld in weld 1 and weld 2, it' is clear how area fraction decreases with the distance in both cases, but in weld 1 this decrease is much more definite; in order to emphasize how the oxidation occurred in the slit affects the oxides area fraction, also the slit region has been taken into account in graph in *figure 67.*

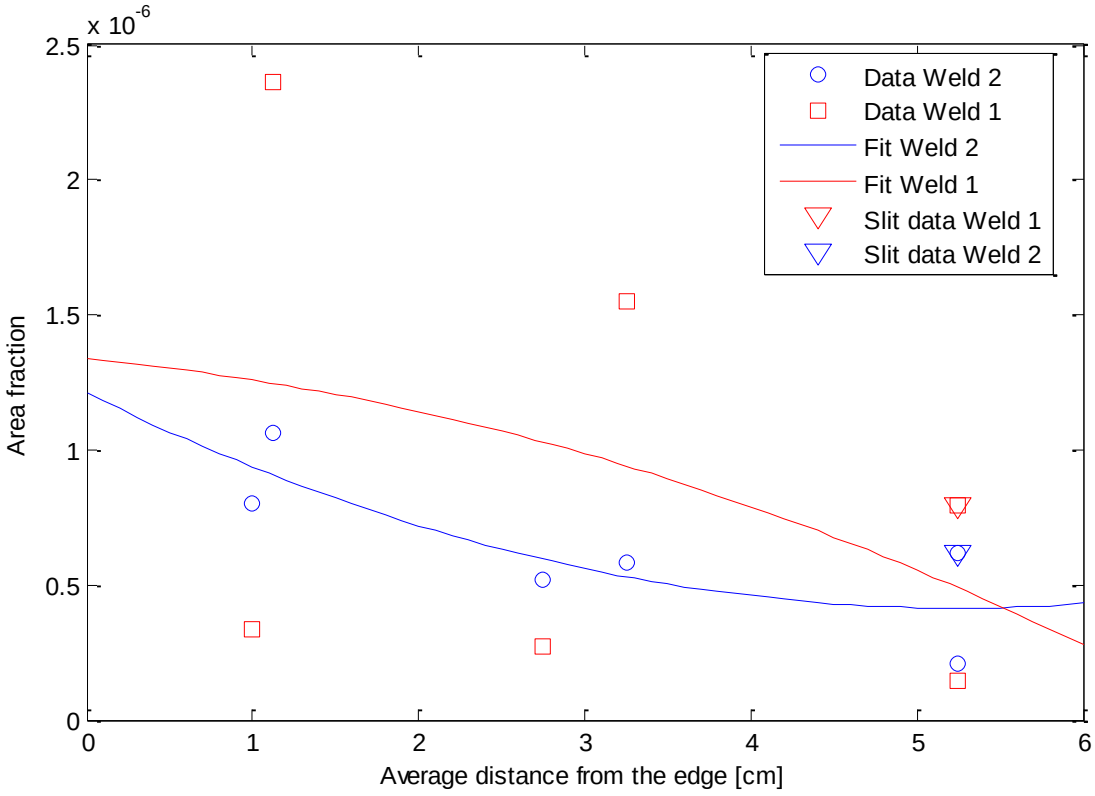

Fig. 67: Relation between area fraction and average distance from the edge of the weld, weld 1,weld 2.

As outlined in graph in *figure 67*, there is also a difference in area fraction between advancing side and retreating side even if this difference is not very relevant (22%) in weld 2; comparing oxides area fraction with weld 1 in advancing, retreating side and slit region, comes out that the in retreating side weld 2 presents a lower oxides area fraction, on the other hand, in advancing side weld 2 presents an higher oxides area fraction, in the slit region oxides area fraction is lower in weld 2. In order to deepen what is show in graph in *figure 67* and to highlight in a more clear way the differences between advancing side and retreating side regarding area fraction graph in *figure 68* in plotted, to sharpen the role of the oxidation occurred along slit and Joint Line Hooking also the latter has been taken into account in this graph.

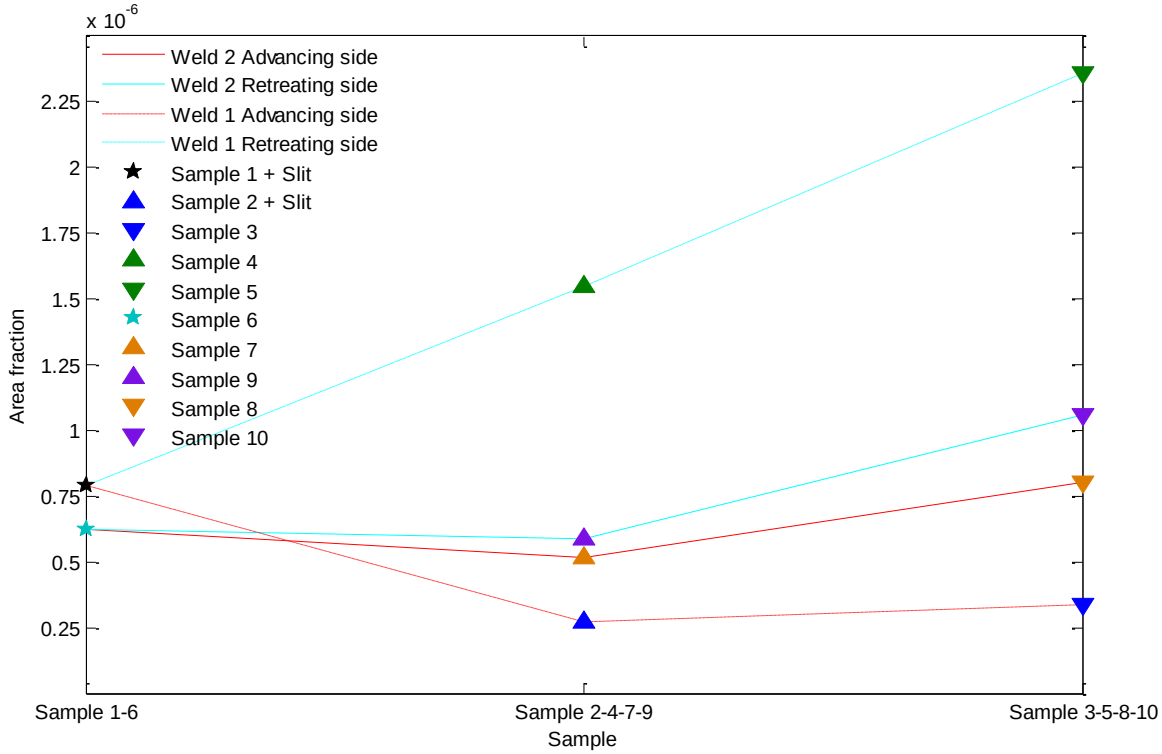

Fig. 68: Relation between area fraction and retreating and advancing side

Considering the total oxides area fraction among the 2 welds including also the slit region, weld 2 presents a lower area fraction by 34% if compared to weld 1.

Table 10: Area fraction in weld 1 and weld 2

Area fraction Weld 1	Area fraction Weld 2
1,1E-06	7,0E-07

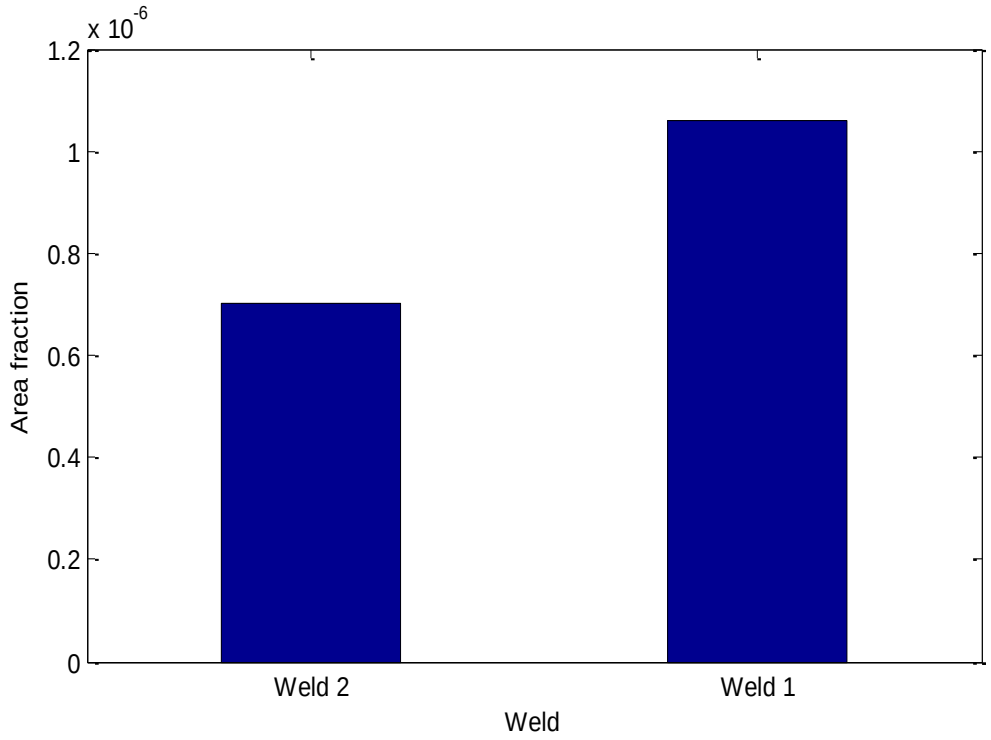

Fig. 69: Area fraction in weld 1 and weld 2

In weld 2, like in weld 1, the morphology of strings is not unique, in the retreating side, closer to the edge of the weld, strings are usually situated at grain boundaries and are usually composed by more than 3 inclusions with a distance between them that can vary from 8 to 30µm, getting further from the edge of the weld, strings are still situated at grain boundaries, they are composed by 5 inclusions which tend to be very far from each others, around 10-20µm; on the other side of the weld, closer to the edge, strings are composed by 3,4 or 5 inclusion quite close to each others; getting further from the edge, strings are composed by a number between 3 and 10 inclusions with a distance between them that can vary from 1µm to 25µm. In the slit region oxide inclusions can be organized both in strings that can be situated at grain boundaries or in the middle of grains composed by 3,4 or 5 inclusions with 4-5 µm and, in some rare cases, 20µm between them, and in clusters composed by 6, 7 inclusions very close to each others, in weld 2 the slit line and the Joint Line Hooking are not presenting a strong oxidation as in weld 1; unlikely weld 1, in weld 2, oxide strings haven't shown up any particular orientation. As well as in weld 1, besides in morphology, inclusions inside strings can be analyzed taking into account their size and oxygen content; there is not a big difference in size between inclusions detected in the retreating side and in the advancing side, however this difference is evident for weld 1 (137%), in order to show how the slit oxidation

can affect the average inclusions size, also the average inclusions size in the slit region has been considered.

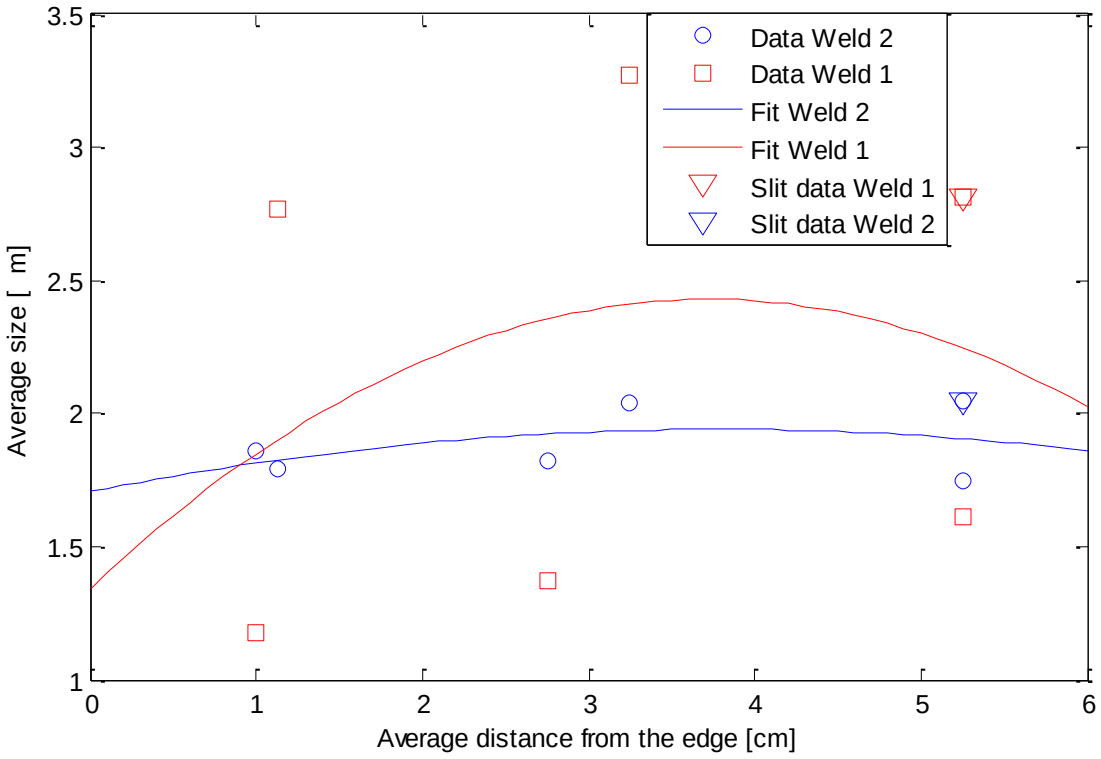

Fig. 70: Relation between average size of inclusions and average distance from the edge of the weld, weld 1, weld 2

Average inclusions size detected in weld 2 is 1,88µm and it is lower by 18% compared with weld 1. This comparison has been made including also the slit in both cases.

Table 11: Average size of inclusion in weld 1 and weld 2

Average size Weld 1 [µm]	Average size Weld 2 [µm]
2,29	1,88

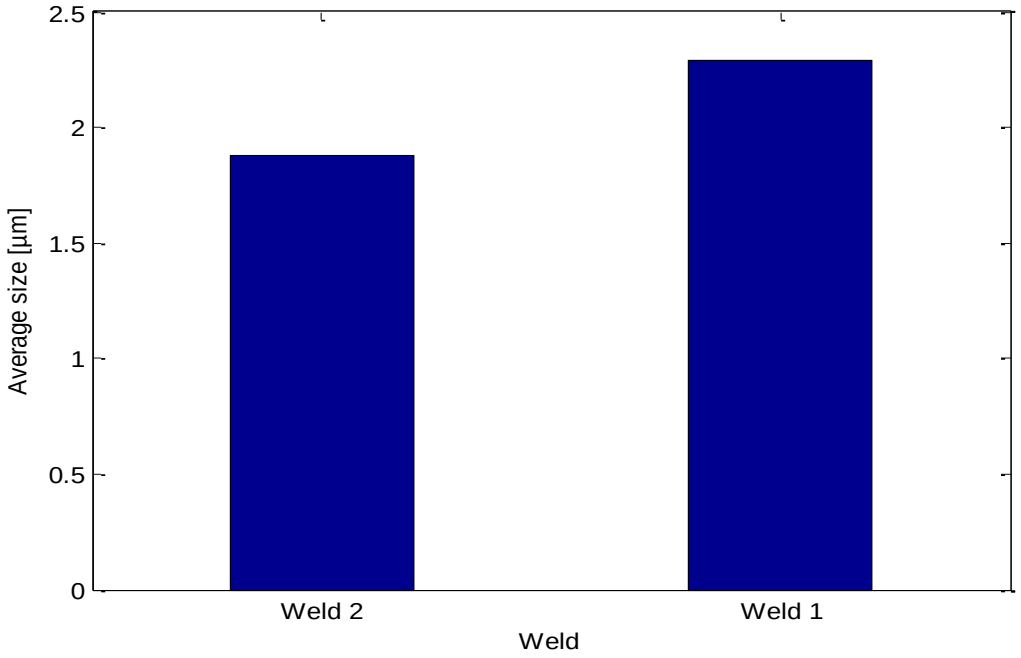

Fig. 71: Average size of inclusions in weld 1 and weld 2

Taking into account the oxygen content, as in weld 1, it increases getting further from the edge of the weld, 15% increase from sample 10 to 9 from 34,61%at in sample 10 to 39,97%at in sample 9 in the retreating side and 43% from 35,07 in 8 to 50,34 in 7 in the advancing side; advancing side present an higher oxygen content by 14% if compared with the retreating side. As previously done, also the average oxygen content of the inclusion disclosed in the slit region is here considered.

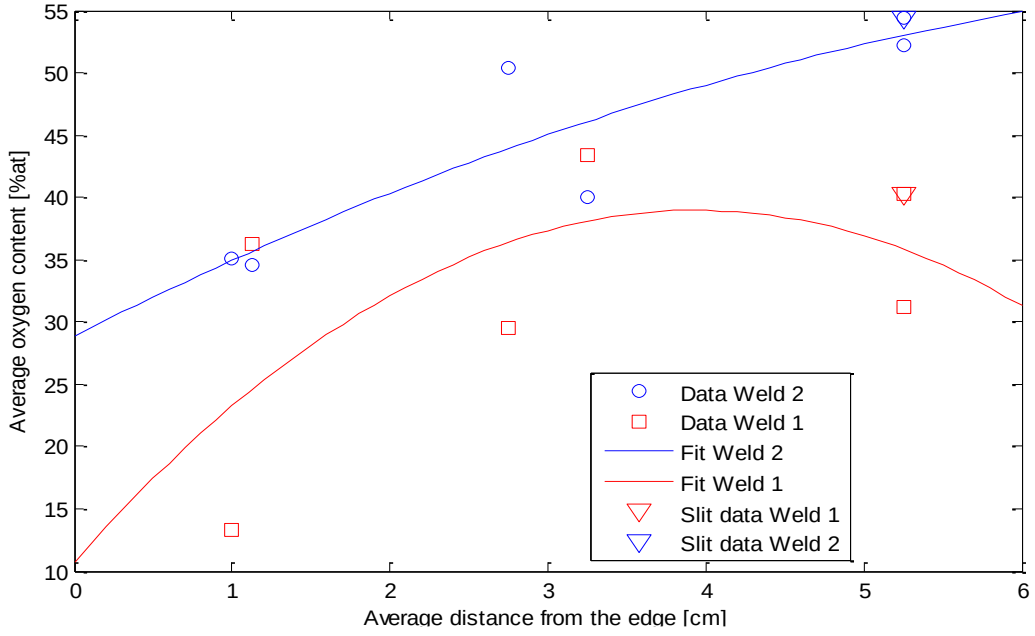

Fig.72: Relation between average oxygen content of inclusions and average distance from the edge of the weld.

The average oxygen content of inclusions in weld 2 is 42,02%at and it is 33% higher of the value disclosed in weld 1 (31,47). This comparison has been made considering also the slit.

Table 12: Average oxygen content of inclusions disclosed in weld 1 and weld 2

Average oxygen content Weld 1 [%at]	Average oxygen content Weld 2 [%at]
31,5	42

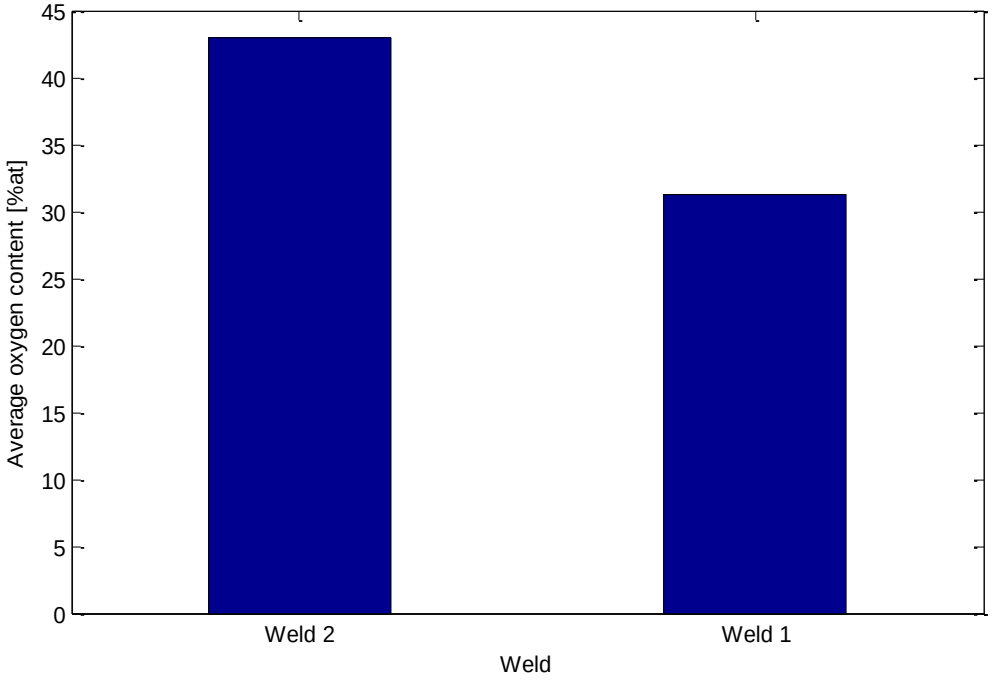

Fig. 73: Average oxygen content of inclusions in weld 1 and weld 2

Since inclusions disclosed in weld 2 are not significantly different in size, unlike weld 1, in weld 2 it is not possible to underline a correlation between average oxygen content and average inclusion's size since data are quite scattered.

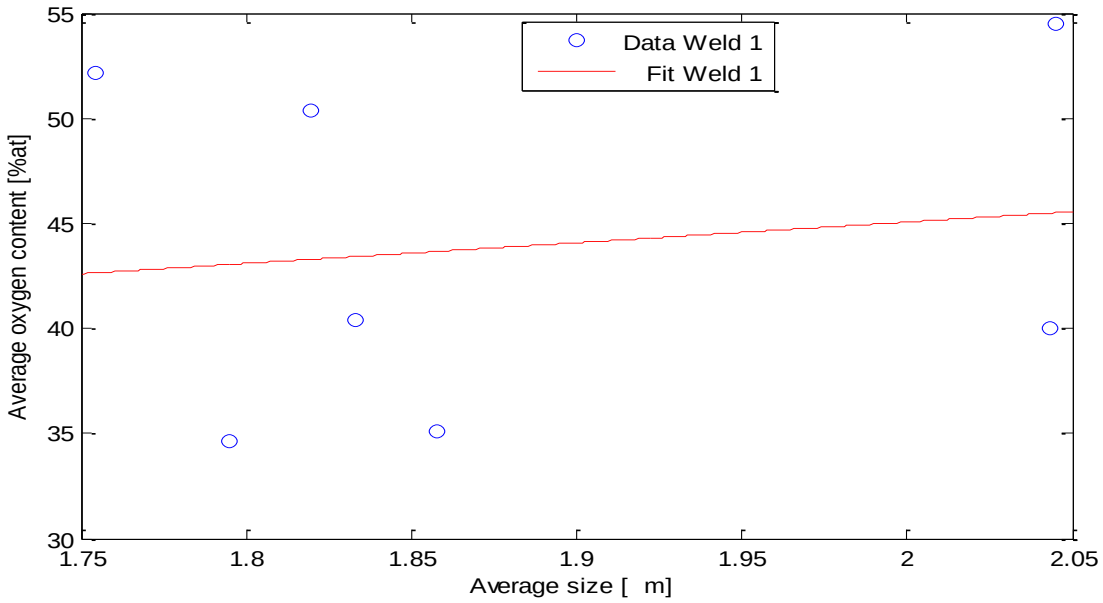

Fig. 74: Relation between average oxygen content and average size of inclusions, weld2.

Considering the slit region, a further clarification is needed: oxides inclusions detected in this part of the weld can be divided into 2 categories: inclusion uniformly distributed among sample 6 and inclusions that follow the slit and the Joint Line Hooking, the latter are bigger in size by 33% and higher in oxygen content by 8%, these results show that, unlikely in weld 1, in weld 2 oxide inclusions following the slit line and the Joint Line Hooking are not affecting that much the average size and oxygen content of the inclusions disclosed in sample 6, in order to underline this, a comparison among average oxygen content and average inclusion size has been made between inclusions disclosed right above the slit in weld 1 and weld 2.

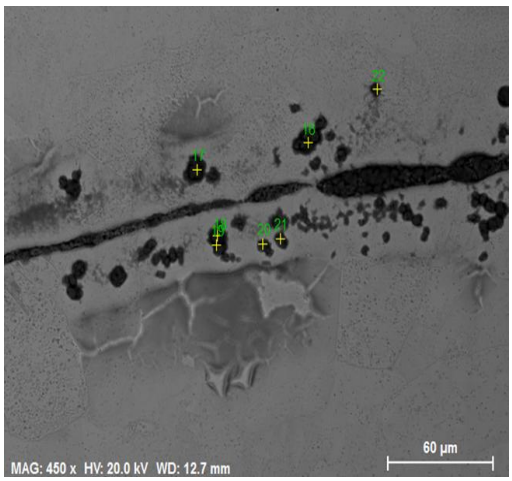

Fig.75: Oxidation in the slit, weld 1, SEM backscattered electrons

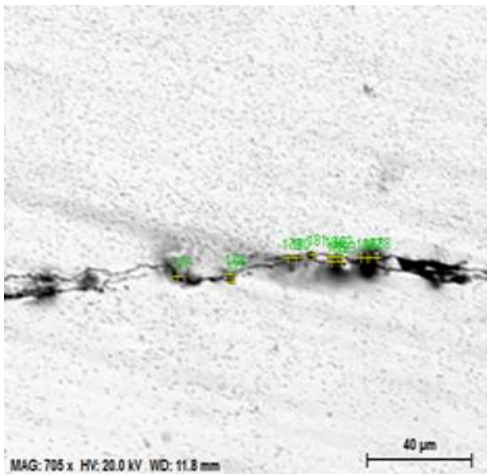

Fig.76:Oxidation in the slit, weld 2, SEM, backscattered electrons

Table 13: Average size of inclusions disclosed in the slit in weld 1 and weld 2

Average size Slit 1 [µm]	Average size Slit 2 [µm]
5,11	2,34

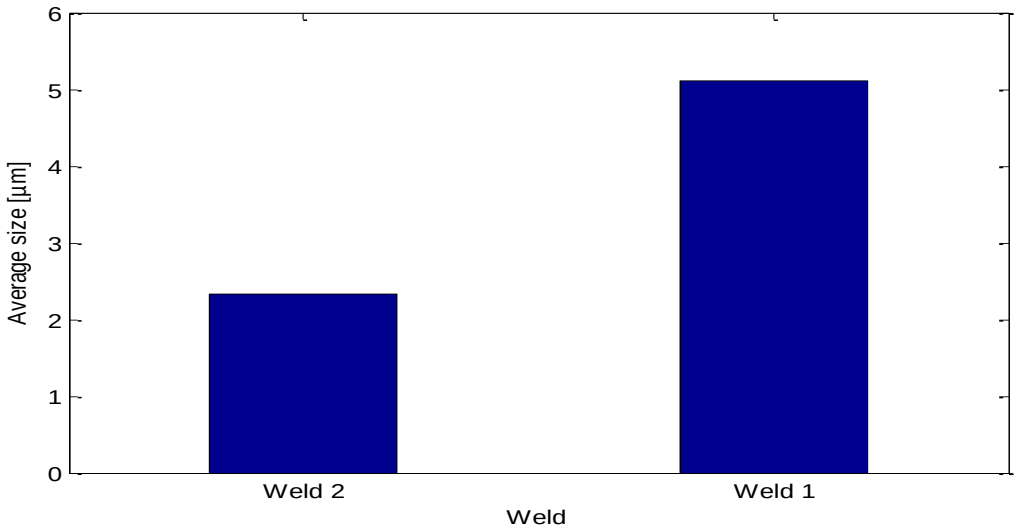

Fig. 77: Average size of inclusions in the slit, weld 1 and weld 2

Table 14: Average oxygen content of inclusions disclosed in the slit in weld 1 and weld 2

Average oxygen content Slit 1 [%at]	Average oxygen content Slit 2 [%at]
76,5	56,8

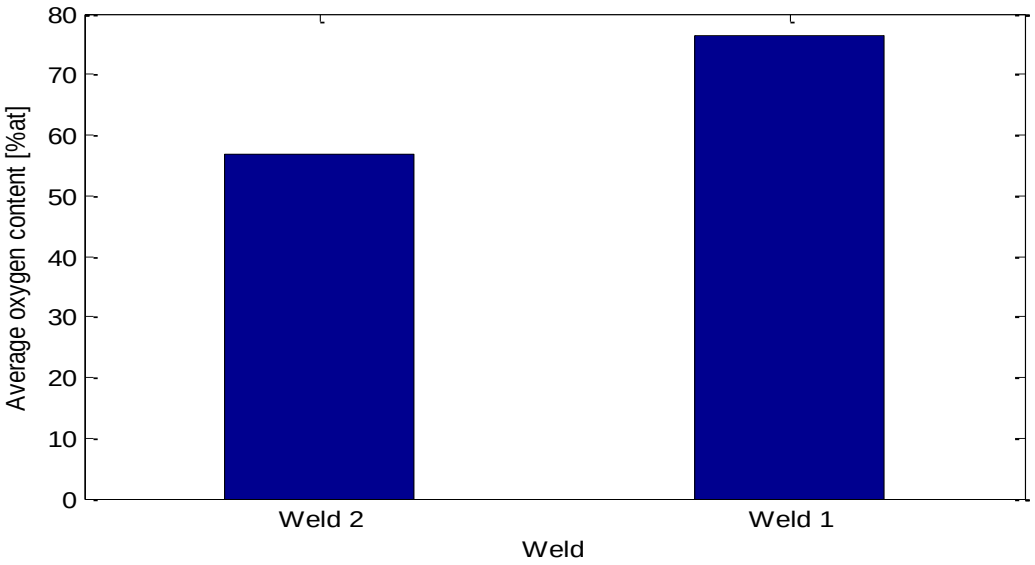

Fig. 78: Average oxygen content of inclusions in the slit, weld 1 and weld 2.

As for weld 1, another important parameter that have been investigated is the number of inclusion disclosed, as expected this number decreases getting further from the edge of the

weld 16% decrease from sample 8 (111) to 7 (93) and 61% from 10 (138) to 9 (53), there is not a notable difference between retreating side and advancing side concerning their number, this is shown, considering also the role of the slit oxidation, in graph in *figure 79.*

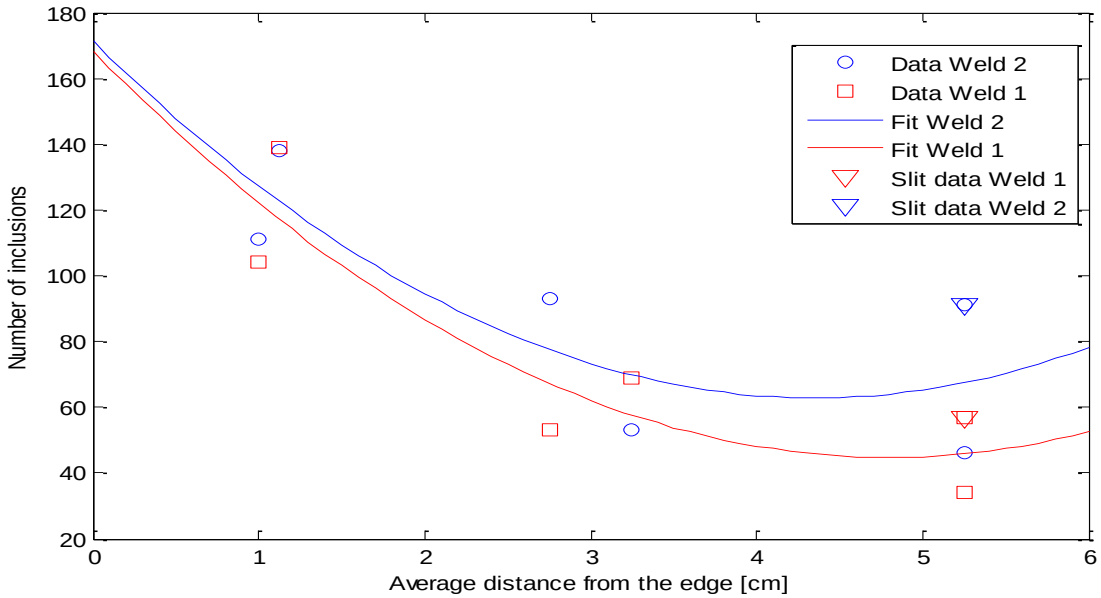

Fig. 79: Relation between number of inclusions and average distance from the edge of the weld

The total number of inclusions disclosed in weld 2 is higher by 16% if compared with weld 1. This comparison has been made considering also the slit.

Table 15: Number of inclusions disclosed in weld 1 and weld 2

Number of inclusions Weld 1	Number of inclusions Weld 2
422	486

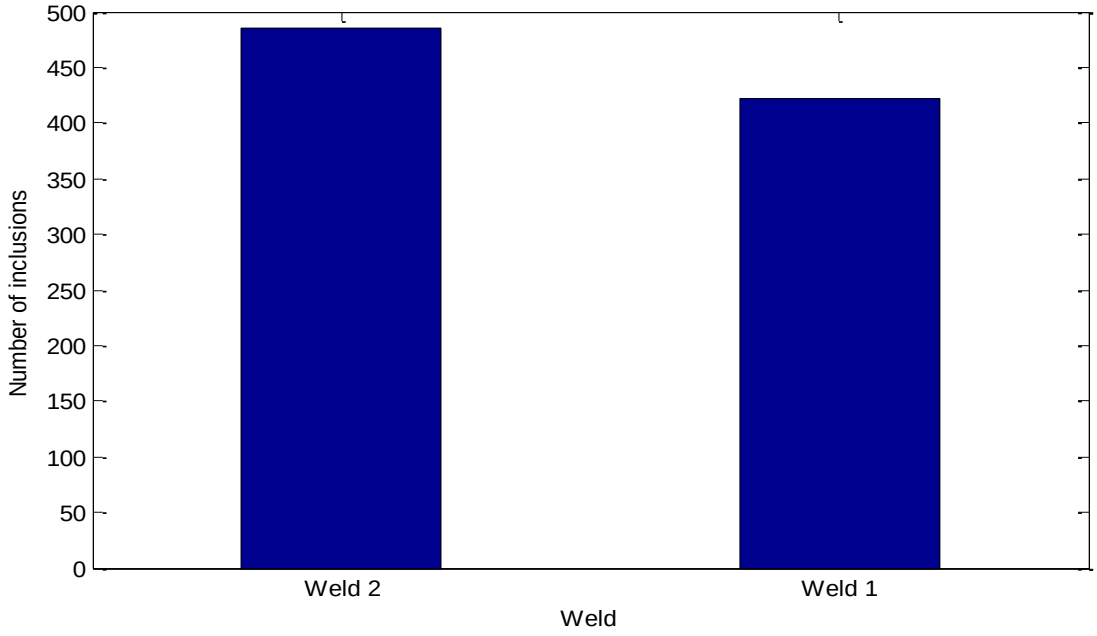

Fig. 80: Number of inclusions weld 1 and weld 2

Inclusions that have been disclosed in weld 2 are mainly composed by oxygen, copper, phosphorous, aluminium and silicon, with sometimes small traces of iron, calcium, potassium and sulphur. Almost no voids have been disclosed. Likewise for weld 1, for weld 2 also the nugget have been taken into account, it presents a lower oxides area fraction and inclusions number if compared with the rest of the weld.

In order to show results in a more concentrated form, data obtained are summarized in *table 16*, *17* and *18.*

Weld 1:

Table 16: Data obtained from Weld 1

	Sample 1	Sample 1 + Slit	Sample 2	Sample 3	Sample 4	Sample 5
Average size [µm]	1,61	2,81	1,37	1,18	3,27	2,77
Average oxygen content [%at]	31,2	40,2	29,5	13,4	43,4	36,3
Area fraction	1,4E-07	7,9E-07	2,7E-07	3,4E-07	1,6E-06	2,4E-06
Average distance from the edge [cm]	5,25	5,25	2,75	1	3,25	1,125
Number of inclusions	34	57	53	104	69	139

Weld 2:

Table 17: Data obtained from Weld 2

	Sample 6	Sample 6 + Slit	Sample 7	Sample 8	Sample 9	Sample 10
Average size [µm]	1,75	2,05	1,82	1,86	2,04	1,79
Average oxygen content [%at]	52,2	54,5	50,3	35,1	40,0	34,6
Area fraction	2,0E-07	6,2E-07	5,2E-07	8,0E-07	5,9E-07	1,1E-06
Average distance from the edge [cm]	5,25	5,25	2,75	1	3,25	1,125
Number of inclusions	46	91	93	111	53	138

Table 18: Data obtained from weld 1 and weld 2

	Weld 1	Weld 2
Average size [µm]	2,29	1,88
Average oxygen content [%at]	31,5	42
Area fraction	1,1E-06	7,0E-07
Number of inclusions	422	486

A comparison has been proposed also considering the nuggets of both welds.

Table 19: Data obtained from nugget 1

	Nugget Weld 1	Nugget Weld 2
Average size [µm]	1,60	1,83
Average oxygen content [%at]	39,5	40,4
Area fraction	1,8E-07	1,3E-07
Number of inclusions	29	21

Results show that weld 1 was subjected to a stronger oxidation if compared with weld 2, this is in line with what was expected, since weld 1 was conducted in air atmosphere and weld 2 was conducted under Argon as shielding gas; then the stronger oxidation presented right above the slit by weld 1 is justified by the fact that the weld probe in weld 1 penetrated a bit deeper.

Results have also been compared also with Cu-OFP thermodynamic model, taking into account graph in *figure 81*, it's clear that results are not fitting this model, first of all, from the model the presence of compounds like Cu_2S, Cu_9S_5, $Cu_2P_2O_7$, $Cu_3P_2O_8$ and P_4O_{10} is expected, conversely, from SEM analysis only Cu_2O is detected with, in some cases, very small traces of sulfur, potassium, iron, calcium, aluminum and silicon; regarding the presence of phosphorous, since electrolytic polishing was performed using, as electrolyte, a solution

containing distilled water and phosphoric acid, every inclusion analyzed showed the presence of phosphorous, the presence of this element is therefore due to electrolytic polishing; this is also proved by the fact that sample 2, previously analyzed after oxides polishing, presents almost no phosphorous. These small traces of P and S are not enough to consider the presence of sulphates and phosphates. Is therefore necessary hereafter to discover and analyze these compounds; regarding this there are some theories, one of these assumes that phosphates and sulphates are not present in copper because, they tend to separate gravitationally in the melt, in the production process; another theory asserts that phosphates and sulphates are too small to be detected with conventional SEM. In this case a more detailed analysis with TEM is suggested.

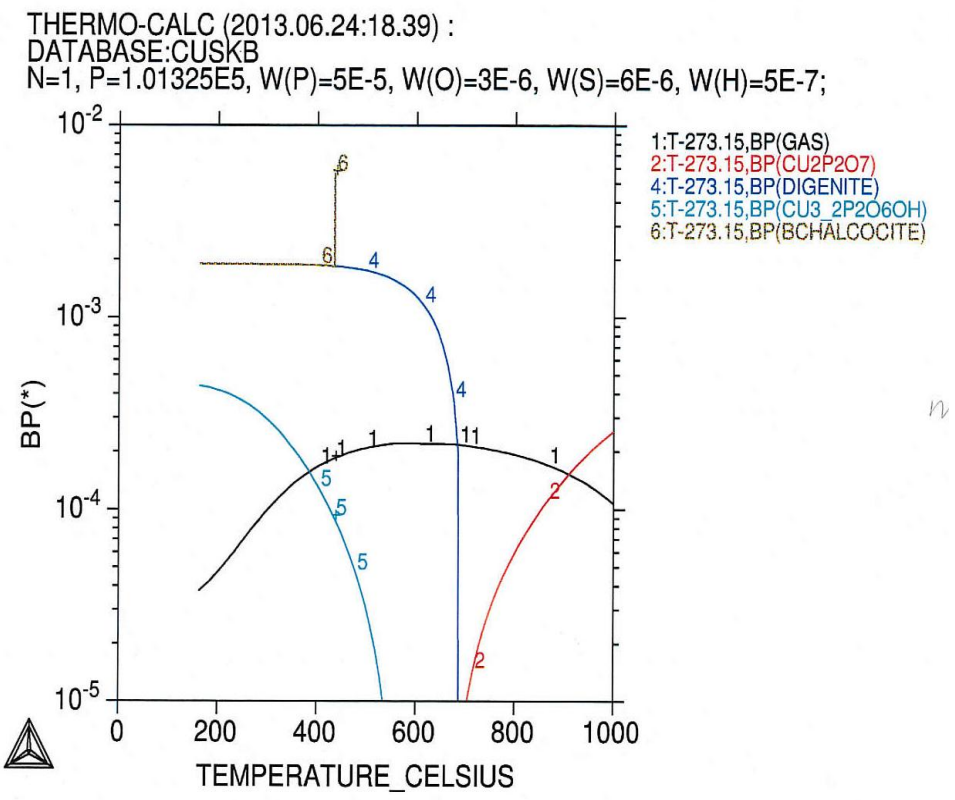

Fig. 81: Thermodynamic model of Cu-OFP normal oxygen content

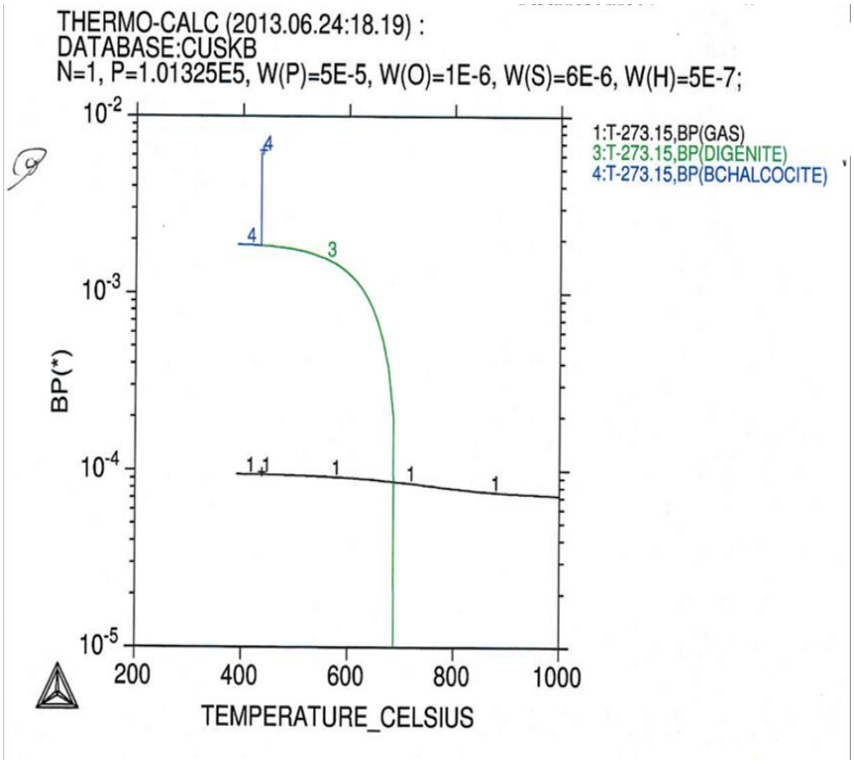

Fig. 62: Thermodynamic model of Cu-OFP low oxygen content

Another important issue regards the comparison between graph in *figure 81* and graph in *figure 82*, since for normal oxygen content phospathes are expected to form in the material, there are not apparent explanations on why for lower oxygen content no phosphates are expected in the thermodynamic model; for this reason further thermodynamic and experimental investigations are suggested.

8 CONCLUSION

From the results it is clear that weld 1 was subjected to a stronger oxidation than weld 2.

- In both welds the samples closer to the surface present an higher oxides area fraction, area fraction quickly decrease getting further from the edge; in spite of this, in proximity of the slit an high number of oxides strings is detected and area fraction grows by 457% in weld 1 and by 202% in weld 2. In weld 1 oxides area fraction decrease in the retreating side by 33% going trough 2,36E-06 of sample 5, to 1,55E-06 of sample 4; this decrease is lighter in the advancing where oxides area fraction decrease from 3,37E-07 of sample 3 to 2,71E-07 of sample 2 (19%); the difference in oxides area fraction between retreating and advancing side is 84%. In weld 2 the decrease in oxides area fraction along retreating side is by 44%, from 1,06E-06 in sample 10 to 5,86E-07 in sample 9; in the advancing side this decrease is by 35% from 8,05E-07 in sample 8 to 5,19E-07 in sample 7, the difference in oxides area fraction between retreating and advancing side in weld 2 is 22%. Considering the total amount of oxides area fraction, in weld 1 is higher by 34% if compared with weld 2.
- In weld 1, a difference also in average size of inclusions has been detected between advancing and retreating size, the average inclusions size grows from 1,24μm of advancing side to 2,93μm of retreating side (137%), inside each side of the weld the average size of inclusions tends to grow getting further from the edge of the weld. This statement is no longer effective in weld 2 since there is not a big difference in size between inclusions, although it is possible to assert that in weld 2 inclusion's size is lower by 18% if compared with weld 1.
- In both welds the average oxygen content grows getting further from the edge of the weld, in weld 1 inclusions disclosed in advancing side present a lower oxygen content than in retreating side where the average oxygen content is higher by 105%; inside advancing side the average oxygen content of inclusions grows form 13,36%at in sample 3 to 29,48%at in sample 2 (120%), in the retreating side this increase is by 19% from 36,31%at in sample 5 to 43,44%at in sample 4. In weld 2 inclusions disclosed in advancing side present an higher oxygen content than in the retreating side, where the average oxygen content is lower by 14%, inside advancing side the

average oxygen content grows from 35,07%at in sample 8 to 50,34%at in sample 7 (43,%), in the retreating side this increase is by 15% from 34,61%at in sample 10 to 39,97%at in sample 9. The average oxygen content of inclusion is higher in weld 2 by 33%. As well as for oxides area fraction, the presence of the slit alters the oxygen content and average size of inclusions present in sample 1 and 6, this is much more noticeable in weld 1 where the average oxygen content of inclusions following the slit line and the Joint Line Hooking is higher by 145% and their size by 217%, considering weld 2 this difference is set at 33% for average size of inclusions and 8% for average oxygen content.

- Concerning weld 1 it is possible to draw a correlation between average oxygen content of inclusions and average size of inclusions, this correlation is not avaible for weld 2 since data are much more scattered than in weld 1.
- In both welds inclusions are mainly composed by oxygen, copper with traces of aluminium, phosphorous, silicon and in some cases small traces of calcium, potassium and sulfur. In weld 1 several voids have been disclosed even if it is not possible to qualify this voids as intrinsic voids or generated by polishing; in weld 2 almost no voids have been detected.
- Another parameter that have been investigated is the number of inclusions, it decrease in both welds getting further from the edge of the weld and in weld 2 is higher by 15% if compared with weld 1.
- In both welds, as pointed out, a difference in oxides area fraction is detected between retreating and advancing side, this difference is higher for weld 1; the reason of this difference has previously been studied by several authors and it is probably due to the flow of matter that occur around the pin during friction stir welding process, this theory is supported by Colligan who, in his study on aluminum friction stir welding, experimentally analyzed the flow of matter using radiographic techniques.

9 ACKNOWLEDGEMENTS

I desire to thank prof. Irene Calliari and prof. Rolf Sandström for having given me the opportunity to perform my activity of thesis in Stockholm and the company SKB that has provided the materials, besides I would like to thank Matts Björck, Peter Hedström, Rui Wu, Johan Pilhagen and all the people who helped me in solving multiple experimental issues. I thank my family: father, mother and brother, who supported me in all these year of study from all points of view; I also thank my closest friends whit whom I shared nice moments.

10 REFERENCES

1: Tommy Hedman, SKB; Road to a DGR in Sweden; CEG Workshop, Feb.2009.

2: Ulf Ronneteg, Lars Cederqvist, Håkan Rydén, Tomas Öberg, Christina Müller, BAM – Federal Institute for Materials, Research and Testing, Berlin; Reliability in sealing of canister for spent nuclear fuel; June 2006; ISSN 1402-3091; SKB Rapport R-06-26.

3: www.skb.se/Templates/Standard16944.aspx?query=greenland; Greenland Analogue Project; SKB, Posiva; June 2013.

4: B.Rosborg, L.Werme, The Swedish nuclear waste program and the long term corrosion behavior of copper. Journal of nuclear materials. 379(2008) 142-153.

5: www.indexmundi.com/commodities/?commodity=uranium; Uranium, u3o8 restricted price, Nuexco exchange spot; Source: International Monetary Fund; May 2013.

6: K. Colligan; Material flow behavior during friction stir welding of aluminium; Supplement to welding journal july 1999.

7:T. Källgren; Friction stir welding of copper canister for nuclear waste; Licentiate thesis; KTH, Stockholm, Sweden 2005.

8: H. R.Shercliff,P.A.Colegrove; Math. Modelling weld. Phenom; 6, 927-74, 2002.

9: A. P. Reynolds, Z. Khandkar, T. Long, J. Khan; Utility of relatively simple models for understanding process parameter effects on FSW; Materials Science Forum; v 426-432, n 4, p 2959-2964, 2003.

10: Katherine Ling, Is the solution to U.S. nuclear waste problem in France?; The New York Times, May 18,2009.

11: Cu-O (Copper Oxygen); Landolt-Bornstein New Series IV/5; page 2; 2013.

12: Hans Magnusson and Karin Frisk Swerea/KIMAB, Thermodynamic modeling OFP-Cu, Draft report, June 2013.

13: S.Nakahara, Y. Okinaka, The hydrogen effect in copper, Materials Science and Engineering A, 101 (1988) 227-230.

14: Åsa Martinsson, Rolf Sandström;. Hydrogen depth profile in phosphorous doped oxygen-free copper after cathodic charging; J Mater Sci.; DOI 10.1007/10853-012-6592-y.

15:Anders Frank et al; Strålsäkerhetsmyndigheten; Report number 2012:23.

16: Rui Wu; Processing line inclusion (PLI) and joint line hooking (JLH) in Cu-OFP friction stir weld-part1: metallographic examination June 2011; Swerea KIMAB; Report number 264017-8.
17: Paul A. Colegrove, Hugh R. Shercliff; 3-Dimensional CFD modelling of flow round a threaded friction stir welding tool profile; Journal of materials processing technology; Report number 2005.03.015.
18: V. Palmieri; The electrolytic polishing of metals: application to copper and niobium; Istituto Nazionale di Fisica Nucleare, Laboratori Nazionali di Legnaro, Draft report.
19: Vander Voort, George F.; Chemical and electrolytic polishing metallography and microstructures; vol. 9, ASM Handbook, ASM International, 2004 p281-293.
20: G.F. Vander Voort; Metallography: Principles and Practice, McGraw-Hill, 1984, Reprinted ASM, International 1999.
21: Pavel A. Korzhavyi; Hydrogen trapping by copper vacancies; June 2013; Draft report.
22: Malakhov; Standard test methods for determining average grain size; ASTM International; Designation E112-10.
23: Cu-O (Copper Oxygen); Landolt-Bornstein New Series IV/5; page 2.
24: Hans Magnusson and Karin Frisk Swerea/KIMAB, Thermodynamic modeling OFP-Cu, KTH Workshop 18/19 June 2013.
25: Chemical and electrolytic polishing metallography and microstructures, vol. 9, ASM Handbook, ASM International, 2004 p281-293.

11 APPENDICES

Here follows a brief summary of some images that have been obtained with SEM and EDS ordered by sample number and weld.

11.1 Sample 1

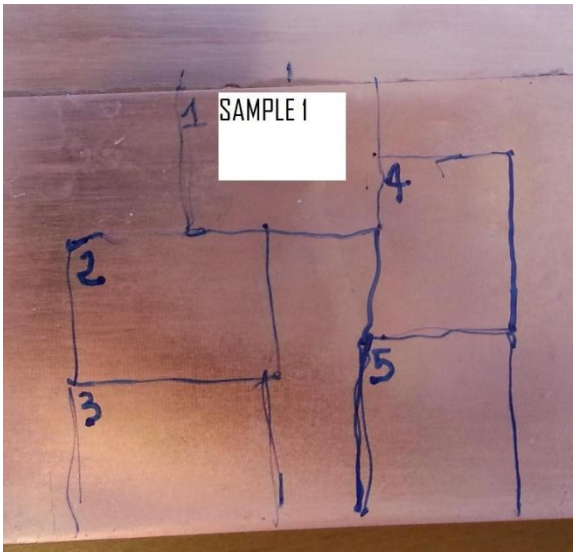

Sample 1 presents the lower oxides concentration among the 5 samples, almost all oxides inclusions are situated nearby grains boundaries, the upper part of the sample is almost free of oxides, this content increase getting closer to sample 2 and 4. Oxides strings are usually composed by at least 5 oxides, even if the largest part is composted just by 2 or 3 inclusions; strings are not oriented in a particular direction. Oxides average size is about 1,61µm and the average oxygen content is around 31,15%at, considering the whole sample the total fraction of oxides is 1,42E-07.

A strong oxidation area has been found in proximity of the slit, this oxidation follows the total length of the slit until the Joint Line Hooking. These oxides are bigger than the oxides revealed in the main body of the sample and have an average diameter of 5,10µm with an average oxygen content of 76,49%at; for this reason they strongly affect the total fraction of oxides of the sample, considering the total amount of oxides, the fraction of area is 7,92E-07 increasing the previous value of 457%. As well as oxygen and copper, also phosphorous has been detected in these inclusions, no voids have been disclosed.

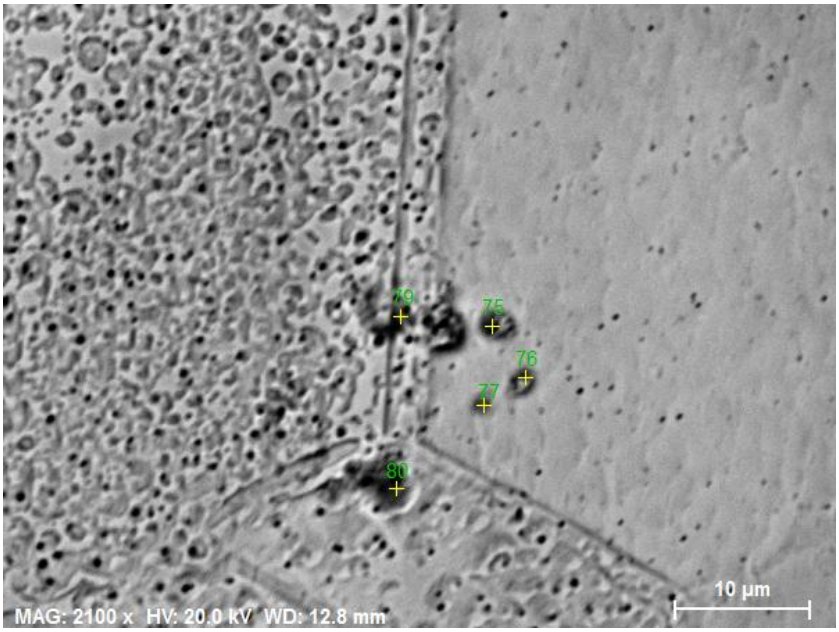

Spectrum: 77

Element	Series	norm. C [wt.%]	Atom. C [at.%]
Oxygen	K-series	9.65	29.79
Copper	K-series	90.35	70.21
Total:		100.00	100.00

Spectrum: 76

Element	Series	norm. C [wt.%]	Atom. C [at.%]
Oxygen	K-series	3.27	11.84
Copper	K-series	96.73	88.16
Total:		100.00	100.00

Spectrum: 75

Element	Series	norm. C [wt.%]	Atom. C [at.%]
Oxygen	K-series	5.36	18.36
Copper	K-series	94.64	81.64
Total:		100.00	100.00

Spectrum: 78

Element	Series	norm. C [wt.%]	Atom. C [at.%]
Oxygen	K-series	2.30	8.54
Copper	K-series	97.70	91.46
Total:		100.00	100.00

Spectrum: 79

Element	Series	norm. C [wt.%]	Atom. C [at.%]
Oxygen	K-series	7.14	23.39
Copper	K-series	92.86	76.61
Total:		100.00	100.00

Spectrum: 80

Element	Series	norm. C [wt.%]	Atom. C [at.%]
Oxygen	K-series	4.74	16.50
Copper	K-series	95.26	83.50
Total:		100.00	100.00

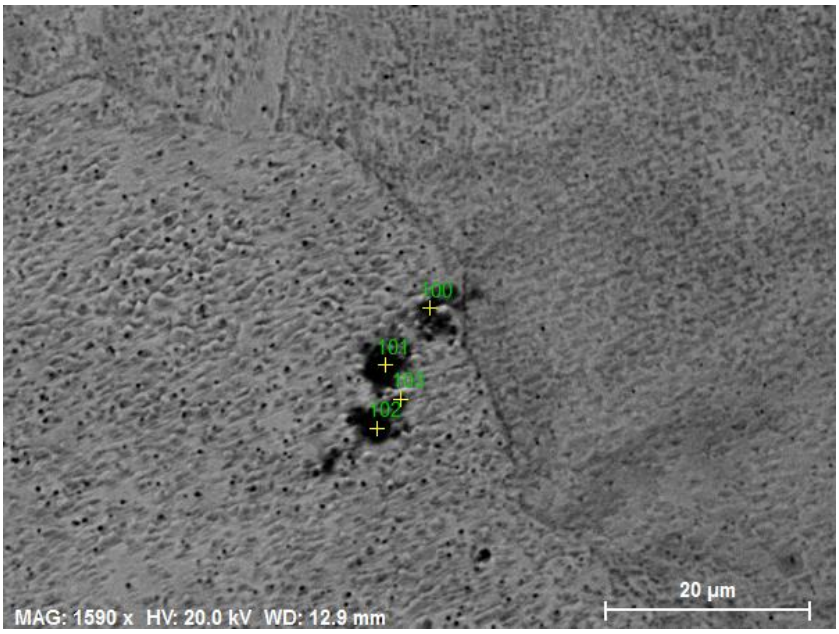

Spectrum: 103

Element	Series	norm. C [wt.%]	Atom. C [at.%]
Oxygen	K-series	14.68	40.59
Copper	K-series	85.32	59.41
Total:		100.00	100.00

Spectrum: 102

Element	Series	norm. C [wt.%]	Atom. C [at.%]
Oxygen	K-series	16.88	44.65
Copper	K-series	83.12	55.35
Total:		100.00	100.00

Spectrum: 101

Element	Series	norm. C [wt.%]	Atom. C [at.%]
Oxygen	K-series	12.75	36.73
Copper	K-series	87.25	63.27
Total:		100.00	100.00

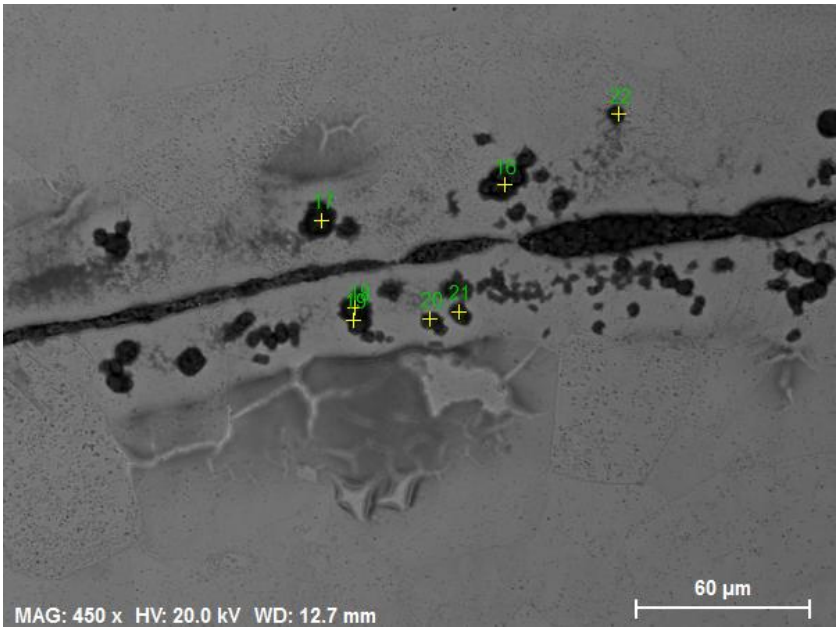

Spectrum: 16

Element	Series	norm. C [wt.%]	Atom. C [at.%]
Oxygen	K-series	49.78	79.74
Copper	K-series	50.22	20.26
Total:		100.00	100.00

Spectrum: 21

Element	Series	norm. C [wt.%]	Atom. C [at.%]
Oxygen	K-series	47.27	78.07
Copper	K-series	52.73	21.93
Total:		100.00	100.00

Spectrum: 20

Element	Series	norm. C [wt.%]	Atom. C [at.%]
Oxygen	K-series	51.10	80.58
Copper	K-series	48.90	19.42
Total:		100.00	100.00

Spectrum: 19

Element	Series	norm. C [wt.%]	Atom. C [at.%]
Oxygen	K-series	34.14	67.31
Copper	K-series	65.86	32.69
Total:		100.00	100.00

11.2 Sample 2

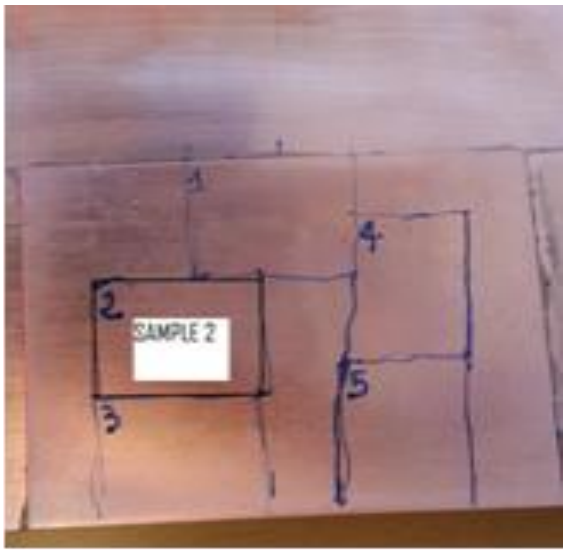

Oxides string in sample 2 are generally located in proximity of the grain boundaries, their amount increase getting closer to specimen 3 and decrease getting closer to specimen 1, strings contains 3,4 oxides inclusions. The average size of these inclusion is 1,37μm and the average oxygen content is around 29,48%at, considering the total amount of oxides, their area fraction is 2,71E-07. As well as oxygen, phosphorous, silicon and aluminum were detected. Some voids have been disclosed though it is not possible to understand if they are generated from the polishing process or are intrinsic voids.

11.3 Sample 3

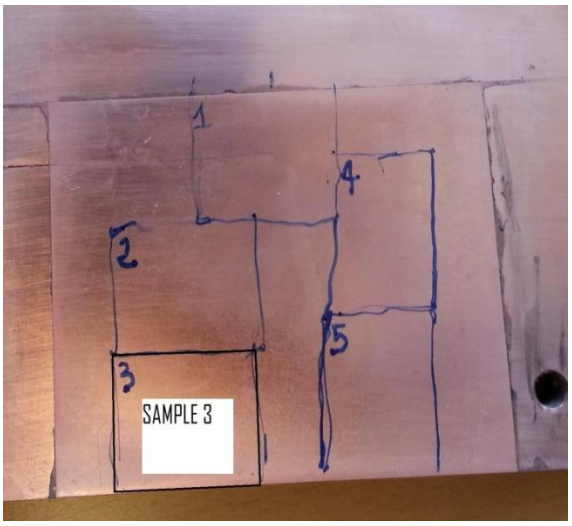

Oxides strings were disclosed also in sample 3, their amount increases getting closer to the edge of the welded zone and decreases getting closer to sample 2. These strings are usually longer than strings in sample 2. The total oxides area fraction is 3,37E-07; the oxide

inclusions disclosed have an average oxygen content of 13,36%at with an average size of 1,18µm. Strings are often composed by more than 4 oxides inclusion and they are situated exactly at grain boundaries, many strings are orientated at 45° to the edge line. As well as oxygen and copper, silicon, aluminum and phosphorous have been detected. Voids have been disclosed, their amount is higher than in sample 2, also in this case it is not possible to say if these voids are generated by the polishing or are intrinsic voids.

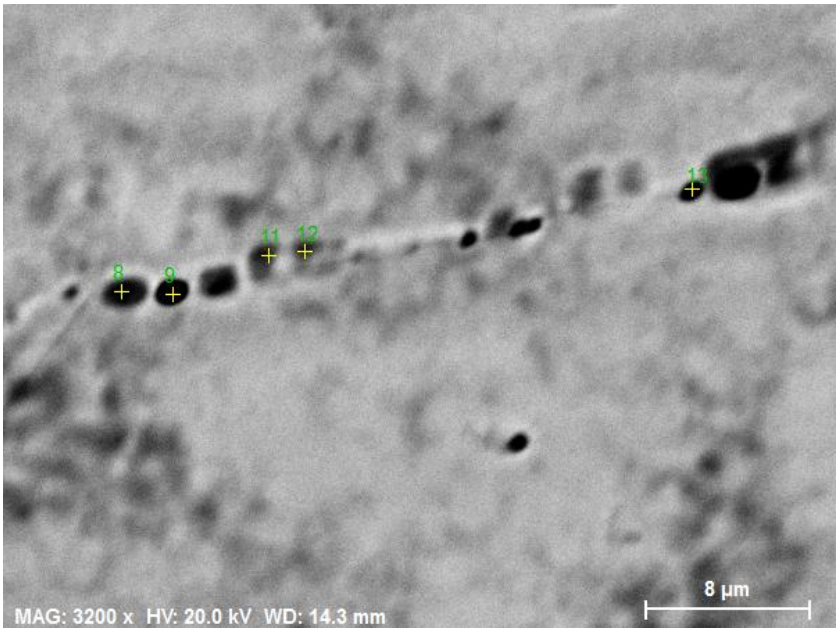

Spectrum: 13

Element	Series	norm. C [wt.%]	Atom. C [at.%]
Oxygen	K-series	1.44	5.49
Copper	K-series	98.56	94.51
Total:		100.00	100.00

Spectrum: 12

Element	Series	norm. C [wt.%]	Atom. C [at.%]
Oxygen	K-series	3.66	13.12
Copper	K-series	96.34	86.88
Total:		100.00	100.00

Spectrum: 11

Element	Series	norm. C [wt.%]	Atom. C [at.%]
Oxygen	K-series	2.11	7.88
Copper	K-series	97.89	92.12
Total:		100.00	100.00

Spectrum: 9

Element	Series	norm. C [wt.%]	Atom. C [at.%]
Oxygen	K-series	3.10	11.27
Copper	K-series	96.90	88.73
Total:		100.00	100.00

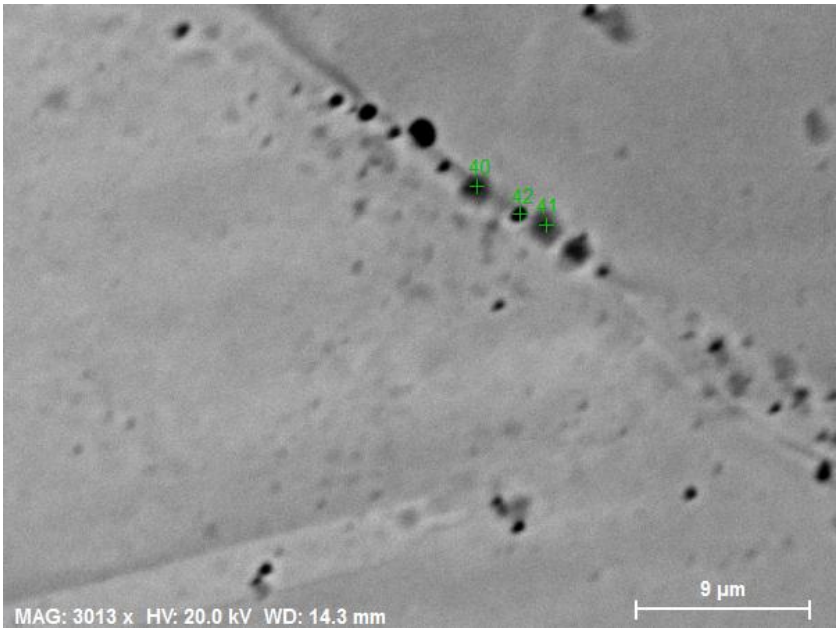

Spectrum: 41

Element	Series	norm. C [wt.%]	Atom. C [at.%]
Oxygen	K-series	0.90	3.47
Copper	K-series	99.10	96.53
Total:		100.00	100.00

Spectrum: 40

Element	Series	norm. C [wt.%]	Atom. C [at.%]
Oxygen	K-series	0.87	3.39
Copper	K-series	99.13	96.61
Total:		100.00	100.00

Spectrum: 39

Element	Series	norm. C [wt.%]	Atom. C [at.%]
Oxygen	K-series	0.64	2.49
Copper	K-series	99.36	97.51
Total:		100.00	100.00

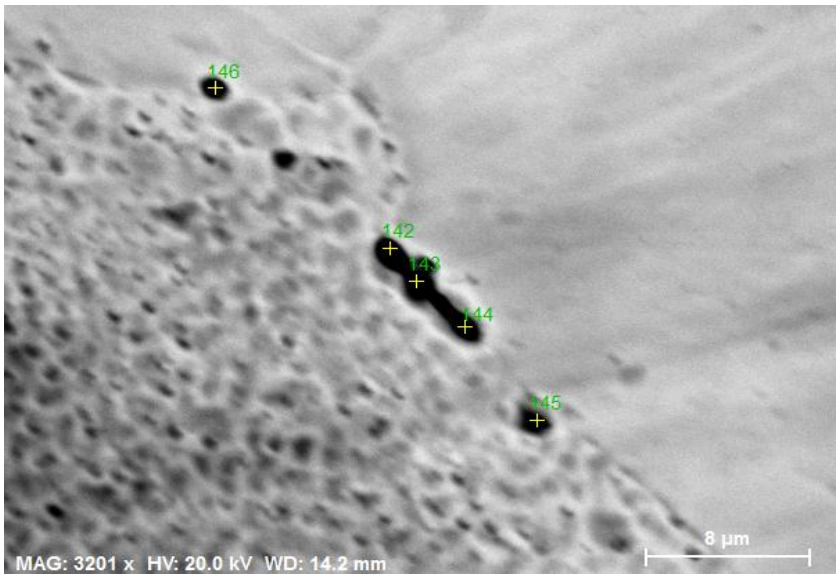

Spectrum: 144

Element	Series	norm. C [wt.%]	Atom. C [at.%]
Oxygen	K-series	8.69	27.44
Copper	K-series	91.31	72.56
Total:		100.00	100.00

Spectrum: 143

Element	Series	norm. C [wt.%]	Atom. C [at.%]
Oxygen	K-series	10.32	31.36
Copper	K-series	89.68	68.64
Total:		100.00	100.00

Spectrum: 142

Element	Series	norm. C [wt.%]	Atom. C [at.%]
Oxygen	K-series	5.20	17.90
Copper	K-series	94.80	82.10
Total:		100.00	100.00

Spectrum: 145

Element	Series	norm. C [wt.%]	Atom. C [at.%]
Oxygen	K-series	8.14	26.02
Copper	K-series	91.86	73.98
Total:		100.00	100.00

11.4 Sample 4

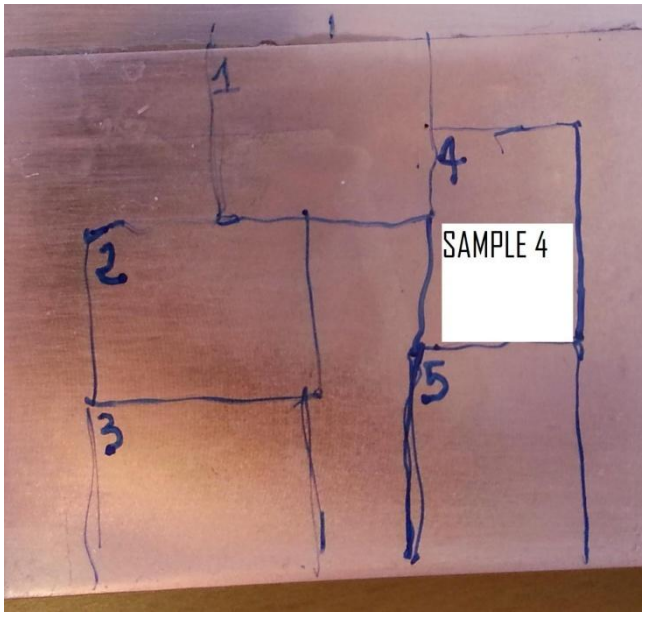

The total amount of oxides found in sample 4 is higher compared to sample 1,2 and 3; increasing getting closer to sample 5 and decreasing getting close to sample 1, besides this, the amount of oxides is higher in the right part of the sample. The total area fraction of oxides is 1,55E-06. Oxide inclusions found in sample 4 have different morphologies: small clusters composed by 3,4 inclusion and long strings composed by more than 3 usually orientated at 90 degrees to the edge line. Strings are different from the ones found in sample 3, they are usually longer and they don't follow completely grain boundaries, then the separation between every inclusion is higher than in sample 3, the average separation between string's inclusions here is about 20µm. The average size of oxides disclosed in sample 4 is 3,27µm. Besides oxygen, with an average content of 43,44%at and copper, inclusions disclosed in this sample show phosphorous, sulfur, aluminum and silicon. Sample 4 presents a lower content of voids if compared with sample 3.

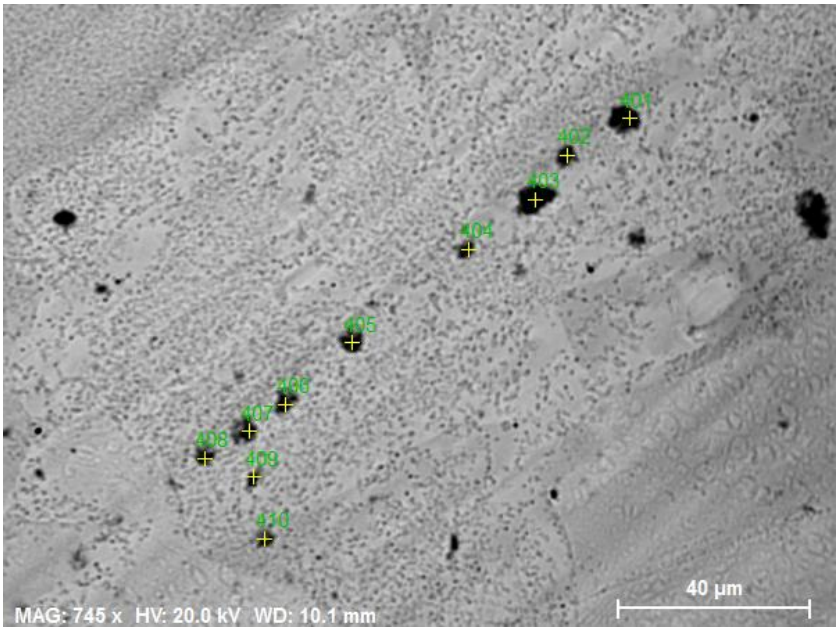

Spectrum: 410

Element	Series	norm. C [wt.%]	Atom. C [at.%]
Oxygen	K-series	10.34	30.64
Phosphorus	K-series	3.14	4.80
Copper	K-series	86.52	64.55
	Total:	100.00	100.00

Spectrum: 409

Element	Series	norm. C [wt.%]	Atom. C [at.%]
Oxygen	K-series	13.18	36.47
Phosphorus	K-series	4.12	5.90
Copper	K-series	82.70	57.63
	Total:	100.00	100.00

Spectrum: 408

Element	Series	norm. C [wt.%]	Atom. C [at.%]
Oxygen	K-series	17.11	43.52
Phosphorus	K-series	5.06	6.65
Copper	K-series	77.83	49.83
	Total:	100.00	100.00

Spectrum: 407

Element	Series	norm. C [wt.%]	Atom. C [at.%]
Oxygen	K-series	16.18	41.75
Phosphorus	K-series	5.55	7.40
Copper	K-series	78.27	50.86
	Total:	100.00	100.00

Spectrum: 406

Element	Series	norm. C [wt.%]	Atom. C [at.%]
Oxygen	K-series	13.56	37.18
Phosphorus	K-series	4.34	6.14
Copper	K-series	82.10	56.68
	Total:	100.00	100.00

Spectrum: 405

Element	Series	norm. C [wt.%]	Atom. C [at.%]
Oxygen	K-series	17.09	43.28
Phosphorus	K-series	5.73	7.50
Copper	K-series	77.18	49.22
	Total:	100.00	100.00

Spectrum: 404

Element	Series	norm. C [wt.%]	Atom. C [at.%]
Oxygen	K-series	14.54	39.10
Phosphorus	K-series	4.30	5.96
Copper	K-series	81.16	54.94
	Total:	100.00	100.00

Spectrum: 403

Element	Series	norm. C [wt.%]	Atom. C [at.%]
Oxygen	K-series	20.62	48.63
Phosphorus	K-series	6.77	8.25
Copper	K-series	72.61	43.12
	Total:	100.00	100.00

Spectrum: 402

Element	Series	norm. C [wt.%]	Atom. C [at.%]
Oxygen	K-series	16.90	42.69
Phosphorus	K-series	6.69	8.73
Copper	K-series	76.41	48.58
	Total:	100.00	100.00

Spectrum: 401

Element	Series	norm. C [wt.%]	Atom. C [at.%]
Oxygen	K-series	18.55	45.18
Phosphorus	K-series	7.55	9.50
Copper	K-series	73.90	45.32
	Total:	100.00	100.00

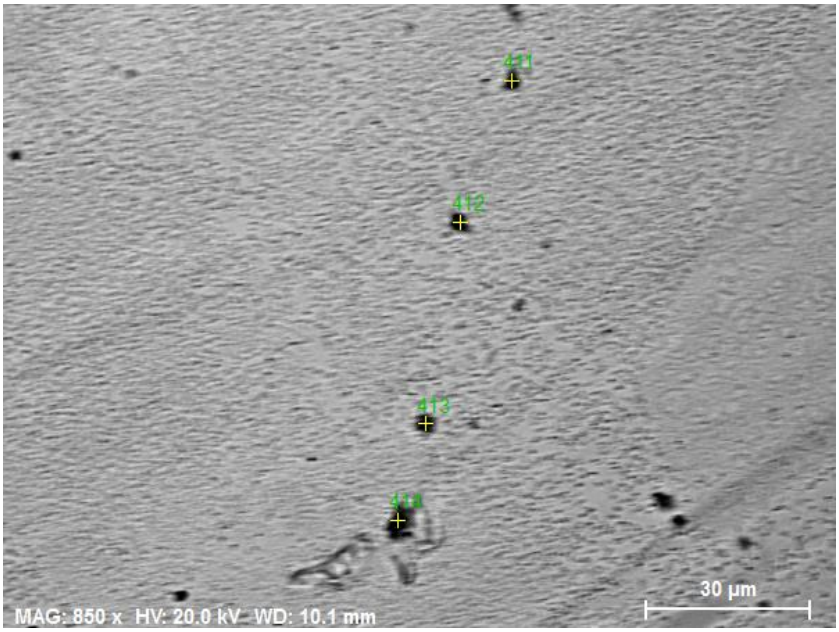

Spectrum: 414

Element	Series	norm. C [wt.%]	Atom. C [at.%]
Oxygen	K-series	20.70	50.91
Copper	K-series	79.30	49.09
Total:		100.00	100.00

Spectrum: 413

Element	Series	norm. C [wt.%]	Atom. C [at.%]
Oxygen	K-series	28.55	56.70
Copper	K-series	59.44	29.72
Silicon	K-series	12.01	13.58
Total:		100.00	100.00

Spectrum: 412

Element	Series	norm. C [wt.%]	Atom. C [at.%]
Oxygen	K-series	17.85	41.56
Aluminium	K-series	7.26	10.02
Silicon	K-series	6.08	8.07
Copper	K-series	68.81	40.35
Total:		100.00	100.00

Spectrum: 411

Element	Series	norm. C [wt.%]	Atom. C [at.%]
Oxygen	K-series	14.44	36.10
Aluminium	K-series	6.67	9.89
Silicon	K-series	5.46	7.78
Copper	K-series	73.43	46.23
Total:		100.00	100.00

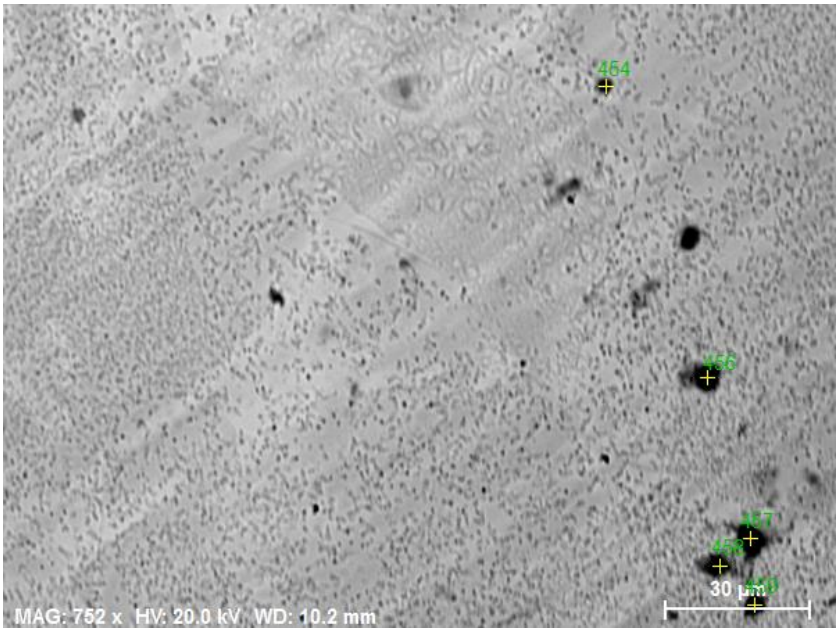

Spectrum: 459

Element	Series	norm. C [wt.%]	Atom. C [at.%]
Oxygen	K-series	22.82	51.79
Phosphorus	K-series	6.84	8.02
Copper	K-series	70.34	40.19
Total:		100.00	100.00

Spectrum: 458

Element	Series	norm. C [wt.%]	Atom. C [at.%]
Oxygen	K-series	16.05	41.42
Phosphorus	K-series	5.91	7.88
Copper	K-series	78.04	50.70
Total:		100.00	100.00

Spectrum: 457

Element	Series	norm. C [wt.%]	Atom. C [at.%]
Oxygen	K-series	21.25	49.16
Phosphorus	K-series	8.09	9.67
Copper	K-series	70.66	41.17
	Total:	100.00	100.00

Spectrum: 456

Element	Series	norm. C [wt.%]	Atom. C [at.%]
Oxygen	K-series	21.25	49.60
Phosphorus	K-series	6.64	8.01
Copper	K-series	72.11	42.39
	Total:	100.00	100.00

Spectrum: 454

Element	Series	norm. C [wt.%]	Atom. C [at.%]
Oxygen	K-series	21.02	49.01
Phosphorus	K-series	7.52	9.06
Copper	K-series	71.45	41.93
	Total:	100.00	100.00

11.5 Sample 5

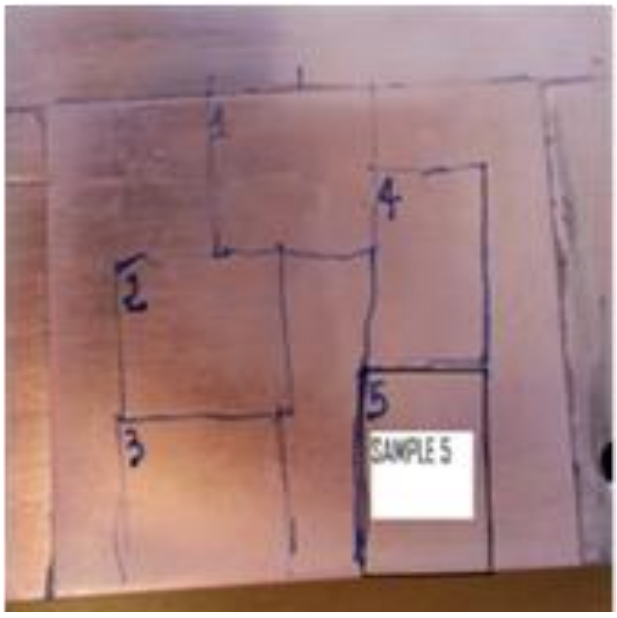

Sample 5 presents the higher oxides amount among the weld. As in sample 4, here, strings can be divided into 2 categories: strings at grain boundary and long strings composed by more than 3 inclusion with high diameter situated in proximity of boundaries with an average distance of about 20 μm between them, since these strings are not following the boundaries they have an average orientation of 45 degrees. The average size of inclusions is about 2,77μm and their average oxygen content is 36,31%at. Considering the total amount of strings and the size of the whole sample, oxides inclusions in sample 5 have an area fraction of 2,36E-06, 52% more than sample 4. As in sample 4, also in this sample an higher content of strings is shown on the right side of the sample increasing getting closer to the edge of the welded zone and decreasing getting closer to sample 4. Considering the chemical composition of these strings, except oxygen and copper, phosphorous, sulfur and aluminum have been detected in small traces. Sample 5 presents a lower content of voids if compared with sample 3.

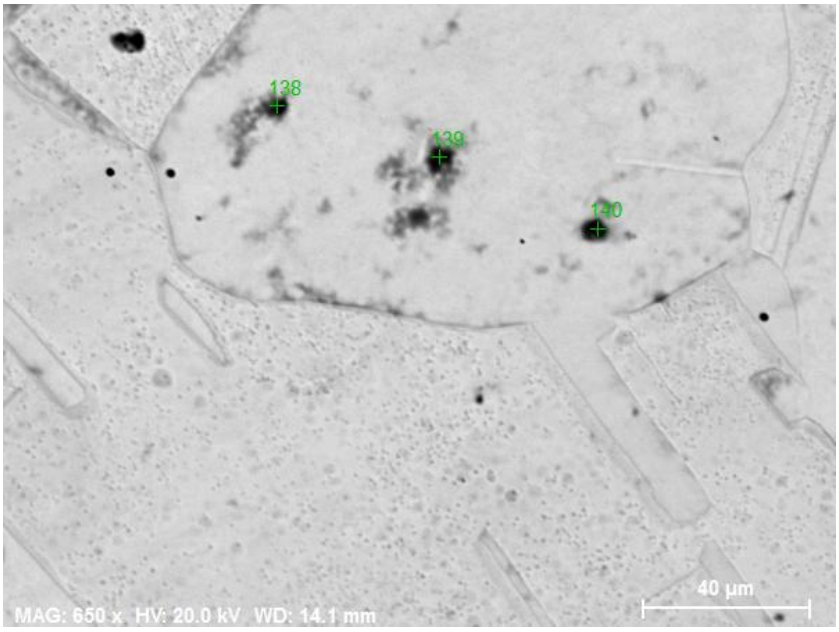

Spectrum: 140

Element	Series	norm. C [wt.%]	Atom. C [at.%]
Oxygen	K-series	23.55	55.03
Copper	K-series	76.45	44.97
Total:		100.00	100.00

Spectrum: 139

Element	Series	norm. C [wt.%]	Atom. C [at.%]
Oxygen	K-series	19.38	48.85
Copper	K-series	80.62	51.15
Total:		100.00	100.00

Spectrum: 138

Element	Series	norm. C [wt.%]	Atom. C [at.%]
Oxygen	K-series	17.96	46.51
Copper	K-series	82.04	53.49
Total:		100.00	100.00

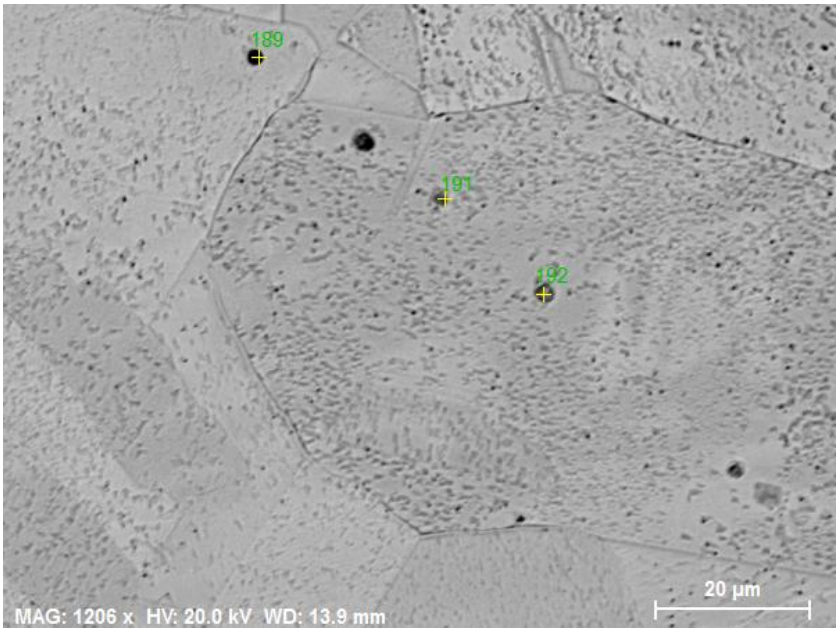

Spectrum: 192

Element	Series	norm. C [wt.%]	Atom. C [at.%]
Oxygen	K-series	2.95	10.78
Copper	K-series	97.05	89.22
Total:		100.00	100.00

Spectrum: 191

Element	Series	norm. C [wt.%]	Atom. C [at.%]
Oxygen	K-series	3.38	12.19
Copper	K-series	96.62	87.81
Total:		100.00	100.00

Spectrum: 190

Element	Series	norm. C [wt.%]	Atom. C [at.%]
Oxygen	K-series	0.78	3.02
Copper	K-series	99.22	96.98
Total:		100.00	100.00

Spectrum: 189

Element	Series	norm. C [wt.%]	Atom. C [at.%]
Oxygen	K-series	1.96	7.35
Copper	K-series	98.04	92.65
Total:		100.00	100.00

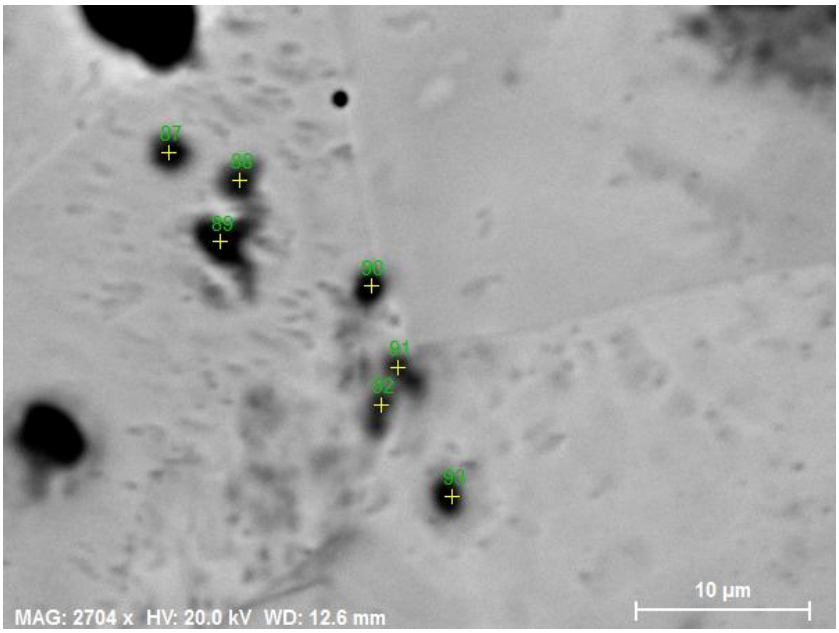

Spectrum: 93

Element	Series	norm. C [wt.%]	Atom. C [at.%]
Oxygen	K-series	14.00	39.27
Copper	K-series	86.00	60.73
Total:		100.00	100.00

Spectrum: 92

Element	Series	norm. C [wt.%]	Atom. C [at.%]
Oxygen	K-series	9.30	28.93
Copper	K-series	90.70	71.07
Total:		100.00	100.00

Spectrum: 91

Element	Series	norm. C [wt.%]	Atom. C [at.%]
Oxygen	K-series	10.32	31.37
Copper	K-series	89.68	68.63
Total:		100.00	100.00

Spectrum: 90

Element	Series	norm. C [wt.%]	Atom. C [at.%]
Oxygen	K-series	16.73	44.38
Copper	K-series	83.27	55.62
Total:		100.00	100.00

Spectrum: 89

Element	Series	norm. C [wt.%]	Atom. C [at.%]
Oxygen	K-series	21.45	52.02
Copper	K-series	78.55	47.98
Total:		100.00	100.00

Spectrum: 88

Element	Series	norm. C [wt.%]	Atom. C [at.%]
Oxygen	K-series	13.17	37.59
Copper	K-series	86.83	62.41
Total:		100.00	100.00

Spectrum: 87

Element	Series	norm. C [wt.%]	Atom. C [at.%]
Oxygen	K-series	16.09	43.24
Copper	K-series	83.91	56.76
Total:		100.00	100.00

11.6 Nugget Weld 1

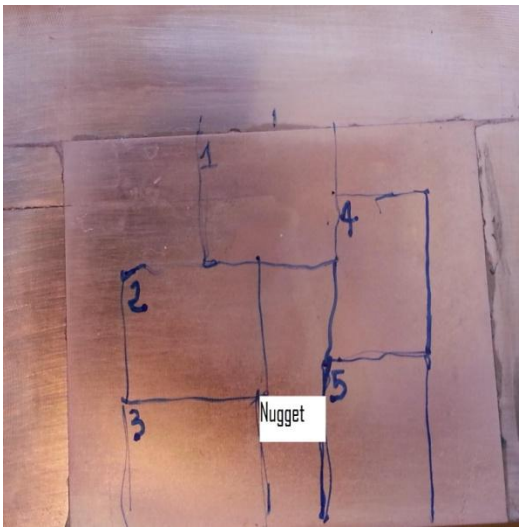

As well as retreating side, advancing side and slit region, also the nugget has been investigated, strings are mainly composed by 3 or 4 inclusions with an average separation of 25µm, and can be detected both at grain boundaries and in the middle of the grain, in one case a string composed by more than 5 inclusions has been found at a grain boundary. The average size of inclusion is 1,60µm with an average oxygen content of 39,54%at; considering the total amount of strings, oxides area fraction is 1,83E-07.

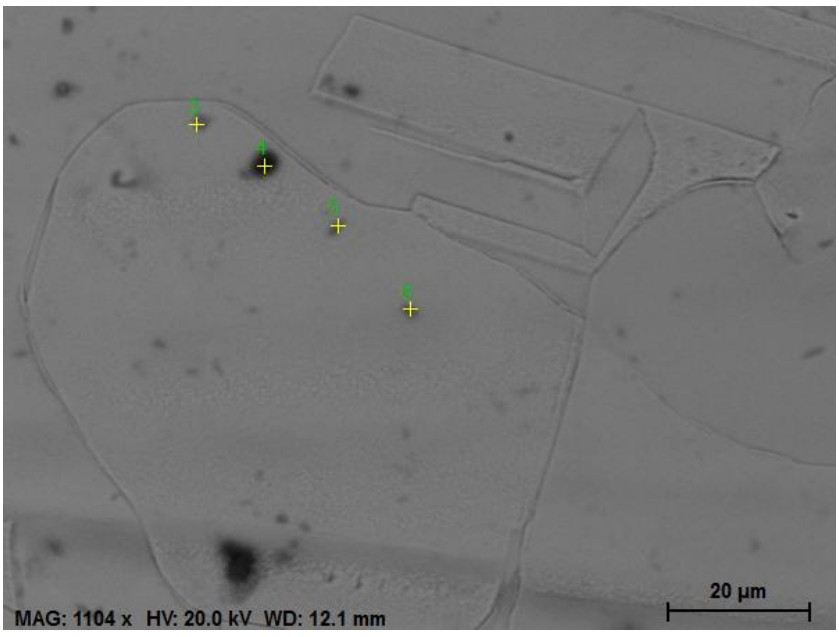

Spectrum: 6

Element	Series	norm. C [wt.%]	Atom. C [at.%]
Oxygen	K-series	11.56	32.84
Phosphorus	K-series	5.15	7.56
Copper	K-series	83.29	59.60
Total:		100.00	100.00

Spectrum: 5

Element	Series	norm. C [wt.%]	Atom. C [at.%]
Oxygen	K-series	7.40	23.62
Phosphorus	K-series	2.31	3.80
Copper	K-series	90.30	72.58
Total:		100.00	100.00

Spectrum: 4

Element	Series	norm. C [wt.%]	Atom. C [at.%]
Oxygen	K-series	29.25	59.09
Phosphorus	K-series	9.19	9.59
Copper	K-series	61.56	31.31
Total:		100.00	100.00

Spectrum: 3

Element	Series	norm. C [wt.%]	Atom. C [at.%]
Oxygen	K-series	10.55	31.18
Phosphorus	K-series	2.84	4.33
Copper	K-series	86.62	64.48
Total:		100.00	100.00

Spectrum: 15

Element	Series	norm. C [wt.%]	Atom. C [at.%]
Oxygen	K-series	27.15	56.93
Phosphorus	K-series	8.29	8.98
Copper	K-series	64.56	34.09
Total:		100.00	100.00

Spectrum: 14

Element	Series	norm. C [wt.%]	Atom. C [at.%]
Oxygen	K-series	30.93	60.55
Phosphorus	K-series	10.45	10.57
Copper	K-series	58.62	28.89
Total:		100.00	100.00

Spectrum: 13

Element	Series	norm. C [wt.%]	Atom. C [at.%]
Oxygen	K-series	24.39	53.32
Phosphorus	K-series	8.72	9.85
Copper	K-series	66.90	36.83
Total:		100.00	100.00

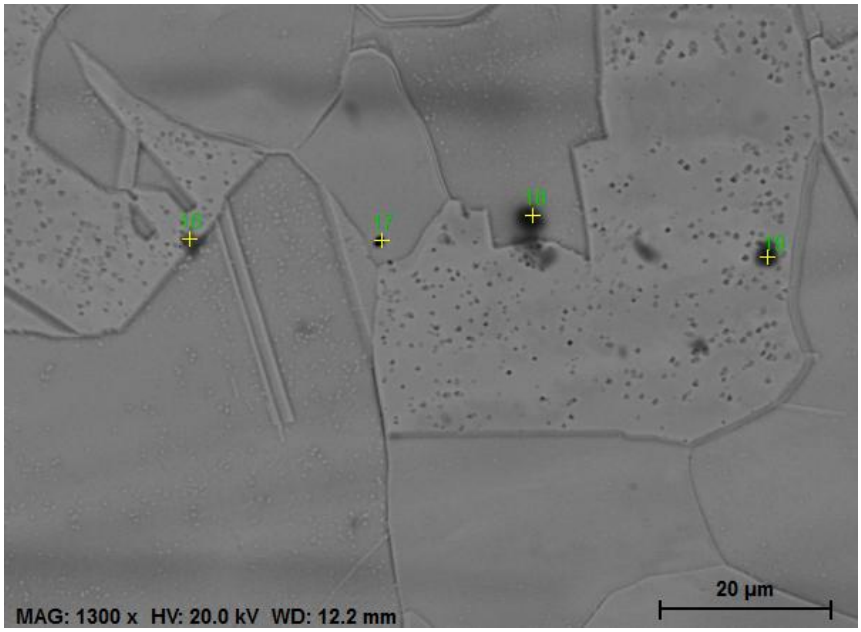

Spectrum: 19

Element	Series	norm. C [wt.%]	Atom. C [at.%]
Oxygen	K-series	31.7	61.28
Phosphorus	K-series	10.91	10.87
Copper	K-series	57.33	27.85
	Total:	100.00	100.00

Spectrum: 18

Element	Series	norm. C [wt.%]	Atom. C [at.%]
Oxygen	K-series	27.20	57.09
Phosphorus	K-series	8.01	8.68
Copper	K-series	64.79	34.23
	Total:	100.00	100.00

Spectrum: 17

Element	Series	norm. C [wt.%]	Atom. C [at.%]
Oxygen	K-series	1.94	7.03
Phosphorus	K-series	3.96	7.39
Copper	K-series	94.10	85.59
	Total:	100.00	100.00

Spectrum: 16

Element	Series	norm. C [wt.%]	Atom. C [at.%]
Oxygen	K-series	17.42	43.92
Phosphorus	K-series	5.50	7.16
Copper	K-series	77.07	48.91
	Total:	100.00	100.00

Weld 2

11.7 Sample 6

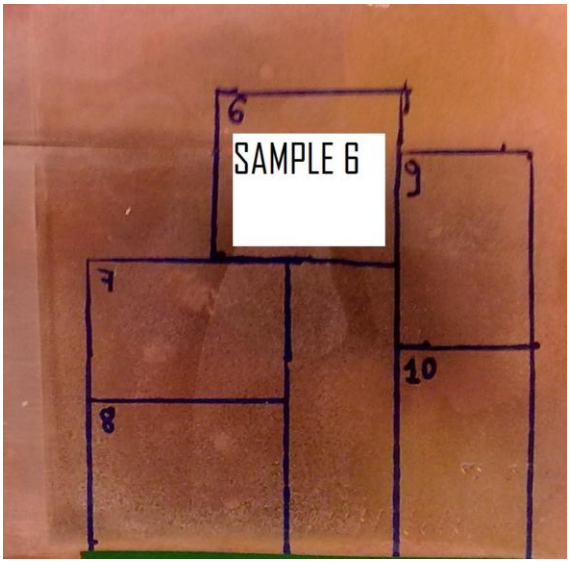

Sample 6 also presents oxide strings, their presence is detected not necessarily at grain boundaries but also in the middle of grains; this sample presents the lower oxides content among the 5 specimens. Strings are usually composed by 5,4 or 3 inclusions usually separated by 4-5µm, rarely some inclusions are separated by more than 20µm. Oxide inclusion in sample 6 are not always in the form of strings, sometimes they are grouped in clusters of 6,7 inclusions very close to each others. Oxides distribution in the sample is quite even, even if, close to the slit, an higher oxides content is detected, this make the oxides inclusions area fraction grows by 203% from 2,05E-07 to 6,21E-07 considering also the slit region. Considering also the slit, average oxides size is about 2,05µm and the average oxygen content is 54,46. Inclusions are composed mainly by oxygen and copper with traces of phosphorous, aluminum, silicon, iron, potassium and calcium. No voids have been detected.

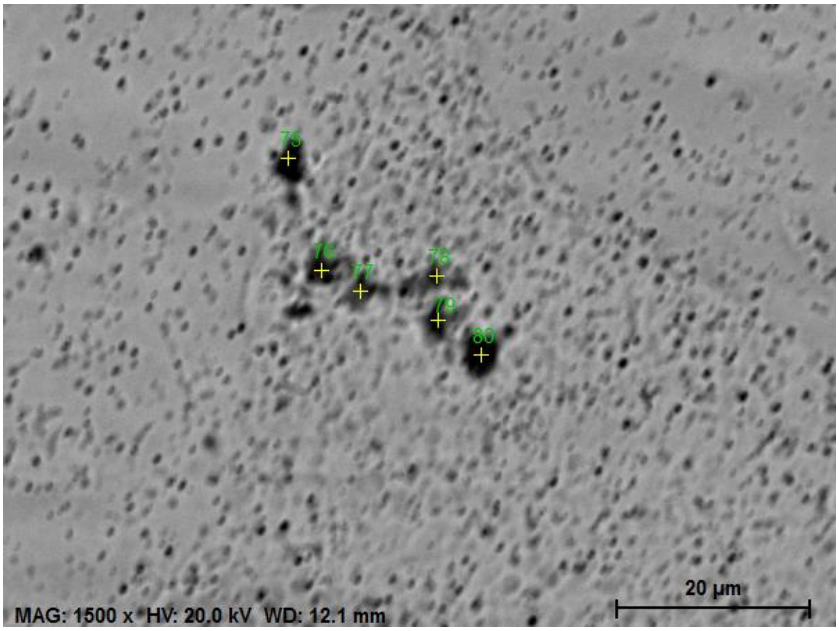

Spectrum: 80

Element	Series	norm. C [wt.%]	Atom. C [at.%]
Oxygen	K-series	43.10	70.90
Phosphorus	K-series	11.94	10.15
Copper	K-series	39.23	16.25
Iron	K-series	5.73	2.70
Total:		100.00	100.00

Spectrum: 79

Element	Series	norm. C [wt.%]	Atom. C [at.%]
Oxygen	K-series	23.22	51.84
Phosphorus	K-series	7.89	9.11
Iron	K-series	4.16	2.66
Copper	K-series	64.73	36.39
Total:		100.00	100.00

Spectrum: 78

Element	Series	norm. C [wt.%]	Atom. C [at.%]
Oxygen	K-series	22.68	51.52
Phosphorus	K-series	7.07	8.30
Copper	K-series	70.25	40.18
Total:		100.00	100.00

Spectrum: 77

Element	Series	norm. C [wt.%]	Atom. C [at.%]
Oxygen	K-series	19.94	48.01
Phosphorus	K-series	5.42	6.75
Copper	K-series	74.64	45.24
Total:		100.00	100.00

Spectrum: 76

Element	Series	norm. C [wt.%]	Atom. C [at.%]
Oxygen	K-series	12.78	35.57
Phosphorus	K-series	4.48	6.44
Copper	K-series	82.74	57.98
Total:		100.00	100.00

Spectrum: 75

Element	Series	norm. C [wt.%]	Atom. C [at.%]
Oxygen	K-series	21.64	49.21
Phosphorus	K-series	9.81	11.53
Copper	K-series	68.55	39.26
Total:		100.00	100.00

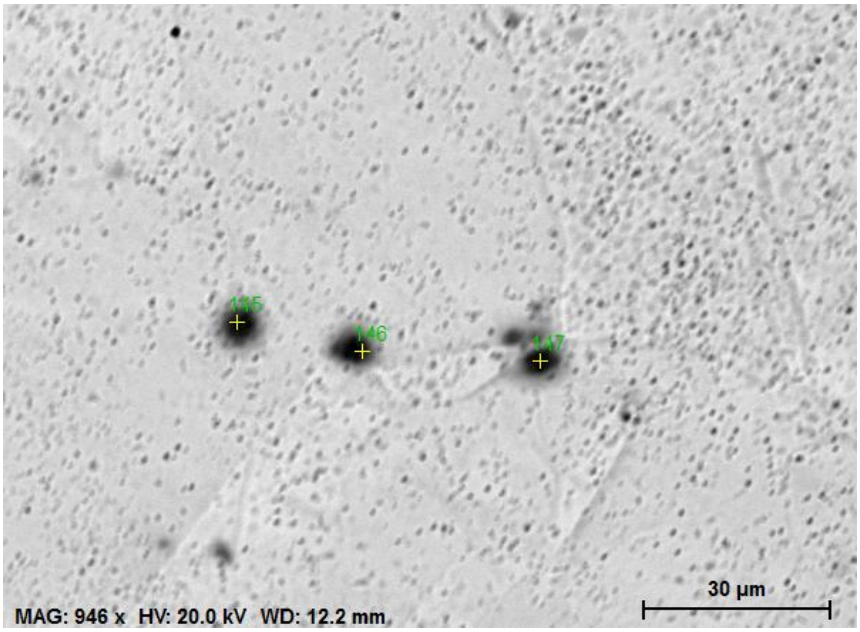

Spectrum: 147

Element	Series	norm. C [wt.%]	Atom. C [at.%]
Oxygen	K-series	45.88	72.49
Phosphorus	K-series	13.31	10.86
Iron	K-series	7.43	3.36
Copper	K-series	33.38	13.28
Total:		100.00	100.00

Spectrum: 146

Element	Series	norm. C [wt.%]	Atom. C [at.%]
Oxygen	K-series	43.11	71.00
Phosphorus	K-series	12.41	10.56
Copper	K-series	44.47	18.44
Total:		100.00	100.00

Spectrum: 145

Element	Series	norm. C [wt.%]	Atom. C [at.%]
Oxygen	K-series	37.99	66.79
Phosphorus	K-series	11.50	10.45
Iron	K-series	6.73	3.39
Copper	K-series	43.78	19.38
Total:		100.00	100.00

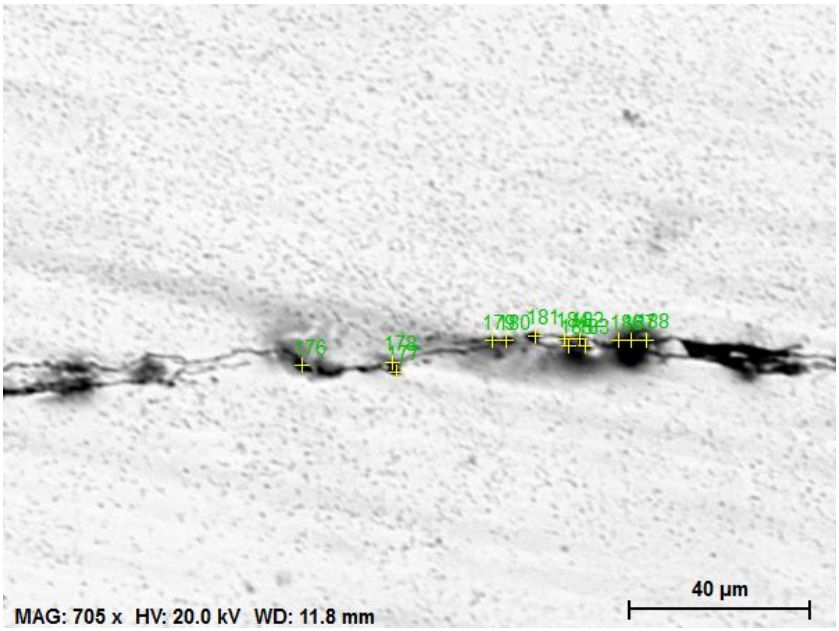

Spectrum: 188

Element	Series	norm. C [wt.%]	Atom. C [at.%]
Oxygen	K-series	26.42	55.50
Phosphorus	K-series	8.37	9.09
Copper	K-series	63.82	33.75
Silicon	K-series	1.39	1.66
Total:		100.00	100.00

Spectrum: 187

Element	Series	norm. C [wt.%]	Atom. C [at.%]
Oxygen	K-series	44.06	71.98
Phosphorus	K-series	11.60	9.79
Copper	K-series	44.34	18.24
Total:		100.00	100.00

Spectrum: 186

Element	Series	norm. C [wt.%]	Atom. C [at.%]
Oxygen	K-series	35.18	64.28
Phosphorus	K-series	12.18	11.49
Copper	K-series	52.65	24.22
Total:		100.00	100.00

Spectrum: 185

Element	Series	norm. C [wt.%]	Atom. C [at.%]
Oxygen	K-series	25.93	55.00
Phosphorus	K-series	9.70	10.63
Copper	K-series	64.36	34.37
Total:		100.00	100.00

Spectrum: 184

Element	Series	norm. C [wt.%]	Atom. C [at.%]
Oxygen	K-series	17.39	43.08
Silicon	K-series	1.70	2.40
Phosphorus	K-series	6.17	7.90
Copper	K-series	74.74	46.62
Total:		100.00	100.00

Spectrum: 183

Element	Series	norm. C [wt.%]	Atom. C [at.%]
Oxygen	K-series	19.44	46.60
Phosphorus	K-series	7.52	9.32
Copper	K-series	73.04	44.08
Total:		100.00	100.00

Spectrum: 182

Element	Series	norm. C [wt.%]	Atom. C [at.%]
Oxygen	K-series	23.26	51.63
Silicon	K-series	1.66	2.11
Phosphorus	K-series	7.34	8.41
Copper	K-series	67.74	37.85
Total:		100.00	100.00

Spectrum: 181

Element	Series	norm. C [wt.%]	Atom. C [at.%]
Oxygen	K-series	18.95	45.21
Phosphorus	K-series	9.67	11.92
Copper	K-series	71.38	42.87
Total:		100.00	100.00

Spectrum: 180

Element	Series	norm. C [wt.%]	Atom. C [at.%]
Oxygen	K-series	19.88	46.50
Phosphorus	K-series	10.22	12.34
Copper	K-series	69.90	41.16
Total:		100.00	100.00

Spectrum: 179

Element	Series	norm. C [wt.%]	Atom. C [at.%]
Oxygen	K-series	21.43	49.03
Phosphorus	K-series	9.46	11.17
Copper	K-series	69.11	39.80
Total:		100.00	100.00

11.8 Sample 7

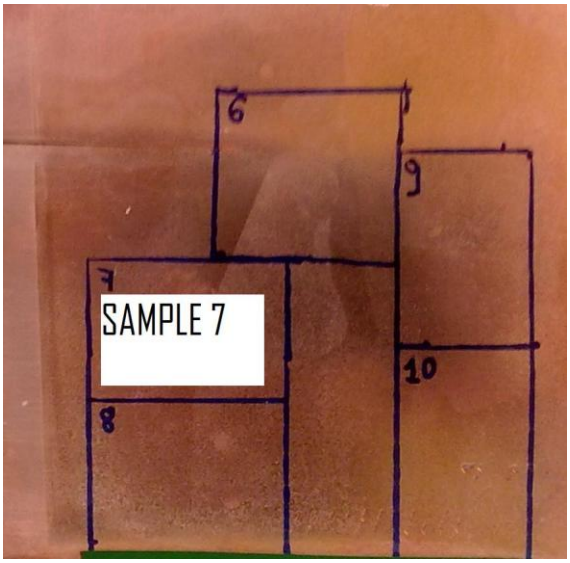

Oxide strings detected in sample 7 are not necessarily situated at grain boundaries, they are composed by a minimum of 3 inclusion and a maximum of 10; the separation between inclusions inside a string can vary a lot: some inclusions can be very close to each other (1µm), others can be separated by 20-30µm. Oxides distribution is not completely even since there are some parts of the sample that present more inclusions for example in the middle of the sample, oxides concentration grows getting closer to sample 8, and decreases getting closer to sample 6. The average oxides size is 1,82µm with an average oxygen content of

50,34%at. Considering the total amount of strings, the oxides are fraction is about 5,19E-07. As well as, copper and oxygen, also traces of phosphorous, iron, aluminum and silicon have been detected, almost no void have been found.

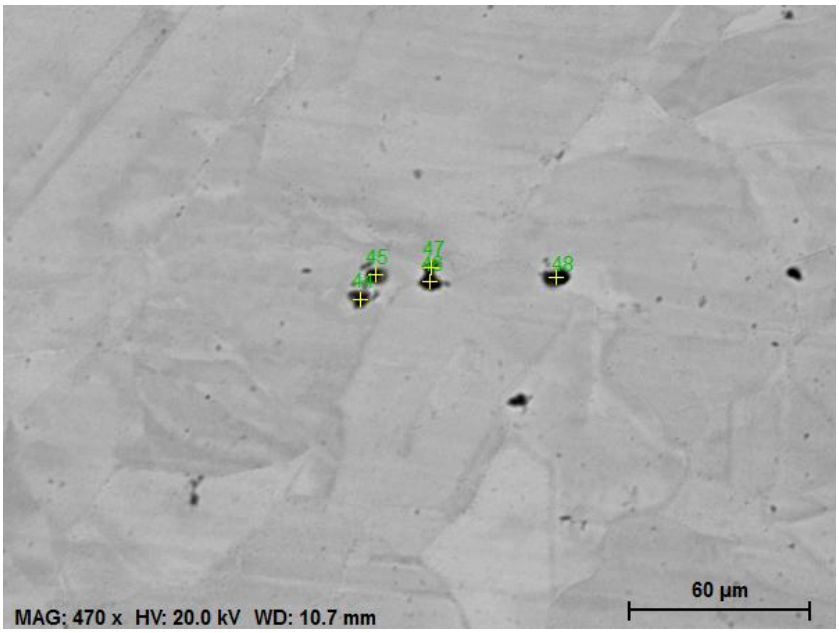

Spectrum: 47

Element	Series	norm. C [wt.%]	Atom. C [at.%]
Oxygen	K-series	25.38	55.16
Phosphorus	K-series	6.94	7.79
Copper	K-series	67.68	37.04
Total:		100.00	100.00

Spectrum: 46

Element	Series	norm. C [wt.%]	Atom. C [at.%]
Oxygen	K-series	39.13	67.96
Phosphorus	K-series	11.79	10.58
Copper	K-series	49.07	21.46
Total:		100.00	100.00

Spectrum: 45

Element	Series	norm. C [wt.%]	Atom. C [at.%]
Oxygen	K-series	38.07	67.77
Phosphorus	K-series	9.49	8.73
Copper	K-series	52.44	23.50
Total:		100.00	100.00

Spectrum: 44

Element	Series	norm. C [wt.%]	Atom. C [at.%]
Oxygen	K-series	25.07	54.48
Phosphorus	K-series	7.86	8.83
Copper	K-series	67.07	36.70
Total:		100.00	100.00

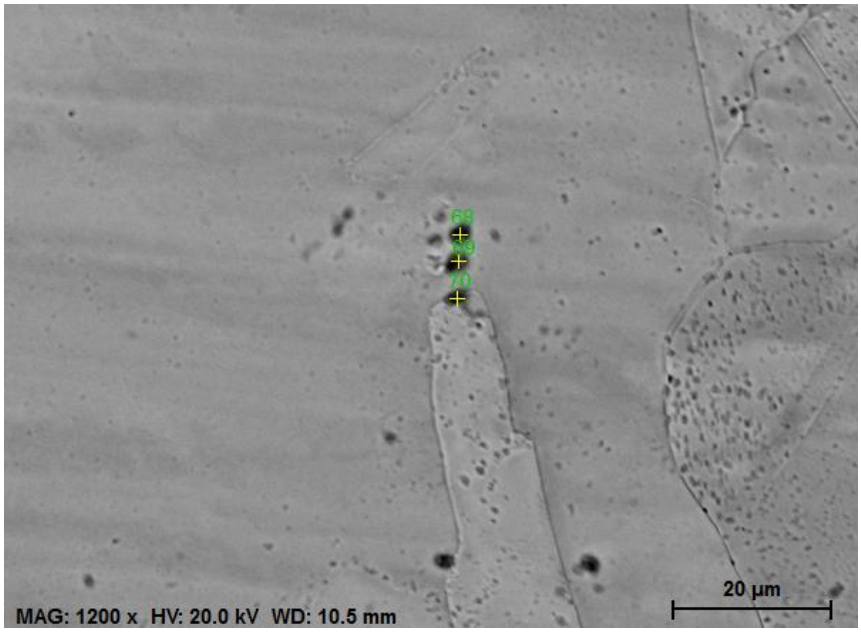

Spectrum: 70

Element	Series	norm. C [wt.%]	Atom. C [at.%]
Oxygen	K-series	16.44	42.22
Phosphorus	K-series	5.52	7.33
Copper	K-series	78.04	50.45
Total:		100.00	100.00

Spectrum: 69

Element	Series	norm. C [wt.%]	Atom. C [at.%]
Oxygen	K-series	24.91	53.20
Phosphorus	K-series	9.08	10.02
Copper	K-series	64.25	34.55
Aluminium	K-series	1.77	2.24
Total:		100.00	100.00

Spectrum: 68

Element	Series	norm. C [wt.%]	Atom. C [at.%]
Oxygen	K-series	23.52	52.33
Phosphorus	K-series	8.19	9.42
Copper	K-series	68.29	38.25
Total:		100.00	100.00

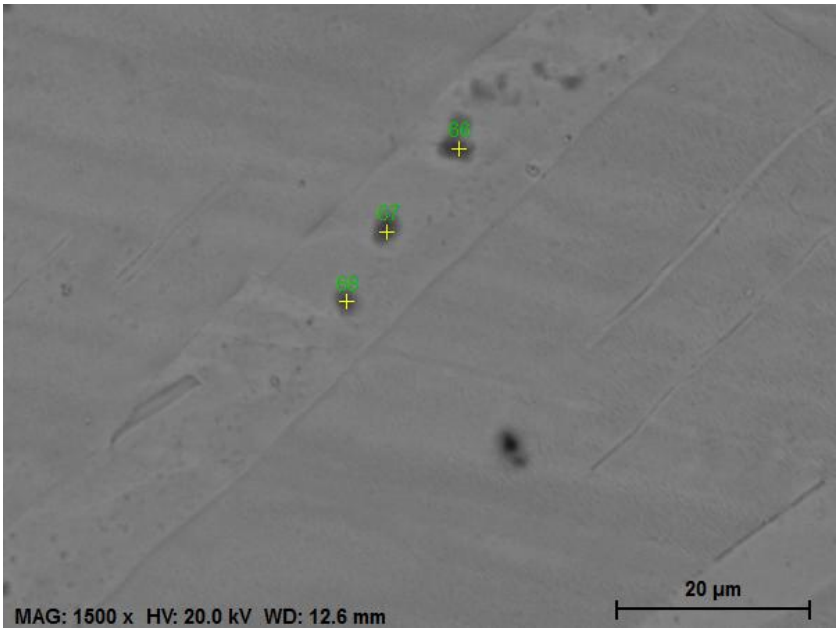

Spectrum: 68

Element	Series	norm. C [wt.%]	Atom. C [at.%]
Oxygen	K-series	19.22	46.52
Phosphorus	K-series	6.61	8.27
Copper	K-series	74.17	45.21
Total:		100.00	100.00

Spectrum: 67

Element	Series	norm. C [wt.%]	Atom. C [at.%]
Oxygen	K-series	33.65	63.64
Phosphorus	K-series	9.52	9.30
Copper	K-series	56.83	27.06
Total:		100.00	100.00

Spectrum: 66

Element	Series	norm. C [wt.%]	Atom. C [at.%]
Oxygen	K-series	31.61	61.65
Phosphorus	K-series	9.23	9.30
Copper	K-series	59.16	29.05
Total:		100.00	100.00

11.9 Sample 8

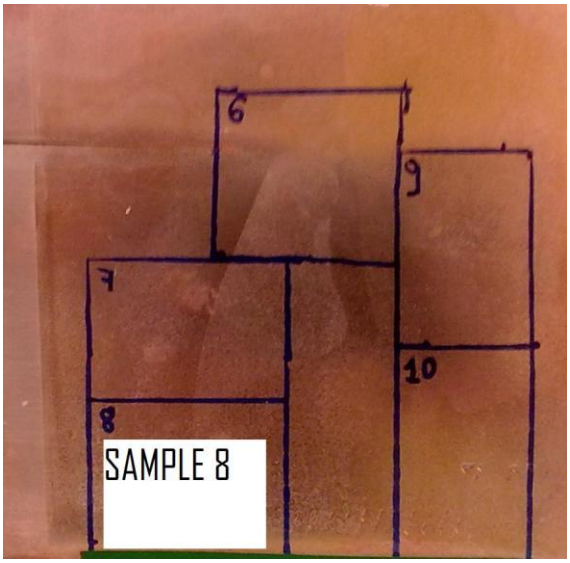

Sample 8 presents oxide strings that can be both at grain boundaries and in the middle of the grain, they are composed by 3, 4, 5 or 6 inclusions. Most oxide strings are not following a particular direction, and sometimes they are also curved, between every inclusion there is an average separation of 5µm. A strong oxidation is detected closer to the edge, the concentration of oxide strings increases getting closer to the edge of the weld and decreases getting closer to sample 7. Usually the distribution of these strings is quite even, even though,

sometimes, in some random parts of the sample some strings are very closer to each others. Inclusions average size is about 1,86 µm with an average oxygen content of 35,07%at. The total oxides area fraction is 8,05E07. Besides copper and oxygen, inclusions are composed by phosphorous, aluminum, silicon, iron with, in some inclusions, small traces of sulfur. No voids have been detected.

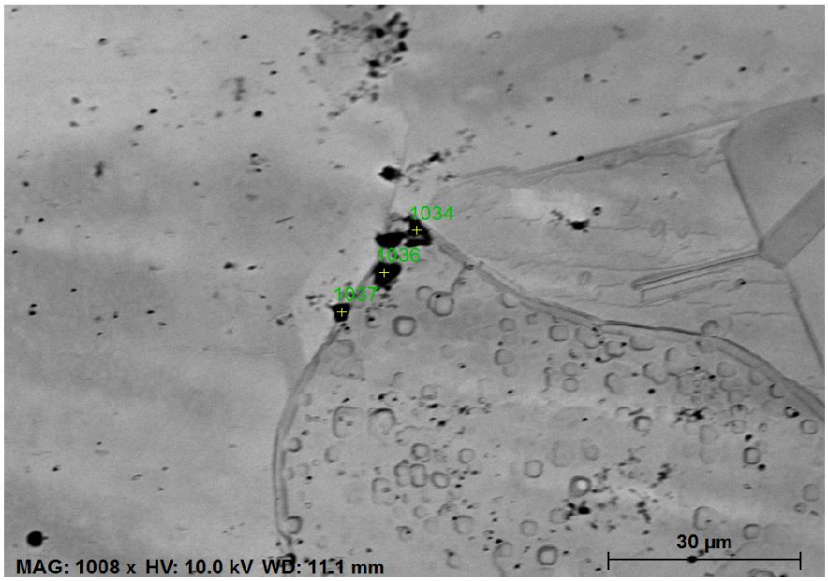

Spectrum: 1037

Element	Series	norm. C [wt.%]	Atom. C [at.%]
Oxygen	K-series	39.87	66.62
Phosphorus	K-series	18.26	15.76
Copper	K-series	41.87	17.62
Total:		100.00	100.00

Spectrum: 1036

Element	Series	norm. C [wt.%]	Atom. C [at.%]
Oxygen	K-series	49.81	76.77
Phosphorus	K-series	9.20	7.32
Copper	K-series	40.99	15.90
Total:		100.00	100.00

Spectrum: 1034

Element	Series	norm. C [wt.%]	Atom. C [at.%]
Oxygen	K-series	19.43	46.48
Phosphorus	K-series	7.85	9.71
Copper	K-series	72.72	43.81
Total:		100.00	100.00

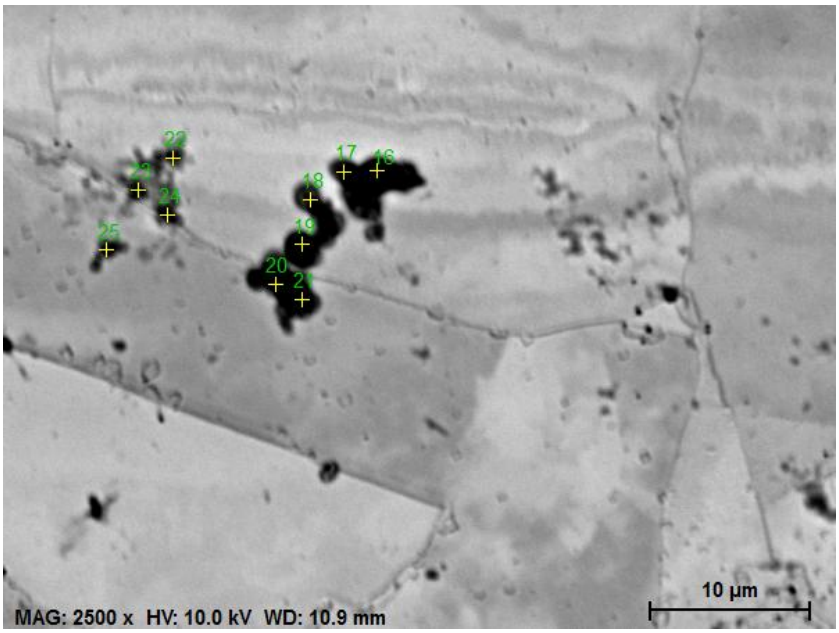

Spectrum: 25

Element	Series	norm. C [wt.%]	Atom. C [at.%]
Oxygen	K-series	12.61	35.14
Phosphorus	K-series	4.82	6.93
Copper	K-series	82.57	57.93
Total:		100.00	100.00

Spectrum: 24

Element	Series	norm. C [wt.%]	Atom. C [at.%]
Oxygen	K-series	11.36	32.70
Phosphorus	K-series	3.96	5.89
Copper	K-series	84.69	61.41
Total:		100.00	100.00

Spectrum: 23

Element	Series	norm. C [wt.%]	Atom. C [at.%]
Oxygen	K-series	14.41	38.70
Phosphorus	K-series	4.82	6.69
Copper	K-series	80.77	54.61
Total:		100.00	100.00

Spectrum: 22

Element	Series	norm. C [wt.%]	Atom. C [at.%]
Oxygen	K-series	10.42	30.66
Phosphorus	K-series	3.83	5.83
Copper	K-series	85.74	63.51
Total:		100.00	100.00

Spectrum: 21

Element	Series	norm. C [wt.%]	Atom. C [at.%]
Oxygen	K-series	8.82	26.96
Phosphorus	K-series	3.57	5.63
Copper	K-series	87.61	67.41
Total:		100.00	100.00

Spectrum: 20

Element	Series	norm. C [wt.%]	Atom. C [at.%]
Oxygen	K-series	13.91	36.92
Phosphorus	K-series	7.85	10.77
Copper	K-series	78.24	52.31
Total:		100.00	100.00

Spectrum: 19

Element	Series	norm. C [wt.%]	Atom. C [at.%]
Oxygen	K-series	30.01	58.94
Phosphorus	K-series	12.43	12.61
Copper	K-series	57.55	28.45
Total:		100.00	100.00

Spectrum: 18

Element	Series	norm. C [wt.%]	Atom. C [at.%]
Oxygen	K-series	21.73	48.90
Phosphorus	K-series	10.65	12.38
Sulfur	K-series	0.73	0.82
Copper	K-series	66.90	37.91
Total:		100.00	100.00

Spectrum: 17

Element	Series	norm. C [wt.%]	Atom. C [at.%]
Oxygen	K-series	17.43	43.16
Phosphorus	K-series	8.22	10.51
Copper	K-series	74.35	46.34
Total:		100.00	100.00

Spectrum: 16

Element	Series	norm. C [wt.%]	Atom. C [at.%]
Oxygen	K-series	33.57	62.33
Phosphorus	K-series	13.45	12.90
Copper	K-series	52.98	24.77
Total:		100.00	100.00

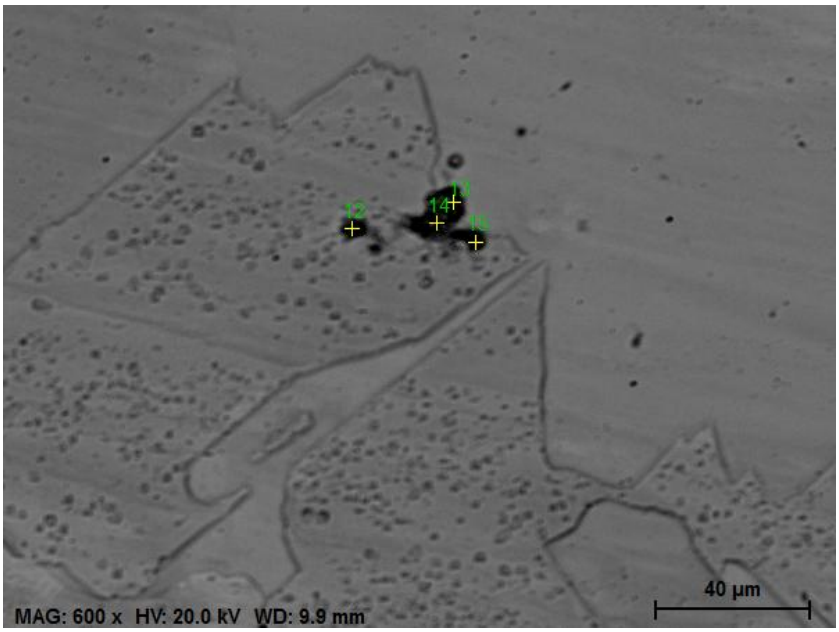

Spectrum: 15

Element	Series	norm. C [wt.%]	Atom. C [at.%]
Oxygen	K-series	33.10	62.42
Phosphorus	K-series	10.69	10.42
Copper	K-series	48.96	23.25
Iron	K-series	7.25	3.92
Total:		100.00	100.00

Spectrum: 14

Element	Series	norm. C [wt.%]	Atom. C [at.%]
Oxygen	K-series	11.44	32.47
Phosphorus	K-series	3.35	4.92
Sulfur	K-series	1.70	2.40
Iron	K-series	5.09	4.14
Copper	K-series	78.43	56.07
Total:		100.00	100.00

Spectrum: 13

Element	Series	norm. C [wt.%]	Atom. C [at.%]
Oxygen	K-series	10.95	30.80
Phosphorus	K-series	4.75	6.90
Sulfur	K-series	2.65	3.72
Iron	K-series	7.97	6.42
Copper	K-series	73.67	52.16
Total:		100.00	100.00

Spectrum: 12

Element	Series	norm. C [wt.%]	Atom. C [at.%]
Oxygen	K-series	22.36	50.46
Phosphorus	K-series	8.32	9.70
Iron	K-series	5.58	3.61
Copper	K-series	63.75	36.23
Total:		100.00	100.00

11.10 Sample 9

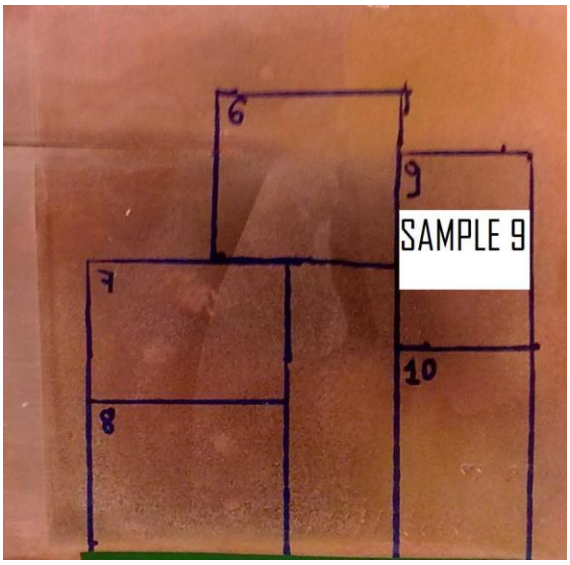

Oxide inclusions in sample 9 are situated mostly at grain boundaries, seldom strings don't follow a particular boundary but are situated in the middle of the grain; they are composed at least by 5 oxide inclusions and the separation between them is around 10-30μm, also in this case they don't follow a particular direction. Their concentration increases getting closer to sample 10 and decreases getting closer to sample 6, perpendicular to the weld axis, the distribution is quite even. Oxides average size is about 2,04μm with an average oxygen content of 39,97%at , the total area fraction of oxides is 5,86E-07. Inclusions are mostly composed by oxygen, copper, phosphorous, aluminum, iron, silicon, calcium with, in some case, small traces of sulfur. Also in this case, almost no voids are detected.

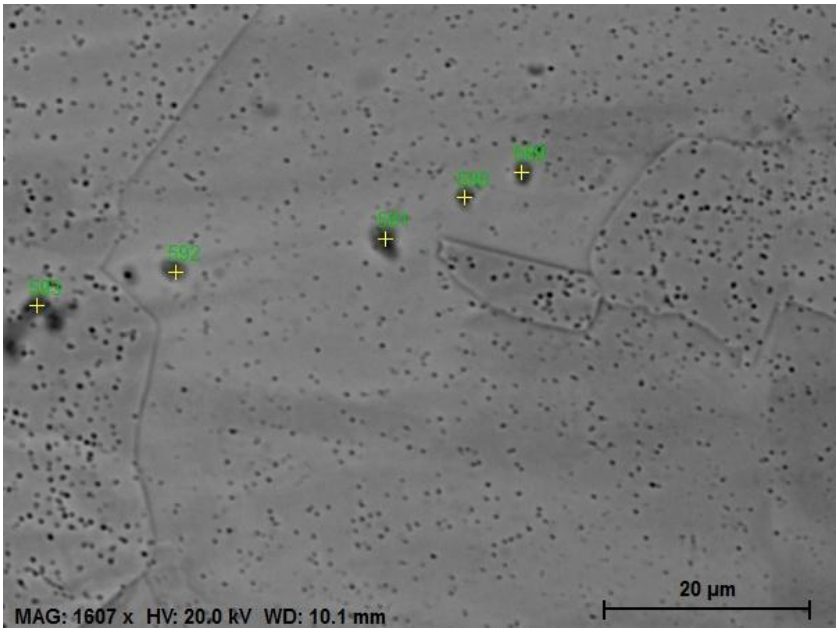

Spectrum: 593

Element	Series	norm. C [wt.%]	Atom. C [at.%]
Oxygen	K-series	10.86	31.77
Phosphorus	K-series	3.28	4.97
Copper	K-series	85.86	63.27
Total:		100.00	100.00

Spectrum: 592

Element	Series	norm. C [wt.%]	Atom. C [at.%]
Oxygen	K-series	6.36	20.81
Phosphorus	K-series	2.31	3.91
Copper	K-series	91.33	75.28
Total:		100.00	100.00

Spectrum: 591

Element	Series	norm. C [wt.%]	Atom. C [at.%]
Oxygen	K-series	7.91	24.92
Phosphorus	K-series	2.38	3.87
Copper	K-series	89.72	71.21
Total:		100.00	100.00

Spectrum: 590

Element	Series	norm. C [wt.%]	Atom. C [at.%]
Oxygen	K-series	10.14	30.05
Phosphorus	K-series	3.67	5.62
Copper	K-series	86.1	64.33
Total:		100.00	100.00

Spectrum: 589

Element	Series	norm. C [wt.%]	Atom. C [at.%]
Oxygen	K-series	6.75	21.99
Phosphorus	K-series	1.71	2.89
Copper	K-series	91.54	75.13
Total:		100.00	100.00

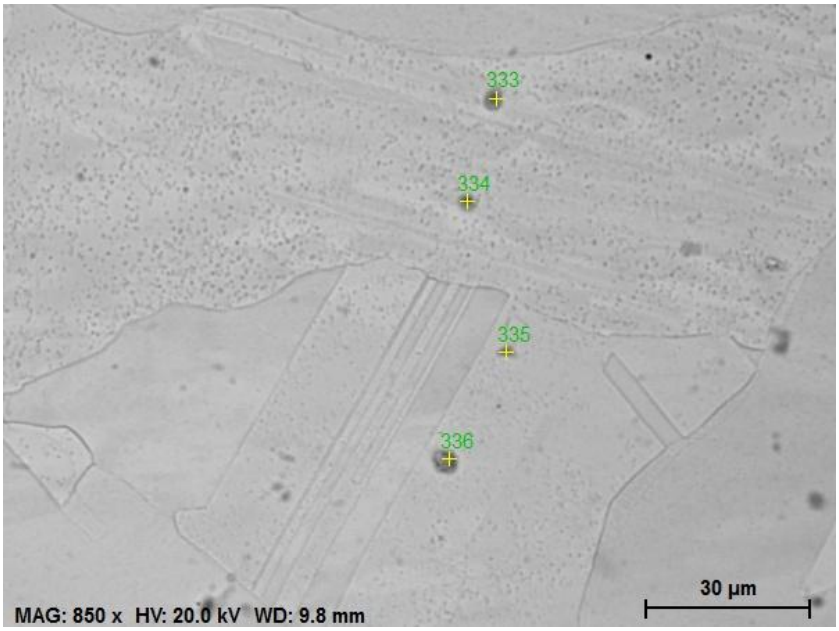

Spectrum: 336

Element	Series	norm. C [wt.%]	Atom. C [at.%]
Oxygen	K-series	33.86	65.24
Phosphorus	K-series	1.55	1.54
Copper	K-series	36.43	17.67
Iron	K-series	28.16	15.55
Total:		100.00	100.00

Spectrum: 335

Element	Series	norm. C [wt.%]	Atom. C [at.%]
Oxygen	K-series	15.87	41.29
Phosphorus	K-series	5.18	6.96
Copper	K-series	78.96	51.74
Total:		100.00	100.00

Spectrum: 334

Element	Series	norm. C [wt.%]	Atom. C [at.%]
Oxygen	K-series	20.35	46.94
Silicon	K-series	8.64	11.36
Phosphorus	K-series	0.73	0.87
Copper	K-series	70.28	40.83
Total:		100.00	100.00

Spectrum: 333

Element	Series	norm. C [wt.%]	Atom. C [at.%]
Oxygen	K-series	25.25	54.31
Aluminium	K-series	1.69	2.16
Phosphorus	K-series	2.23	2.48
Sulfur	K-series	2.52	2.71
Copper	K-series	66.33	35.92
Silicon	K-series	1.97	2.41
Total:		100.00	100.00

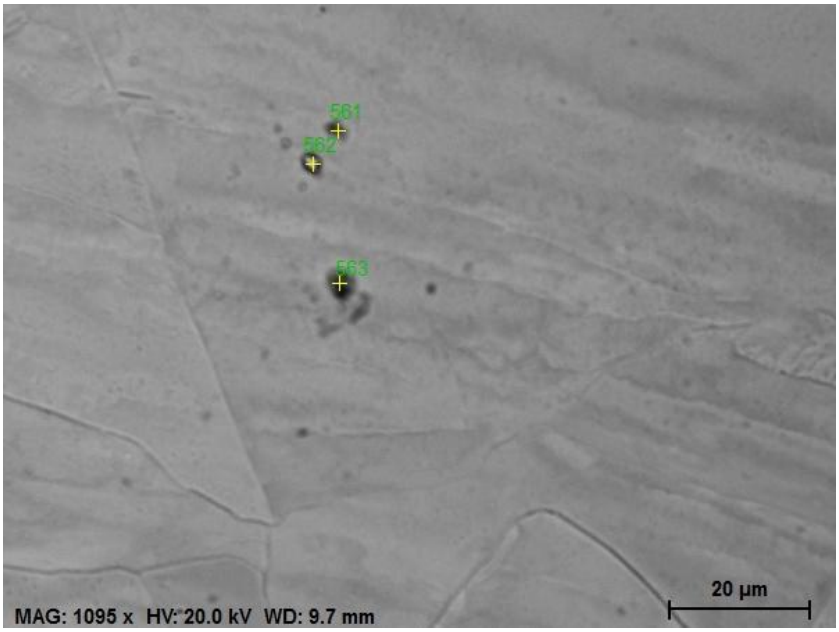

Spectrum: 563

Element	Series	norm. C [wt.%]	Atom. C [at.%]
Oxygen	K-series	6.58	21.08
Silicon	K-series	3.52	6.42
Copper	K-series	89.90	72.50
Total:		100.00	100.00

Spectrum: 562

Element	Series	norm. C [wt.%]	Atom. C [at.%]
Oxygen	K-series	2.36	8.77
Copper	K-series	97.64	91.23
Total:		100.00	100.00

Spectrum: 561

Element	Series	norm. C [wt.%]	Atom. C [at.%]
Oxygen	K-series	8.73	26.17
Silicon	K-series	5.17	8.83
Copper	K-series	86.10	65.00
Total:		100.00	100.00

11.11 Sample 10

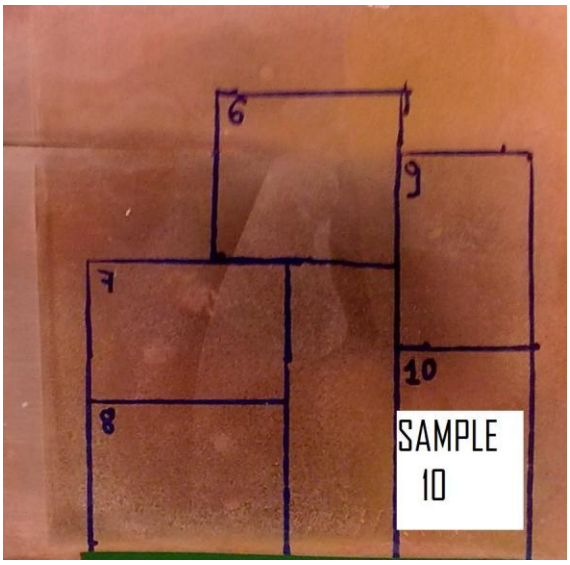

Sample 10 presents the higher oxides concentration among the 5 samples, oxides inclusion are usually situated at grain boundaries and their concentration grows getting closer to the edge of the weld, similarly, the concentration of oxides decrease getting closer to sample 9, besides decreasing in number getting further from the edge, oxide inclusions increase in number in the left part of the sample, closer to the friction zone. Strings are usually composed by more than 3 oxide inclusions and sometimes even more than 5 or 6, strings are composed by inclusions that present almost the same size and they are not orientated following a particular direction. The separation between inclusions in a string can vary a lot from 30µm to 5µm. Oxides average size is about 1,79µm, with an average oxygen content of 34,61 %at. Considering the whole sample, the total area fraction of oxides is 1,06E-06. As well as oxygen and copper, also phosphorous, calcium, aluminum and some traces of potassium have been detected. Almost no voids have been detected.

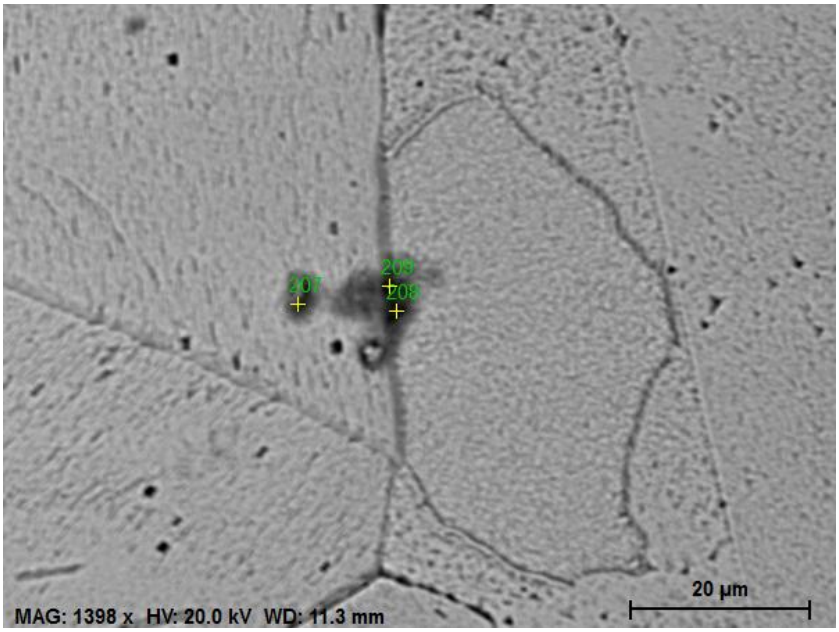

Spectrum: 209

Element	Series	norm. C [wt.%]	Atom. C [at.%]
Oxygen	K-series	17.74	44.27
Phosphorus	K-series	6.12	7.89
Copper	K-series	76.14	47.84
Total:		100.00	100.00

Spectrum: 208

Element	Series	norm. C [wt.%]	Atom. C [at.%]
Oxygen	K-series	16.01	40.99
Phosphorus	K-series	7.17	9.49
Copper	K-series	76.82	49.52
Total:		100.00	100.00

Spectrum: 207

Element	Series	norm. C [wt.%]	Atom. C [at.%]
Oxygen	K-series	13.77	37.51
Phosphorus	K-series	4.67	6.57
Copper	K-series	81.56	55.92
Total:		100.00	100.00

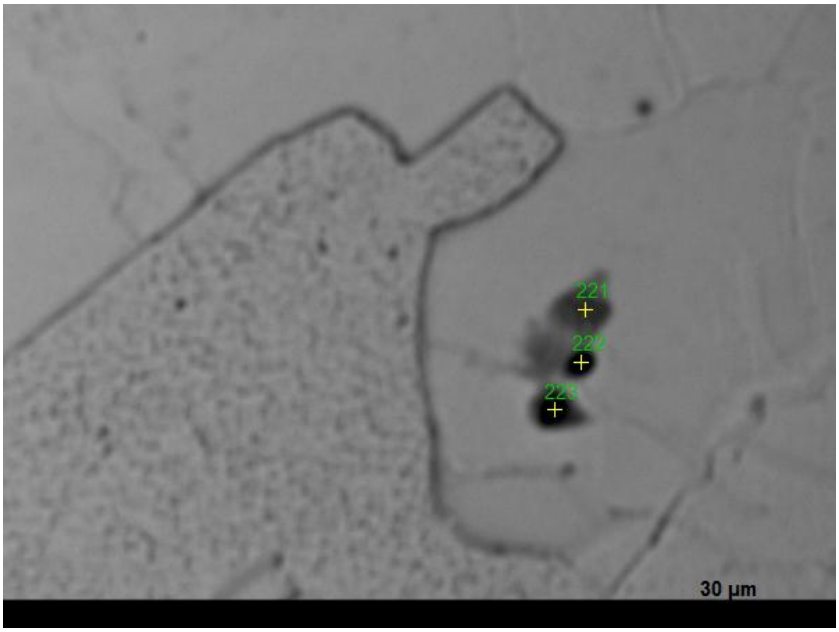

Spectrum: 223

Element	Series	norm. C [wt.%]	Atom. C [at.%]
Oxygen	K-series	17.98	44.44
Phosphorus	K-series	6.87	8.78
Copper	K-series	75.15	46.78
Total:		100.00	100.00

Spectrum: 222

Element	Series	norm. C [wt.%]	Atom. C [at.%]
Oxygen	K-series	49.13	74.58
Phosphorus	K-series	14.85	11.64
Copper	K-series	36.03	13.77
Total:		100.00	100.00

Spectrum: 221

Element	Series	norm. C [wt.%]	Atom. C [at.%]
Oxygen	K-series	17.86	44.45
Phosphorus	K-series	6.18	7.94
Copper	K-series	75.97	47.61
Total:		100.00	100.00

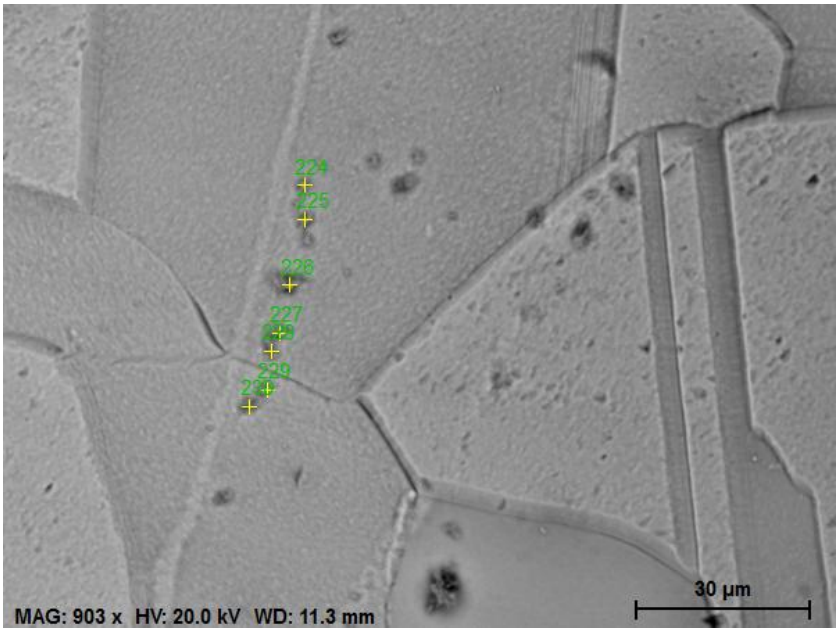

Spectrum: 230

Element	Series	norm. C [wt.%]	Atom. C [at.%]
Oxygen	K-series	21.33	49.92
Phosphorus	K-series	6.00	7.26
Copper	K-series	72.67	42.82
Total:		100.00	100.00

Spectrum: 229

Element	Series	norm. C [wt.%]	Atom. C [at.%]
Oxygen	K-series	6.12	20.30
Phosphorus	K-series	1.45	2.48
Copper	K-series	92.43	77.22
Total:		100.00	100.00

Spectrum: 228

Element	Series	norm. C [wt.%]	Atom. C [at.%]
Oxygen	K-series	10.12	30.14
Phosphorus	K-series	3.08	4.74
Copper	K-series	86.80	65.12
Total:		100.00	100.00

Spectrum: 227

Element	Series	norm. C [wt.%]	Atom. C [at.%]
Oxygen	K-series	14.29	38.53
Phosphorus	K-series	4.56	6.35
Copper	K-series	81.15	55.11
Total:		100.00	100.00

Spectrum: 226

Element	Series	norm. C [wt.%]	Atom. C [at.%]
Oxygen	K-series	22.43	51.32
Phosphorus	K-series	6.61	7.81
Copper	K-series	70.96	40.87
Total:		100.00	100.00

Spectrum: 225

Element	Series	norm. C [wt.%]	Atom. C [at.%]
Oxygen	K-series	12.28	34.81
Phosphorus	K-series	3.44	5.03
Copper	K-series	84.28	60.16
Total:		100.00	100.00

Spectrum: 224

Element	Series	norm. C [wt.%]	Atom. C [at.%]
Oxygen	K-series	19.20	46.68
Phosphorus	K-series	6.02	7.55
Copper	K-series	74.78	45.77
Total:		100.00	100.00

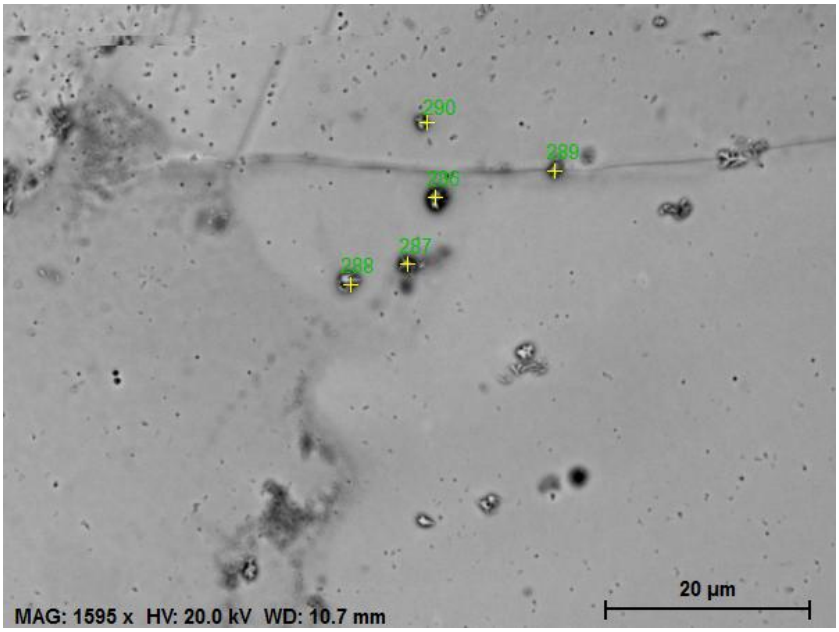

Spectrum: 290

Element	Series	norm. C [wt.%]	Atom. C [at.%]
Oxygen	K-series	7.87	24.88
Phosphorus	K-series	2.11	3.44
Copper	K-series	90.03	71.68
Total:		100.00	100.00

Spectrum: 289

Element	Series	norm. C [wt.%]	Atom. C [at.%]
Oxygen	K-series	10.33	30.82
Phosphorus	K-series	2.29	3.52
Copper	K-series	87.39	65.65
Total:		100.00	100.00

Spectrum: 288

Element	Series	norm. C [wt.%]	Atom. C [at.%]
Oxygen	K-series	9.13	27.83
Phosphorus	K-series	3.01	4.73
Copper	K-series	87.87	67.44
Total:		100.00	100.00

Spectrum: 287

Element	Series	norm. C [wt.%]	Atom. C [at.%]
Oxygen	K-series	15.94	41.98
Phosphorus	K-series	3.25	4.42
Copper	K-series	80.82	53.60
Total:		100.00	100.00

Spectrum: 286

Element	Series	norm. C [wt.%]	Atom. C [at.%]
Oxygen	K-series	15.15	40.39
Phosphorus	K-series	3.78	5.21
Copper	K-series	81.06	54.40
Total:		100.00	100.00

11.12 Nugget Weld 2

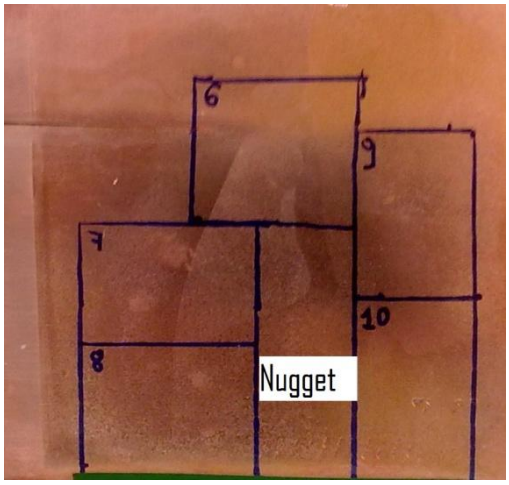

Oxide strings detected in the nugget are composed by 3,4 inclusions usually with a distance between them of 20-25µm, only in one case a string at a grain boundary has been detected, in this case the distance between the inclusions inside the latter was around 2-5µm; the average size of the inclusions detected inside strings is 1,83µm, with an average oxygen content of 40,41%at. Considering the total amount of oxide strings, oxide area fraction is 1,29E-07.

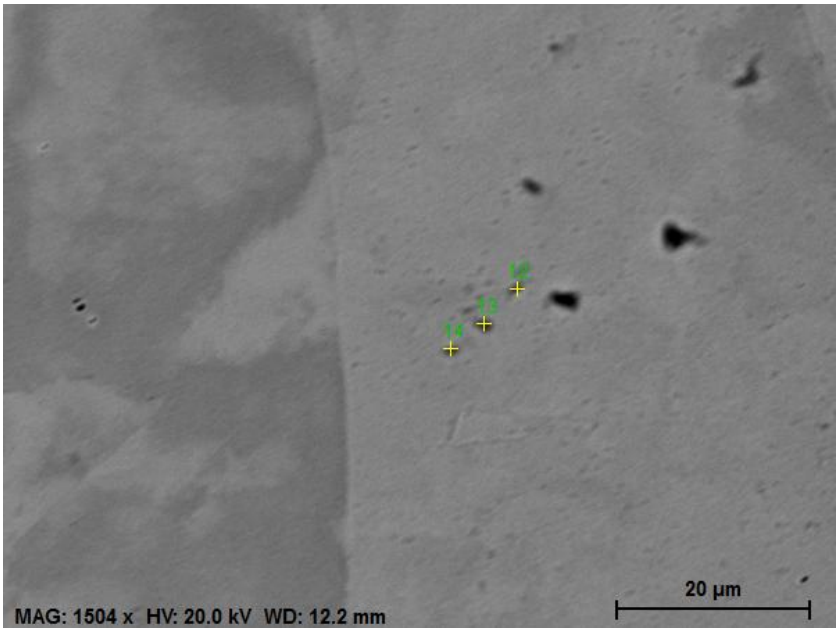

Spectrum: 14

Element	Series	norm. C [wt.%]	Atom. C [at.%]
Oxygen	K-series	12.55	35.46
Phosphorus	K-series	3.12	4.55
Copper	K-series	84.33	59.99
Total:		100.00	100.00

Spectrum: 13

Element	Series	norm. C [wt.%]	Atom. C [at.%]
Oxygen	K-series	13.77	37.91
Phosphorus	K-series	3.18	4.52
Copper	K-series	83.05	57.57
Total:		100.00	100.00

Spectrum: 12

Element	Series	norm. C [wt.%]	Atom. C [at.%]
Oxygen	K-series	7.03	22.72
Phosphorus	K-series	1.83	3.06
Copper	K-series	91.14	74.22
Total:		100.00	100.00

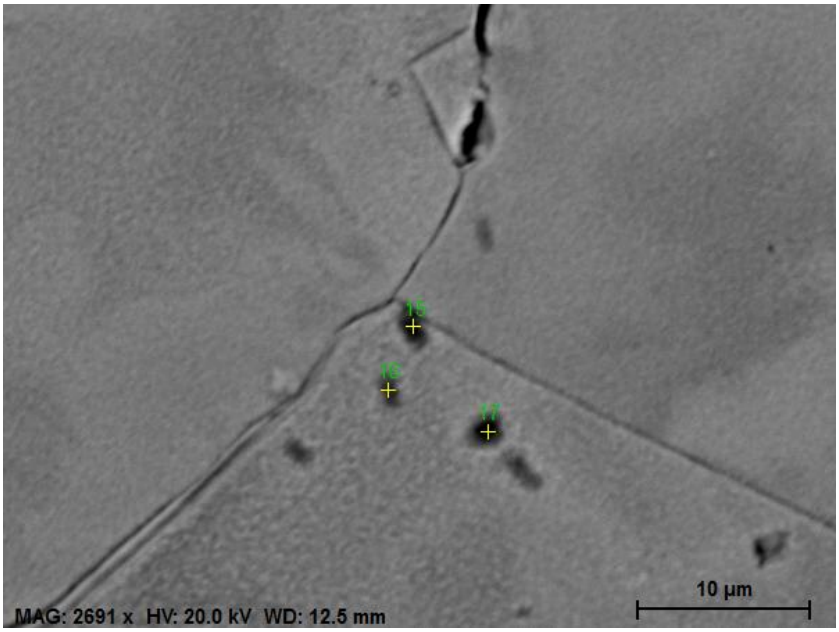

Spectrum: 17

Element	Series	norm. C [wt.%]	Atom. C [at.%]
Oxygen	K-series	21.16	49.80
Phosphorus	K-series	5.33	6.48
Copper	K-series	71.60	42.43
Iron	K-series	1.92	1.30
Total:		100.00	100.00

Spectrum: 16

Element	Series	norm. C [wt.%]	Atom. C [at.%]
Oxygen	K-series	14.12	38.36
Phosphorus	K-series	3.78	5.31
Iron	K-series	1.76	1.37
Copper	K-series	80.35	54.97
Total:		100.00	100.00

Spectrum: 15

Element	Series	norm. C [wt.%]	Atom. C [at.%]
Oxygen	K-series	18.31	45.41
Phosphorus	K-series	5.09	6.52
Iron	K-series	2.71	1.93
Copper	K-series	73.89	46.14
Total:		100.00	100.00

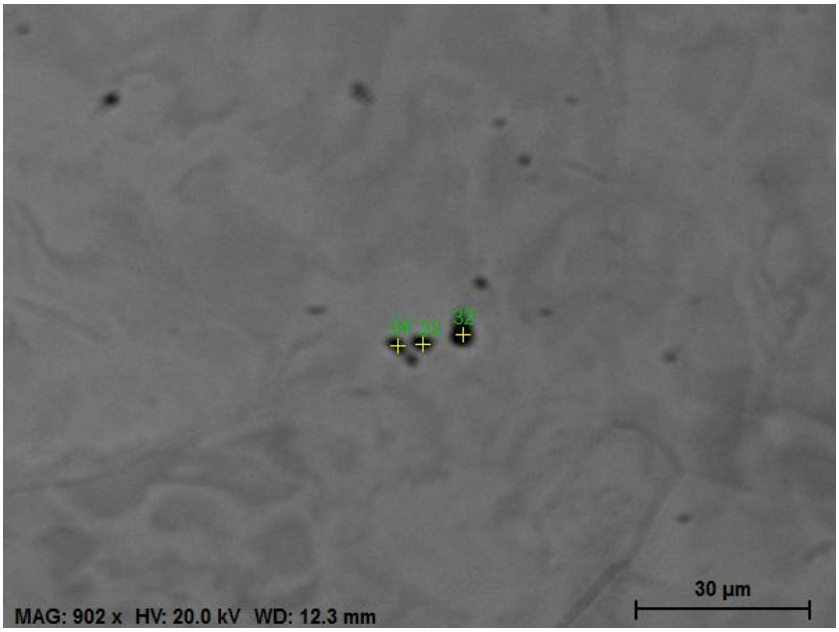

Spectrum: 34

Element	Series	norm. C [wt.%]	Atom. C [at.%]
Oxygen	K-series	16.89	42.49
Aluminium	K-series	1.01	1.50
Phosphorus	K-series	5.78	7.51
Iron	K-series	1.63	1.17
Copper	K-series	74.70	47.32
Total:		100.00	100.00

Spectrum: 33

Element	Series	norm. C [wt.%]	Atom. C [at.%]
Oxygen	K-series	19.15	46.63
Phosphorus	K-series	5.56	6.99
Iron	K-series	2.70	1.88
Copper	K-series	72.59	44.50
Total:		100.00	100.00

Spectrum: 32

Element	Series	norm. C [wt.%]	Atom. C [at.%]
Oxygen	K-series	32.95	61.23
Phosphorus	K-series	13.95	13.39
Iron	K-series	8.35	4.45
Copper	K-series	44.74	20.93
Total:		100.00	100.00